POLYMER PARTICLE SIZE DISTRIBUTIONS IN CONTINUOUS EMULSION POLYMERIZATION

by

James Otto Funderburk, Jr.

A Dissertation Submitted to the
Graduate Faculty in Partial Fulfillment of
The Requirements for the Degree of
DOCTOR OF PHILOSOPHY

Major Subject: Chemical Engineering

Approved:

Signature was redacted for privacy.

In Charge of Major Work

Signature was redacted for privacy.

Head of Major Department

Signature was redacted for privacy.

Dean of Graduate College

Iowa State University
Of Science and Technology
Ames, Iowa

1969

PLEASE NOTE:

Not original copy.
Some pages have very
light type. Filmed
as received.

University Microfilms

TABLE OF CONTENTS

INTRODUCTION

Although such substances as rubber, cellulose, protein, resins, and gum have been known for years, the study of polymerization and polymers as molecules of high molecular weight is a relatively new field for chemists and engineers. This is partly due to the inability of earlier chemists to isolate a pure polymeric compound which could be represented by a single molecular formula. It was thought that polymeric substances were colloidal aggregates of smaller molecules held together by an intermolecular force. It is now known that these substances consist of molecules of very high molecular weight, for example, from 20,000 (nylon) to 1,000,000 or more (cellulose in cotton). A specific polymeric substance will exhibit a molecular weight distribution rather than consist of identical molecules.

There are two basic polymeric growth reactions: addition and condensation. In addition polymerization the polymer becomes "activated" by being transformed into a free radical or an ion. Monomer molecules continually add to the growing polymeric chain until the activity is terminated. The polymerization of styrene is an example of addition polymerization:

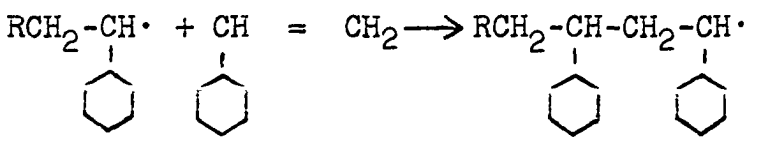

In condensation polymerization a side product, such as H_2O or CO_2, will be split off as each additional monomer molecule joins the polymeric chain. The combination of hexamethylenediamine and adipic acid is an example of condensation polymerization:

$$NH_2(CH_2)_6NH_2 + HOOC(CH_2)_4COOH \rightarrow NH_2(CH_2)_6NH\underset{\underset{O}{\|}}{C}(CH_2)_4CHOOH + H_2O$$

The method in which the reactants for the two types of growth reactions given above are brought together is used to classify the type of polymerization. The four characteristic types of polymerization are bulk, solution, suspension, and emulsion polymerization. In the first three types, the polymerization takes place in the phase of the monomer. In bulk polymerization the polymerization takes place in the pure liquid monomer phase itself. In solution polymerization the polymerization takes place in the solution in which the monomer is dissolved. In suspension polymerization small beads of monomer are suspended in a medium. The polymerization takes place in the liquid monomer within the beads.

Emulsion polymerization, like suspension polymerization, is a two phase reaction consisting of a dispersion medium and a dispersed phase which is the monomer. However the polymerization does not take place in the monomer phase in emulsion polymerization. The polymerization begins at specific loci in the dispersion medium and continues outside the monomer

phase. This characteristic of emulsion polymerization is the source of its principle advantage. By using the techniques of emulsion polymerization, the propagation rate can be increased without a significant decrease in the average molecular weight. In most other types of polymerization, an increase in propagation rate will result in a corresponding decrease in average molecular weight.

There are other advantages as well as disadvantages to the application of emulsion polymerization. The product of emulsion polymerization is in the form of a latex. When the produced polymer is to be deposited on a surface, the latex containing the polymer can serve as a vehicle of direct application, for example as latex paint. The latex properties are affected by the size distribution of the particles in suspension. Therefore in order to properly control the properties of the latex product, the process must be designed to give the desired distribution of polymer particle sizes. The major disadvantage occurs when a solid polymer product is desired; the polymer must be separated from the latex.

The majority of previous research deals with emulsion polymerization carried out in batch reactors. Although continuous polymerizers have been used industrially, there is little information available relating particle size distribution in continuous polymerization to process design variables.

The purpose of this project was to develop a model which would relate the particle size distribution to the process design variables in a continuous emulsion polymerization system. This size distribution model was developed from one of three growth rate models which were incorporated into a particle population balance to determine the particle size distribution of the product. In order to verify the validity of the model, data of the population density of a polystyrene system were obtained and compared with a computer solution of the model.

EXISTING THEORY AND LITERATURE REVIEW

Micelles and Solubilization

The presence of soap or detergent in sufficient quantities to form micelles distinguishes emulsion polymerization from all other techniques of polymerization. The properties of soap and detergent which affect emulsion polymerization are emulsification, solubilization, reduction of surface tension, and protection of polymer particles from flocculation. By lowering the surface tension of the dispersion medium, the soap molecules are able to surround and stabilize small monomer particles to form an emulsion. Above a specific soap concentration, soap molecules come together to form small "pockets" of high soap concentration, called micelles. The concentration at which micelles begin to form is called the critical micelle concentration and depends on the temperature and substances forming the solution.

The structure of micelles, which consist of 50-100 soap molecules, is not exactly known. McBain (21) proposed a laminar structure, and Hartley (18) proposed a spherical one. However, neither has been wholly accepted because the structure may be a function of both the substance used and its concentration.

The role of the micelle is twofold. As proposed by Harkins (16, 17) the micelle serves as a locus for particle nucleation and polymerization during early particle growth.

Also the micelle provides soap molecules to stabilize the growing polymer particles in later stages of growth.

The micelle is capable of serving as a polymerization locus because monomer molecules are solubilized by the micelles. Solubilization was defined by McBain (21) as the "spontaneous passage of molecules of a substance insoluble in water into a dilute aqueous solution of a detergent to form a thermodynamically stable solution." Solubilization differs from emulsification because it is accompanied by a decrease in free energy. It is thought that the solubilized monomer molecules arrange themselves between layers of soap molecules within the micelle.

The role of the micelle as explained by Harkins (16, 17), has been widely accepted as a reasonable explanation of nucleation. However, in 1968, Roe (26) challenged this hypothesis. Since emulsion polymerization has been reported in the absence of micelles, Roe concludes that nucleation takes place in the dissolved phase and the growing radical is absorbed by the micelle.

In general, the role of the soap is entirely physical. The micelle acts as a monomer reservoir for initiation and propagation.

Kinetics

By locating properly the locus of polymerization, Harkins (16, 17) made the first major advancement in the understanding

of emulsion polymerization. The major points of the Harkins theory are as follows:

1. Polymer particles are almost entirely initiated within micelles. The number of particles initiated at other loci is negligible.
2. Most polymerization takes place in the polymer particle; very little polymerization takes place within the monomer droplets and extremely little takes place in the water.
3. Polymerization takes place within the particle by a free radical mechanism.
4. Monomer is supplied to the growing particle by diffusion through the water phase from the monomer droplet.
5. The micelles bring the radicals and monomer together in a higher concentration than in the water.

The relationship of the particles, droplets, and micelles is illustrated in Figure 1.

In order to further characterize emulsion polymerization in a batch process, Gardon (9) divides the process into three intervals (see Table 1). Interval one is distinguished by the presence of micelles. During this interval virtually all the particle nucleation takes place. The initiation of polymerization within a micelle corresponds to the nucleation of a polymer particle. Interval two begins at the time that

Figure 1. Relationship of the particles, droplets, and micelles

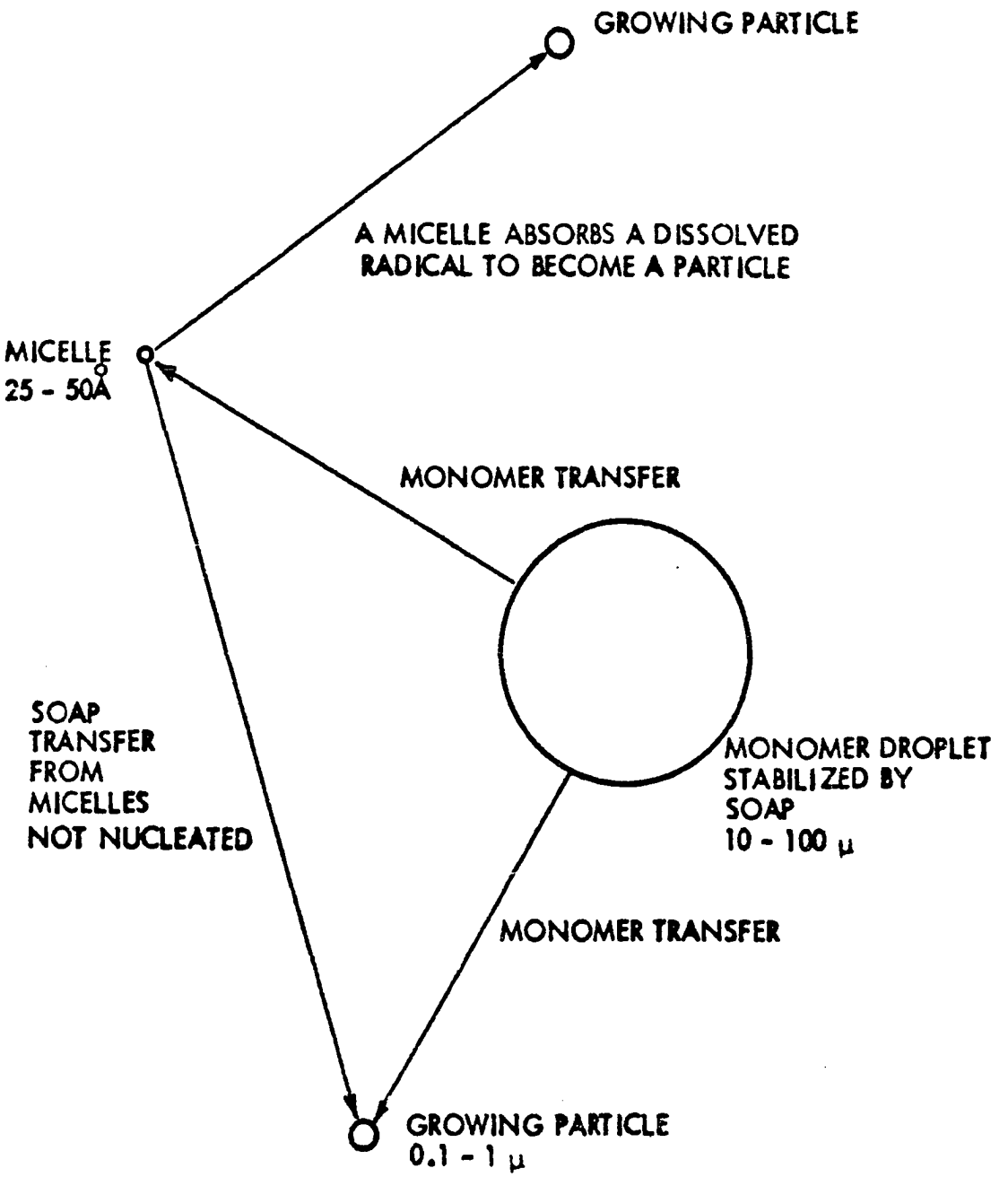
GROWING PARTICLE
A MICELLE ABSORBS A DISSOLVED RADICAL TO BECOME A PARTICLE
MICELLE
25 - 50Å
MONOMER TRANSFER
SOAP TRANSFER FROM MICELLES NOT NUCLEATED
MONOMER DROPLET STABILIZED BY SOAP
10 - 100 μ
MONOMER TRANSFER
GROWING PARTICLE
0.1 - 1 μ

Table 1. Intervals in batch emulsion polymerization[a]

Interval	Processes occurring	Identities present
I	Nucleation Soap molecule transfer Monomer transfer Radical initiation Radical termination Particle growth	Micelles Droplets Particles
II	Monomer transfer Radical initiation Radical termination Particle growth	Droplets Particles
III	Radical initiation Radical termination Particle change (Decreasing monomer volume fraction)	Particles

[a]Source: Gardon (9).

all micelles have become nuclei or the soap molecules of the micelles have migrated to growing polymer particles. During this interval the number of polymer particles remains constant since, according to the Harkins' hypothesis, no new nuclei can be formed in the absence of micelles. After all the monomer in the droplets has diffused to the polymer particles, the latex enters the third interval characterized by the absence of droplets. During this interval propagation is supported entirely by the monomer absorbed by the growing particles during interval two.

Smith and Ewart (30) built on the qualitative theory of Harkins to develop a number of equations describing the quantitative aspects of the process. One of these equations was a recursion relation developed from a radical balance made on the radicals entering and leaving a particle of the average population size at steady state. The balance is made on an emulsion system within interval two such that there is a constant number of growing particles, N, of average volume, $\bar{V}$, and surface area, $\bar{a}$. Since all radicals are formed outside the particles and are assumed to be completely absorbed by the particles, the rate at which the radicals diffuse into a single particle is R/N where R is the rate of production of radicals and N is the number of particles per cc of water. Mutual termination was assumed to be the only form of radical termination. Therefore the rate of termination becomes $(k_t/N_A)\, q\, [\,(q-1)/\bar{V}\,]$ where k_t is the specific rate constant, N_A is Avogadro's number, and q is the number of radicals present in the particle. By assuming no desorption of radicals from the particles, the steady state balance around the total number of particles containing q radicals leads to the recursion formula

$$(q+2)(q+1)\, N_{q+2} + \alpha\, N_{q-1} = N_q\, [\, q(q-1) + \alpha\,] \qquad (1)$$

$$\alpha = (R/N)\, (N_A \bar{V}/k_t) \qquad (2)$$

where

$$N = \Sigma N_q. \tag{3}$$

Smith and Ewart qualitatively solved this relation for the special case of instantaneous termination, and found that the average number of radicals, Q, in a particle was 0.5. This leads to an expression for the rate of propagation, which is proportional to particle growth rate, of the form

$$r_p = k_p (M) (N/2) \tag{4}$$

where M is the concentration of the monomer at the loci of the radical and k_p is the specific rate constant of propagation.

Stockmayer (31) and others (24, 32) have developed general solutions of the Smith-Ewart recursion relation. The Stockmayer solution is

$$a^2 = 8 \alpha \tag{5}$$

$$Q = (a/4) I_o(a)/I_1(a) \tag{6}$$

where α is given in Equation 2, and $I_o(a)$ and $I_1(a)$ are modified Bessel functions of the first kind of zeroth and first order, respectively. This solution provides a size dependent average of the number of radicals in a particle which is free of the assumption of instantaneous termination.

By applying this solution to the assumption that polym-

erization within the polymer particle by free radical addition is the controlling mechanism, Gardon (9) was able to express the particle growth rate as a function of particle size as follows:

$$\frac{dV}{dt} = \left[\frac{k_p}{N_A} \frac{\rho_m}{\rho_p} \phi_m Q \right] / (1 - \phi_m) \qquad (7)$$

where ϕ_m the monomer volume fraction within a polymer particle and ρ_m and ρ_p are the molar densities of the monomer and polymer respectively within the particle. The parameters of this expression are very convenient since they can be determined independent of the emulsion polymerization process. The only exception is the specific rate constant of termination which will be affected by the physical properties of the polymer particle and must be determined from an actual emulsion polymerization process. Gardon (9-14) presents these data for a variety of systems and conditions.

It should be noted that all parameters on the right of Equation 7 are constant except Q. Therefore Equation 7 may be expressed as

$$\frac{dV}{dt} = K Q \qquad (8)$$

where

$$K = \frac{k_p}{N_A} \frac{\rho_m}{\rho_p} \left[\frac{Q_m}{1 - Q_m} \right] \qquad (9)$$

The assumption of constant ϕ_m may require some explanation. Morton et al. (23) explain this lack of variation. They pointed out that the energy of mixing of the polymer and monomer and the total surface energy change due to an increase in particle size have approximately equal magnitudes but opposite signs. The energy of mixing favors monomer entry into the particles; however, the total surface energy change retards monomer entry. Therefore, the two effects tend to balance each other out. This conclusion has been verified by Gardon (14).

In 1954 Medvedev (22) proposed that the locus of propagation is the surface of the polymer particle rather than the interior as Harkins suggested. In experimental studies Brodnyan et al. (6) found the growth rate per unit surface area to be relatively constant which tends to support the Medvedev theory.

By assuming a particle growth rate of the form

$$\frac{dV}{dt} = kr^{\gamma} \tag{10}$$

where γ and k are constants, Brodnyan (5) has shown by statistical analysis that the exponent, γ, could be indicated by the properties of the distribution of the particle sizes from a batch reactor. For example, a normal distribution of the volumes indicates an exponent of zero, a normal distribution of radii indicates an exponent of two, and a normal

distribution of the logarithms of the radii indicates an exponent of three. From Equation 10 it is easily seen that an exponent of zero, two, or three corresponds to a growth rate proportional to a constant as in the Smith-Ewart theory, the surface area, or the particles volume respectively.

Brodnyan (5) points out that while working with styrene Vanderhoff et al. (33) found an exponent of 2.5 for Equation 8 and Ewart and Carr (8), also working with styrene, found that dr/dt was approximately constant which implies an exponent equal to two. This further supports the Medvedev theory.

Continuous Emulsion Polymerization

Although the majority of published work deals with batch systems, there is some work which discusses continuous systems. Wall et al. (34) experimentally demonstrated the general feasibility of continuous emulsion polymerization. Wall concluded that continuous emulsion polymerization could be controlled by the same methods, altering residence time, reactor temperature, catalyst concentration, as batch operations.

Sato and Taniyama (27) developed a kinetic model for emulsion polymerization which predicted the same results as Smith and Ewart. In a later work (28) they applied the model to continuous emulsion polymerization and found that the total number of particles formed is independent of the initiator concentration, proportional to the soap concentration, and

proportional to the -2/3 power of the average residence time. The authors pointed out that the results agreed with the unpublished work of Gershberg and Longfield (15).

Allen et al. (1) compared the polydispersity of a batch polymerizer with that of a cascade of one, two, and three polymerizers. As the authors expected, the theoretical calculations predicted a broader particle size distribution for the continuous systems. The authors investigated the system for two volumetric growth rate models. The first was the Smith-Ewart model, and in the second, growth rate was proportional to the particle diameter raised to the 2.5 power. The latter model approximates the Medvedev model. The polydispersity was greatest for a single continuous polymerizer with the Medvedev approximation applied.

A modified Stockmayer growth rate model was applied to a continuous system by DeGraff and Poehlin (7). The Stockmayer model was modified by use of Flory's diffusion model. DeGraff observed that the number of particles formed in the first tank of a cascade has an important effect on the rate of polymerization, molecular weight, and conversion in following tanks. The number of particles initiated in the first tank as a function of residence time was found to exhibit a maximum.

The methods of classical statistical mechanics and the basic mathematical machinery of the Markov process have been

applied to continuous emulsion polymerization by Katz and Shinnar (20). However, this stochastic approach provides no additional information when the particle populations are as large as they are in emulsion polymerization since the individual flucuations average out.

MATHEMATICAL DEVELOPMENT AND THEORETICAL RESULTS

Population Density and Moments

Since it is more convenient to work with continuous, rather than discrete mathematics, the distribution of discrete polymer particles are represented by a population density function. The population density, n, represents the number of particles within a given size range. A more precise definition is given by the limiting process:

$$\lim_{V \to 0} \frac{\Delta N}{\Delta V} = \frac{dN}{dV} = n. \tag{11}$$

Here N represents the cumulative distribution function and ΔV represents the volume size interval $V_2 - V_1$.

The reverse mathematical operation is used to return to a particle distribution in terms of pure numbers.

$$\int_{V_1}^{V_2} ndV = \begin{array}{l}\text{Total number of} \\ \text{particles between} \\ \text{sizes } V_1 \text{ and } V_2\end{array}. \tag{12}$$

It is convenient to define a second population density, m, which is a function of radius rather than volume. The procedure is exactly the same as before. Thus,

$$\lim_{\Delta r \to 0} \frac{\Delta N}{\Delta r} = \frac{dN}{dr} = m \tag{13}$$

$$\int_{r_1}^{r_2} mdr = \begin{array}{l}\text{Total number of} \\ \text{particles between} \\ \text{radius } r_1 \text{ and } r_2\end{array}. \tag{14}$$

It is possible to obtain from the population density other distributions which relate to the polymer particles. Equation 11 is the zeroth moment of the population density, m. When the lower limit of integration is zero, the zeroth moment generates the cumulative distribution function. As the upper limit goes to infinity, this distribution gives the total number of particles present.

The cumulative radius is obtained from the first moment,

$$R_T = \int_c^r rmdr \tag{15}$$

and represents the total radius (if all the particles are lined up) of the particles of radius r and below.

The second moment may be used to obtain the cumulative surface area. The shape factor 4π is introduced to account for the spherical nature of the particles.

$$A_T = 4\pi \int_o^r r^2 \, mdr. \tag{16}$$

The cumulative volume is related to the third moment by the shape factor $4\pi/3$.

$$V_T = \frac{4\pi}{3} \int_o^r r^3 \, mdr. \tag{17}$$

These distributions are useful in calculating such system parameters as numbers, interfacial area, total volume, and total mass.

Numbers Balance

This work is directed to a continuous, stirred, tank or backmix polymerizer. In such a polymerizer, shown in Figure 2, the product stream has the same characterization as the latex in the polymerizer. To provide the background for such a polymerizer, the latex is defined as an arbitrary polymer particle suspension through the following assumptions.

1. The latex occupies a variable volume enclosed by fixed boundaries except for a free gravity surface.
2. The volume has input and output streams which are completely mixed as they pass through the boundaries of the volume.
3. The particle sizes are considered to be distributed continuously over a given size range and an element of latex volume.
4. No splitting or coalescence of particles occurs.

To apply the population density to a numbers balance, the zeroth moment of the volumetric population density is used. The balance is

Total number of particles accumulated per latex volume	=	Total number of particles in the input stream per latex volume	-	Total number of particles in the output stream per latex volume

Applying the zeroth moment, the balance becomes

$$\frac{d}{dt} \int_V \int_{V_1}^{V_2} \bar{n} a v a v = \int_{V_1}^{V_2} [\bar{Q}_i \bar{n}_i - \bar{Q}_o \bar{n}_o] \, d\bar{v} \qquad (18)$$

Figure 2. Continuous polymerizer

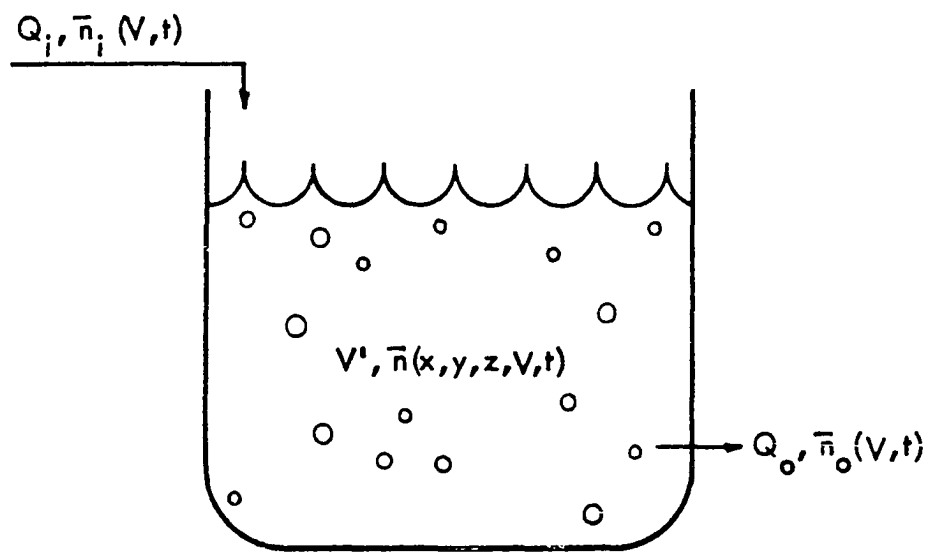
$Q_i, \bar{n}_i\,(V,t)$
$V', \bar{n}(x,y,z,V,t)$
$Q_o, \bar{n}_o(V,t)$

where V' is a unit of latex volume, Q_i, Q_o are volumetric flow rates and $\bar{n}$ is the local population density, $\bar{n} = \bar{n}$ (x, y, z, V, t).

Using Leibnitz's rule on the left hand side of Equation 18, the balance simplifies to

$$\int_{V'} \left[\frac{\partial \bar{n}}{\partial t} + \frac{\partial}{\partial V} \left(\bar{n} \frac{\partial V}{\partial t} \right) \right] dV' + \frac{dV'}{dt} \bar{n}_s - \left[Q_i \bar{n}_i - Q_o \bar{n}_o \right] = 0 \qquad (19)$$

This represents a general population balance subject to the original assumptions. The integral term represents changes in the number of particles within the size range V_1 to V_2 within the latex volume, V', due to non-steady state behavior and growth into or out of the size range. The second term represents changes due to a volume change, and the third and fourth terms represent changes due to the input and output streams.

In order to obtain a more useful form the following assumptions are made:

1. The mixing and product removal is completely ideal. That is, $\bar{n} = \bar{n}_s = \bar{n}_o = n(V,t)$
2. The volume of the latex, V', is constant.
3. There is no induction period in the life of a micelle such that the micelle temporarily cannot become a growing particle.

4. The residence time, τ, is constant and equal to V'/Q_o.

5. There are no particles in the input stream.

The balance further reduces to

$$\frac{\partial n}{\partial t} + \frac{\partial}{\partial V}\left(n \frac{\partial V}{\partial t}\right) + \frac{n}{\tau} = 0 \qquad (20)$$

or for the steady state case,

$$\frac{d}{dV}\left(nR_V\right) + \frac{n}{\tau} = 0. \qquad (21)$$

Here R_V represents the volumetric particle growth rate.

The same balance technique can be applied to the population density as a function of particle radius. The simplified transient balance becomes

$$\frac{\partial m}{\partial t} + \frac{\partial}{\partial r}\left(m \frac{\partial r}{\partial t}\right) + \frac{m}{\tau} = 0. \qquad (22)$$

The steady state balance reduces to

$$\frac{d}{dr}\left(R_r m\right) + \frac{m}{\tau} = 0. \qquad (23)$$

Here R_r represents the radial particle growth rate.

From Equations 21 and 23, the steady state population density can be determined analytically if the size rate of change of the particle growth rate (dR_V/dV or dR_r/dr) is known. The steady state solution for Equation 21 can be obtained by expanding the first term and multiplying the

equation by

$$\frac{1}{R_v} \exp \int_{V^o}^{V} \left(\frac{1}{R_v} \frac{dR_v}{dV} + \frac{1}{\tau R_v} \right) dV.$$

The balance becomes

$$n \left[\frac{1}{R_v} \frac{dR_v}{dV} + \frac{1}{\tau R_v} \right] e^{\int \left(\frac{1}{R_v} \frac{dR_v}{dV} + \frac{1}{\tau R_v} \right) dV} + \frac{dn}{dV} e^{\int \left(\frac{1}{R_v} \frac{dR_v}{dV} + \frac{1}{\tau R_v} \right) dV} = 0 \qquad (24)$$

and by combining terms, it becomes

$$\frac{d}{dV} \left\{ n \exp \left[\int_{V_o}^{V} \left(\frac{1}{R_v} \frac{dR_v}{dV} + \frac{1}{\tau R_v} \right) dV \right] \right\} = 0 \qquad (25)$$

which can be solved to give

$$n = n^o \exp \left[- \int_{V_o}^{V} \left(\frac{1}{R_v} \frac{dR_v}{dV} + \frac{1}{\tau R_v} \right) dV \right] \qquad (26)$$

This is the general analytic steady state solution for Equation 21. For Equation 23 by an analogous process the general steady state solution becomes

$$m = m^o \exp \left[- \int_{r_o}^{r} \left(\frac{1}{R_r} \frac{dR_r}{dr} + \frac{1}{\tau R_r} \right) dr \right] \qquad (27)$$

where m^o and n^o are the population density at the nuclei radius and volume respectively.

Growth Rate Models

From the review of emulsion polymerization literature, three volume growth rate models have been obtained. All three assume that the diffusion of the monomer from the droplet to the growing particle is adequate to support the polymerization rate. The first two can be traced back to Harkins' qualitative theory of emulsion polymerization. The Smith-Ewart model indicates that the volume growth rate will be constant. The Stockmayer solution of the Smith-Ewart recursion relation leads to a model in which the growth rate is a function of volume. However, to be applied to continuous emulsion polymerization, the Stockmayer model must be modified. The third model, Medvedev, does not rely on the assumption of Harkins' theory. It takes the form of a power law relationship indicating dependency on surface area.

To modify the Stockmayer model, it is convenient to determine a recursion equation for n_q, the population density of particles containing q radicals. By definition the particle population density is the sum of all its parts.

$$n = \Sigma n_q . \tag{28}$$

The following development is parallel with that of Smith and Ewart (30) in a batch system. Consider the total number

of particles in the latex having an arbitrary size range V_1 to V_2 and containing exactly q radicals. Inputs into this group of particles take place by either the entry of a radical into any of the particles within the arbitrary size range V_1 to V_2 containing exactly (q - 1) radicals or the mutual termination of two growing radicals in any particle within the size range V_1 to V_2 containing exactly (q + 2) radicals. Outputs take place by either the entry of a radical into a particle between the sizes V_1 to V_2 which contains exactly q radicals, or the mutual termination of two radicals in any particle between the sizes V_1 to V_2 containing q radicals. The assumption of no radical desorption is also made.

The entry of a radical into a particle within the size range V_1 to V_2 depends on the relative surface area of the particle as compared to the total surface area available for absorption. Therefore, if we assume that all produced radicals are absorbed through the oil-water interface which has total surface area of S, the rate of absorption of radicals by particles in the volume range V_1 to V_2 and containing q radicals would be

$$\frac{R}{S}\int_{V_1}^{V_2}(\text{AREA})_q\,dV = \frac{R}{S}\int_{V_1}^{V_2}4\pi r^2 n_q dV = \frac{R}{S}\int_{V_1}^{V_2}4.84V^{2/3}n_q dV. \tag{29}$$

The rate of termination of radicals within the particles of this arbitrary size range containing q radicals would be

$$\int_{V_1}^{V_2} n_q \left[\frac{k_t}{VN_A} \; q(q-1) \right] dV .$$

Therefore, a dynamic balance may be written as follows:

$$\frac{d}{dt} \int_{V_1}^{V_2} n_q dV = \frac{R}{S} \int_{V_1}^{V_2} \left[(AREA)_{q-1} - (AREA)_q \right] dV$$

$$+ \int_{V_1}^{V_2} \frac{k_t}{VN_A} \left[n_{q+2} (q+2)(q+1) - n_q(q-1)q \right] dV \qquad (30)$$

or in another form

$$\int_{V_1}^{V_2} \left[\frac{dn_q}{dt} - \frac{R}{S} \; (4.84) \; V^{2/3} (n_{q-1} - n_q) \right.$$

$$\left. - \frac{k_t}{VN_A} \left(n_{q+2}(q+2)(q+1) - n_q(q-1)q \right) \right] dV = 0 \qquad (31)$$

Since the integral is identically zero for any arbitrary size range, the integrand is also equal to zero, and at steady state the balance leads to the recursion relationship

$$(q+2)(q+1) \; n_{q+2} + \beta n_{q-1} = n_q \left[q(q-1) + \beta \right] \qquad (32)$$

$$\beta = \left[\frac{R}{S} \; (4.84) \; \frac{N_A}{k_t} \right] V^{5/3} \qquad (33)$$

This recursion formula is of the same form as that solved by Stockmayer (31) and O'Toole (24) in terms of Bessel functions. The modified Stockmayer solution is given by

$$b^2 = 8\alpha \tag{34}$$

$$Q = (b/4)\, I_0(b)/I_1(b) \tag{35}$$

where Q is the average number of nuclei in a particle of size V, and $I_0(b)$ and $I_1(b)$ are Bessel functions of the first kind.

From each of the volumetric particle growth rates, R_V, the radial particle growth rate, R_r, can be obtained through the following differential operation:

$$R_V = \frac{dV}{dt} = 4\pi r^2 \frac{dr}{dt} = 4\pi r^2 R_r \tag{36}$$

Table 2 lists R_V and R_r for the three growth rate models discussed.

Analytical Solutions

Equations 26 and 27 represent the general analytical solutions for the population densities m and n, respectively. From these equations, the steady state population density can be determined analytically if the size rate of change of the particle growth rate (dR_V/dV or dR_r/dr) is known. Table 3 shows the analytic solutions for each of the three

Table 2. Kinetic growth rate models

Model	Volumetric	Radial
Smith-Ewart	$R_v = 0.5K$	$R_r = K/8\pi r^2$
	$\frac{dR_v}{dV} = 0$	$\frac{dR_r}{dr} = -K/4\pi r^3$
Medvedev	$R_v = k_M V^{2/3}$	$R_r = k_M/(36\pi)^{1/3}$
	$\frac{dR_v}{dV} = 2k_M/3V^{1/3}$	$\frac{dR_r}{dr} = 0$
Modified Stockmayer	$R_v = K\,Q$	$R_r = KQ/4\pi r^2$
	$\frac{dR_v}{dV} = K\frac{dQ}{dV}$	$\frac{dR_r}{dr} = \frac{K}{4\pi}\left[\frac{-2Q}{r3} + \frac{1}{r^2}\frac{dQ}{dV}\right]$
	where $\frac{dQ}{dV} = \frac{K'}{4V^{1/6}} \frac{bI_1^2(b) + 2I_1(b)I_o(b) - bI_o^2(b)}{I_1^2(b)}$	
	$K' = 11.41\,[\,RN_A/S\,k_t\,]^{0.5}$	

Table 3. Analytic solutions for population density

Model	Volumetric	Radial
Smith-Ewart	$n = n^o \exp\ [-(V-V^o)/\tau R_v]$	$m = m^o \exp\ [\ln(r^o/r)^2 - \frac{8\pi}{3K\tau}(r^3-r^{o3})\ ]$
Medvedev	$n = n^o \exp\ [\ln(V^o/V)^{2/3} - 3(V^{1/3}-V^{o1/3})/\tau k_M]$	$m = m^o \exp\ [(r^o-r)/R_r\tau]$
Modified Stock-mayer	$n = n^o \exp\ [\ln(R_v^o/R_v) - \int_{V^o}^{V} dV/R_v\tau]$	$m = m^o \exp\ [\ln(R_r^o/R_r) - \int_{r_o}^{r} dr/R_r\tau]$

kinetic models as a function of both particle radius and volume.

It should be noted that the volumetric population density for the Smith-Ewart model and the radial population density for the Medvedev model are straight lines on a semilog plot. If the nuclei radius and volume are assumed to be approximately zero, then density can be obtained from the slope and intercept of data which would fit either of these solutions.

Nucleation Rate

At steady state the nucleation, or particle initiation, rate is easily determined for this system. Since all the particles are produced in the polymerizer, the rate of nucleation equals the rate of particle removal. Therefore,

$$\text{nucleation rate} = \frac{dN^{o}}{dt} = \frac{\int_{o}^{\infty} n dV}{\tau} \tag{37}$$

which is equal to $n^{o}R_{v}^{o}$ for the Smith-Ewart kinetic model and $m^{o}R_{r}^{o}$ for the Medvedev model.

Another approach employs the basic assumption for the Smith-Ewart and the Stockmayer theories that all the radicals produced by the initiator are absorbed through the surface area of the soap. It is also assumed that this surface area is the sum of the surface areas of the polymer particles and micelles. Therefore all radicals not absorbed by particles must be absorbed by micelles to produce nuclei. The rate

of nucleation is then given by the rate of absorption by the micelles, or

$$\frac{dN^o}{dt} = R\left[1 - \frac{4\pi}{S}\int_o^\infty r^2\, m\, dr\right]. \tag{38}$$

This is analogous to an expression derived by Gardon (9) for batch polymerization.

Dimensionless Solutions

To obtain the population density in a general form, it is convenient to introduce dimensionless variables. The following variables serve this purpose.

$$\sigma_v = V/R_v^o\tau,\ \rho_v = R_v/R_v^o,\ \eta_v = n/n^o,\ \theta = t/\tau \tag{39}$$

$$\sigma_r = r/R_r^o\tau,\ \rho_r = R_r/R_r^o,\ \eta_r = m/m^o. \tag{40}$$

The volumetric and radial, transient balance become, respectively,

$$\frac{\partial\eta_v}{\partial\theta} + \rho_v\frac{\partial\eta_v}{\partial\sigma_v} + \eta_v\frac{\partial\rho_v}{\partial\sigma_v} + \eta_v = 0 \tag{41}$$

$$\frac{\partial\eta_r}{\partial\theta} + \rho_r\frac{\partial\eta_r}{\partial\sigma_r} + \eta_r\frac{\partial\rho_r}{\partial\sigma_r} + \eta_r = 0. \tag{42}$$

The respective, general, steady state solutions to Equations 41 and 42 are

$$\eta_v = \exp\left[-\int_{\sigma_v^o}^{\sigma_v} \left(\frac{1}{\rho_v}\frac{d\rho_v}{d\sigma_v} + \frac{1}{\rho_v}\right) d\sigma_v\right] \qquad (43)$$

$$\eta_r = \exp\left[-\int_{\sigma_r^o}^{\sigma_r} \left(\frac{1}{\rho_r}\frac{d\rho_r}{d\sigma_r} + \frac{1}{\rho_r}\right) d\sigma_r\right]. \qquad (44)$$

These solutions simplify when a specific kinetic model is applied. Table 4 illustrates these simplified solutions. These solutions will be referred to by the growth rate model they employ.

The radial and volumetric population densities for the three models are illustrated in Figures 3 and 4, respectively. When investigated both as a function of σ_v and σ_r, the different models exhibit radically different behavior. The Smith-Ewart model predicts a straight line relationship as a function of dimensionless volume, σ_v. The Medvedev model is a straight line as a function of dimensionless radius, σ_r. The modified Stockmayer model does not exhibit a straight line relationship, but approaches the Smith-Ewart model at small sizes as expected.

The calculations to develop Figures 3 and 4 were made with the assumption that the dimensionless nuclei radius, σ_r^o, and volume, σ_v^o, are approximately zero. However, note that particles of "zero" radius have finite growth rates R_v^o and R_r^o. The errors introduced by this assumption are not significant.

Table 4. Dimensionless solutions

Model	Volumetric	Radial
Smith-Ewart	$\eta_v = \exp\ (\sigma_v^o - \sigma_v)$	$\eta_r = \exp\ [-\ln\ \rho_r + (\sigma_r^{o3} - \sigma_r^3)/3\sigma^{o2}]$
Medvedev	$\eta_v = \exp\ [-\ln\ \rho_v - 3\ ((\sigma_v/\rho_v) - \sigma_v^o)\ ]$	$\eta_r = \exp\ (\sigma_r^o - \sigma_r)$
Modified Stockmayer	$\eta_v = \exp\ [-\ln\ \rho_v - \int_{\sigma_v^o}^{\sigma_v} d\sigma_v/\rho_v]$	$\eta_r = \exp\ [-\ln\ \rho_r - \int_{\sigma_r^o}^{\sigma_r} d\sigma_r/\rho_r]$

Figure 3. Dimensionless radial population density

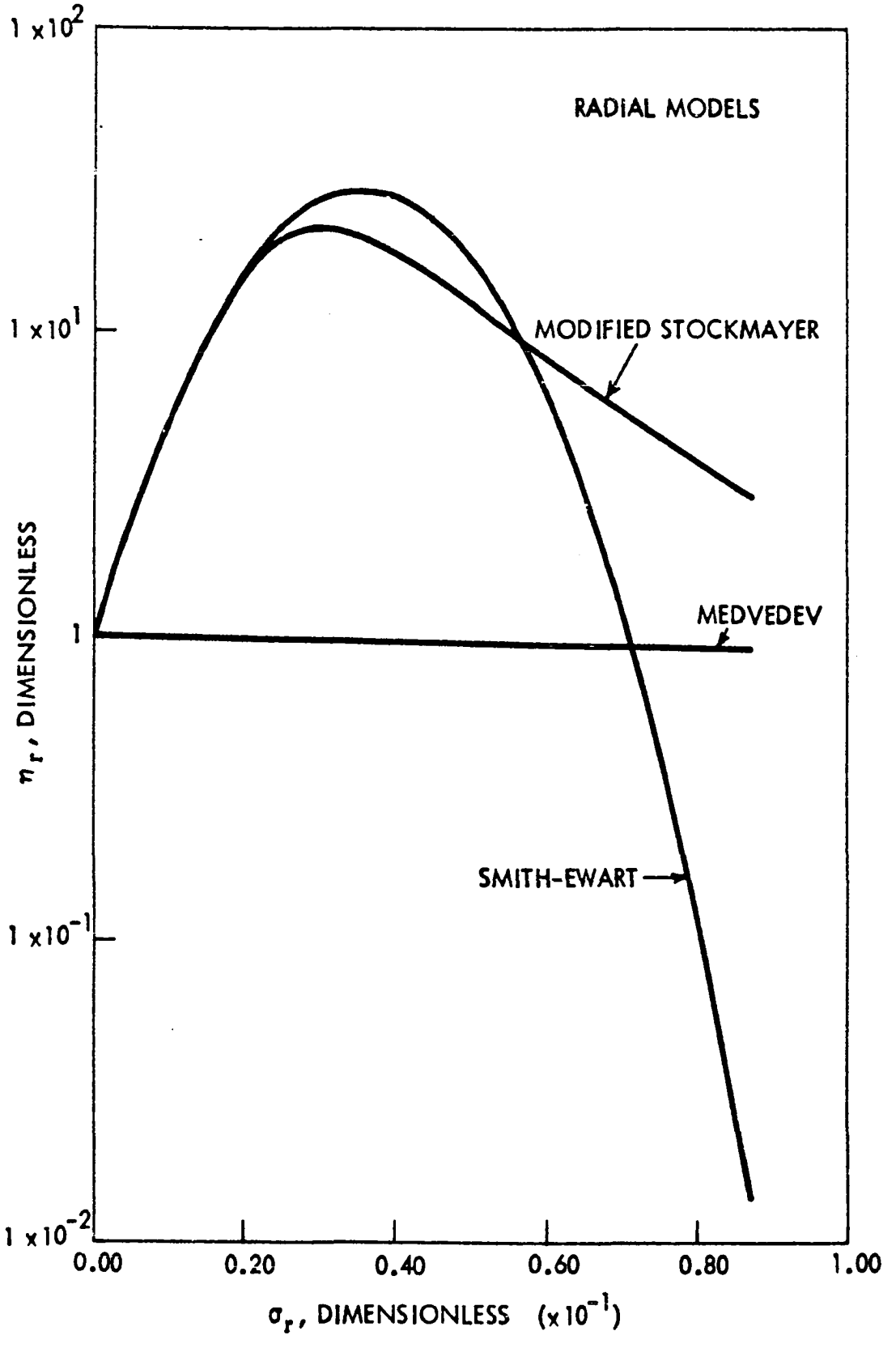
RADIAL MODELS
MODIFIED STOCKMAYER
MEDVEDEV
SMITH-EWART
1 x10^2
1 x10^1
1
1 x10^-1
1 x10^-2
η_r, DIMENSIONLESS
0.00
0.20
0.40
0.60
0.80
1.00
σ_r, DIMENSIONLESS (x10^-1)

Figure 4. Dimensionless volumetric population density

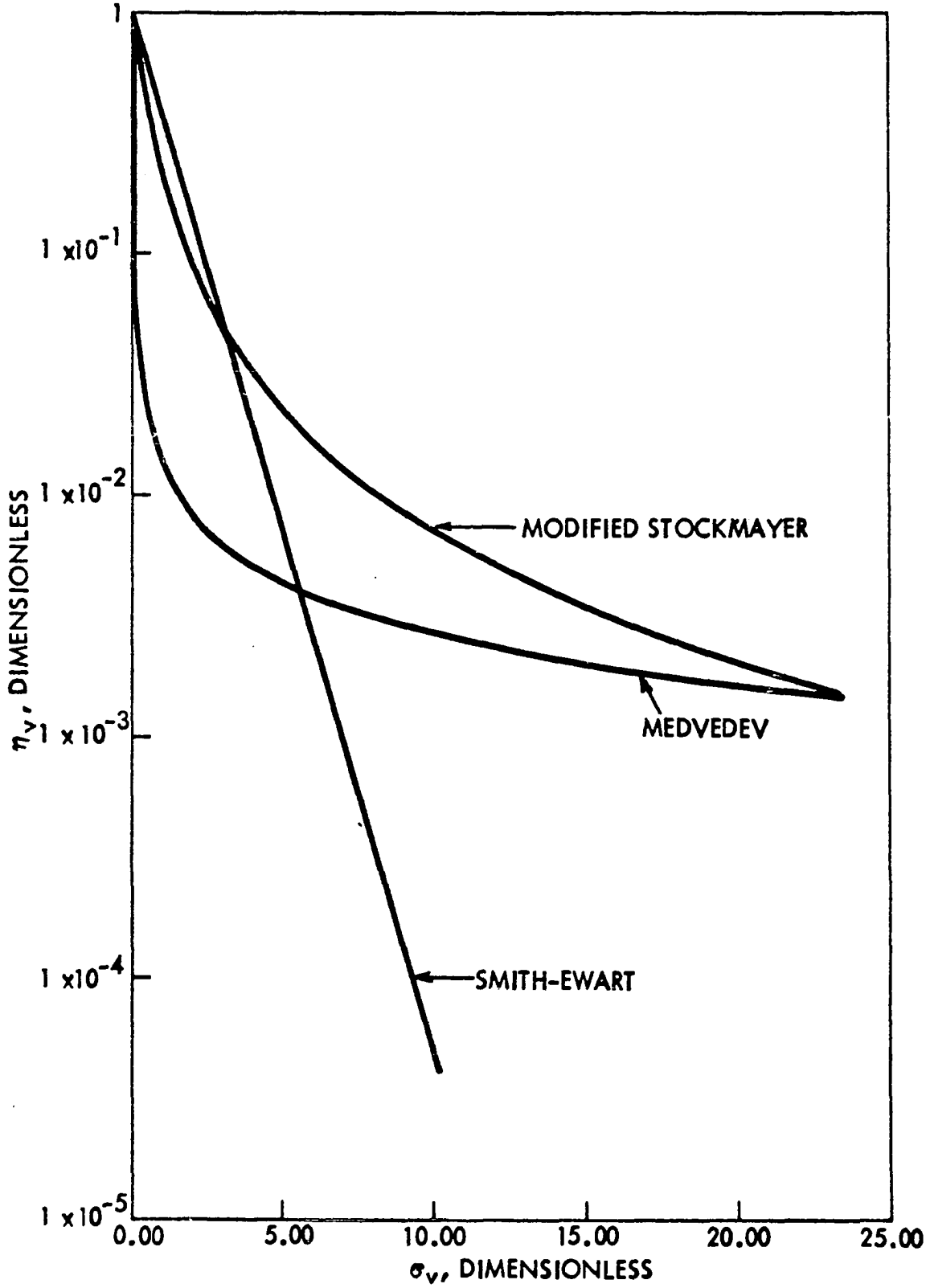
1
1 x10^-1
1 x10^-2
1 x10^-3
1 x10^-4
1 x10^-5
η_v, DIMENSIONLESS
MODIFIED STOCKMAYER
MEDVEDEV
SMITH-EWART
0.00
5.00
10.00
15.00
20.00
25.00
σ_v, DIMENSIONLESS

The similarity of the Smith-Ewart and modified Stockmayer growth rate models at small particle sizes is further illustrated in Figure 5. The two models have the same theoretical development, but the Smith-Ewart model makes the additional assumption of instantaneous termination. This assumption is a good one at small sizes where the two models agree. As the particle size increases, the modified Stockmayer model predicts an increase in the average number of radical, Q, in a particle. When the value of Q increases significantly from 0.5 as shown in Figure 6, the models predict the significant differences in the particle growth rate which affects the population density function.

It is interesting to note that the Medvedev model predicts very large particles. From Figure 7 it can be seen that for the parameter levels used in the calculations, 63 percent of the polymer particles will have a radius larger than 0.5 μ (σ = 0.468) if they obey the Medvedev theory. However, for the Smith-Ewart and modified Stockmayer models, only 10 percent and 30 percent, respectively, of the particles will have a radius larger than 0.06 μ (σ = 0.056). The particle size predictions by the Medvedev theory are much larger than measurement usually observed in practice. Therefore the validity of that model is in doubt.

Although the steady state solutions listed in Table 4 are in a dimensionless form, the curves illustrated in

Figure 5. Dimensionless radial growth rates

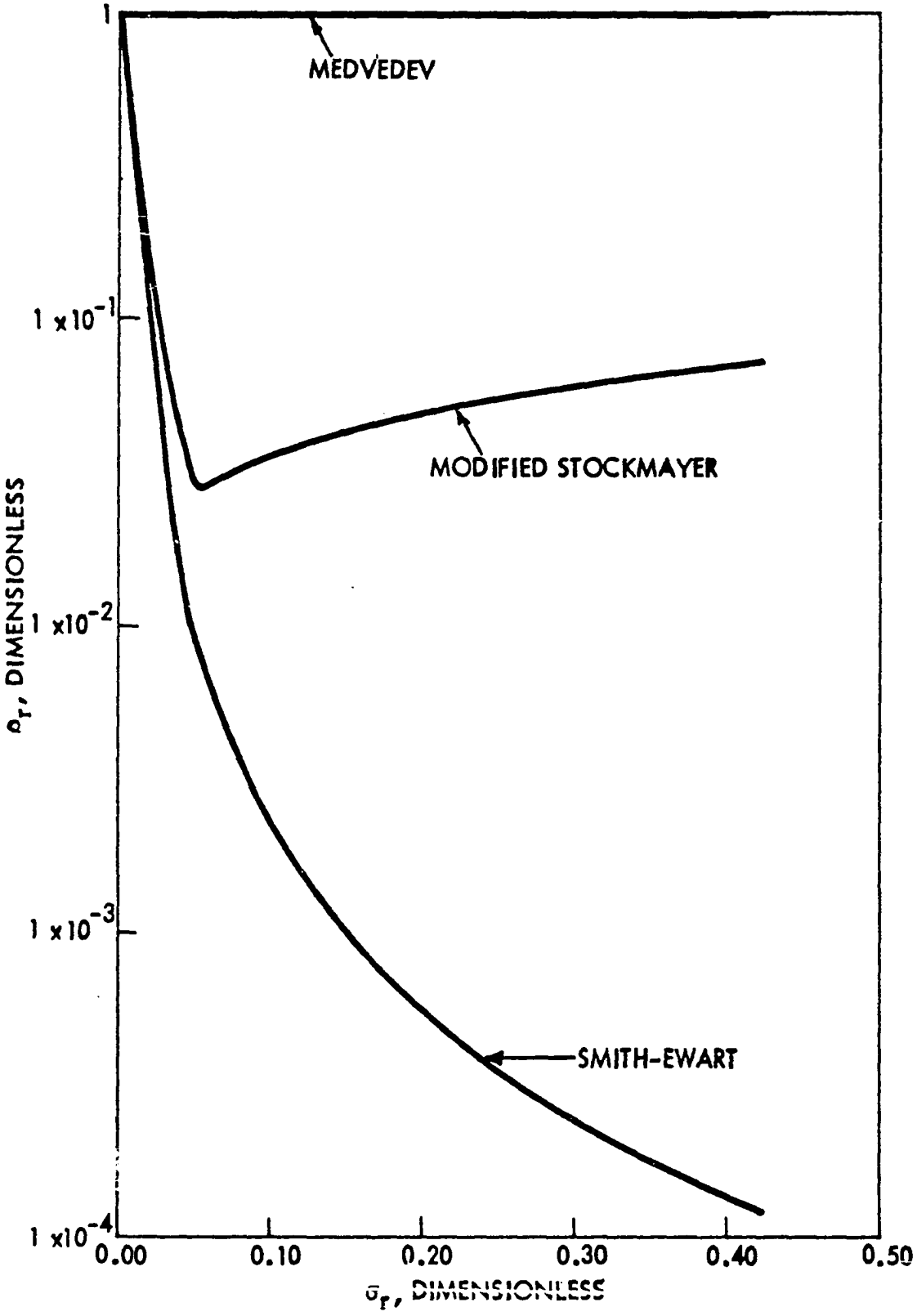
1
1 x10⁻¹
1 x10⁻²
1 x10⁻³
1 x10⁻⁴
MEDVEDEV
MODIFIED STOCKMAYER
SMITH-EWART
0.00
0.10
0.20
0.30
0.40
0.50
σr, DIMENSIONLESS
σr, DIMENSIONLESS

Figure 6. Average number of radicals for a growing particle

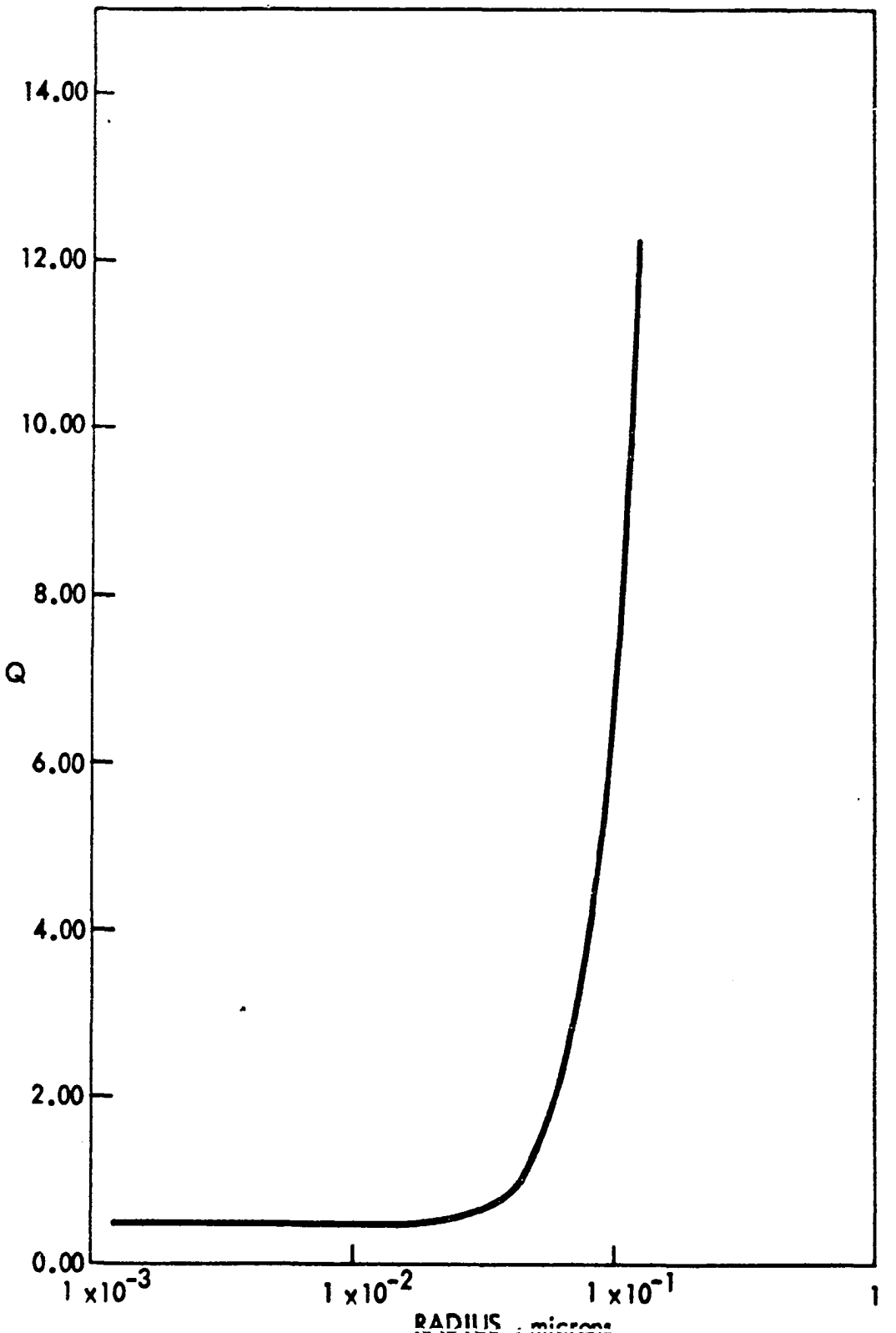
14.00
12.00
10.00
8.00
Q
6.00
4.00
2.00
0.00
1 x10^-3
1 x10^-2
1 x10^-1
1
RADIUS , microns

Figure 7. Dimensionless cumulative distribution function measured by integrating the population density function

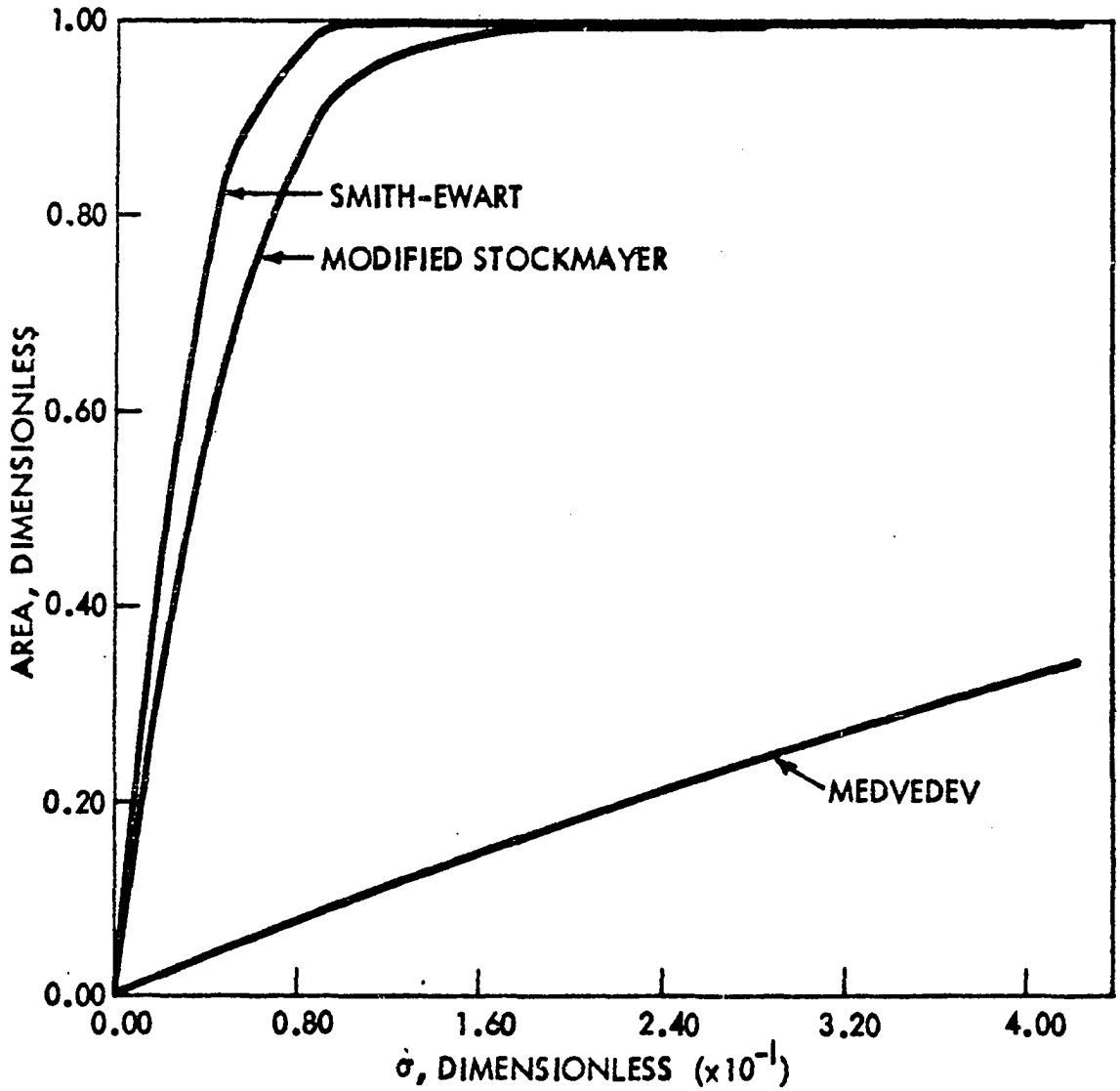
1.00
0.80
0.60
0.40
0.20
0.00
AREA, DIMENSIONLESS
SMITH-EWART
MODIFIED STOCKMAYER
MEDVEDEV
0.00
0.80
1.60
2.40
3.20
4.00
σ̇, DIMENSIONLESS (x10⁻¹)

Figures 3 and 4 are not completely general since their form will change for a change in system parameters. For any case presented in Table 4 in which the particle growth rate is a function of particle size, the density function solution contains two dimensionless variables, dimensionless growth rate and size. To generalize a dimensionless solution from Table 4, it is necessary to relate the dimensionless growth rate and dimensionless size and eliminate one of the dimensionless variables from the solution. The dimensionless growth rate and size are related by a dimensionless group which is a solution of the residence time, nuclei growth rate, and the growth rate model used. Due to the complex nature of this relationship, it is more convenient to present the variation with respect to these dimensionless groups by only the variation of the population density function solution with the product of the residence time and the nuclei growth rate (τR_r^o or τR_V^o). This variation is illustrated in Figures 8, 9, 10, and 11 for the radial Smith-Ewart, radial and volumetric modified Stockmayer, and volumetric Medvedev models respectively. In the case for the growth rate being independent of particle size, the solutions given in Table 4 contain only one dimensionless variable. Therefore the variation with τR_V^o or τR_r^o does not exist.

Figure 8. Change in dimensionless radial Smith-Ewart model due to τR_r^o

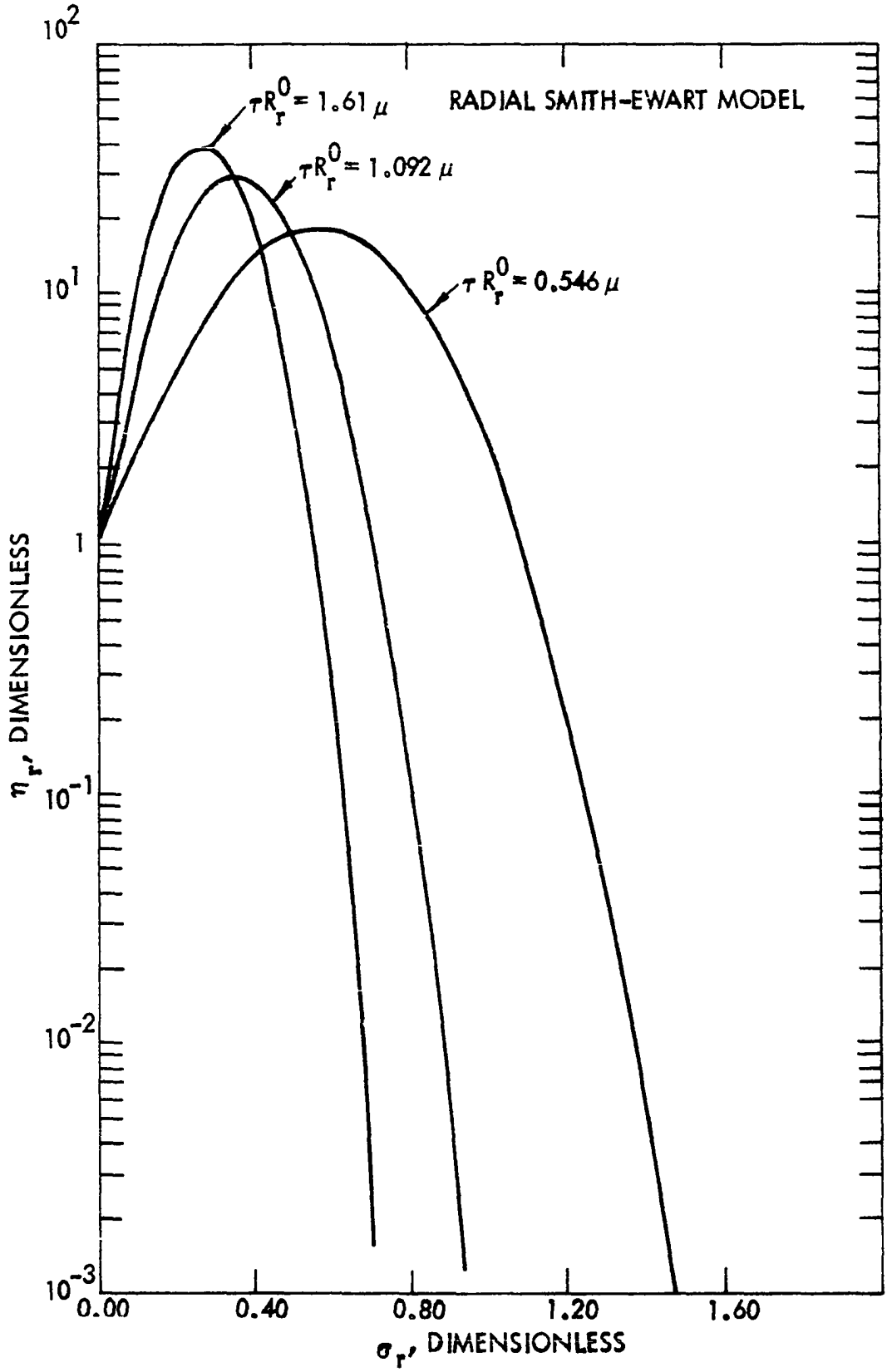
RADIAL SMITH-EWART MODEL
$\tau R_r^0 = 1.61\,\mu$
$\tau R_r^0 = 1.092\,\mu$
$\tau R_r^0 = 0.546\,\mu$
10^2
10^1
1
10^{-1}
10^{-2}
10^{-3}
η_r, DIMENSIONLESS
0.00
0.40
0.80
1.20
1.60
σ_r, DIMENSIONLESS

Figure 9. Change in dimensionless radial modified Stockmayer model due to τR_r^o

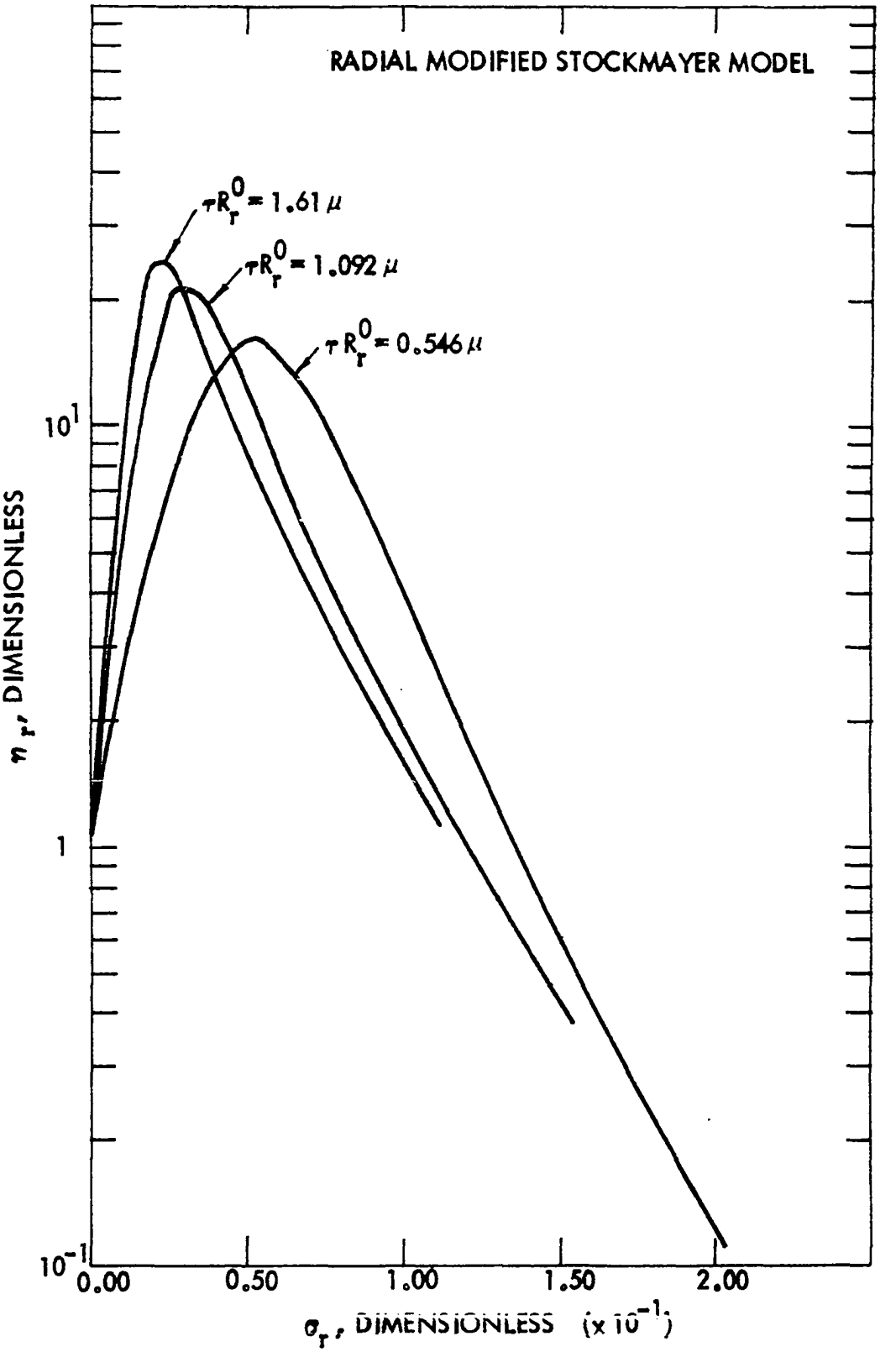
RADIAL MODIFIED STOCKMAYER MODEL
$\tau R_r^0 = 1.61\,\mu$
$\tau R_r^0 = 1.092\,\mu$
$\tau R_r^0 = 0.546\,\mu$
10^1
1
10^{-1}
η_r, DIMENSIONLESS
0.00
0.50
1.00
1.50
2.00
σ_r, DIMENSIONLESS ($\times 10^{-1}$)

Figure 10. Change in dimensionless volumetric modified Stockmayer model due to τR_V^0

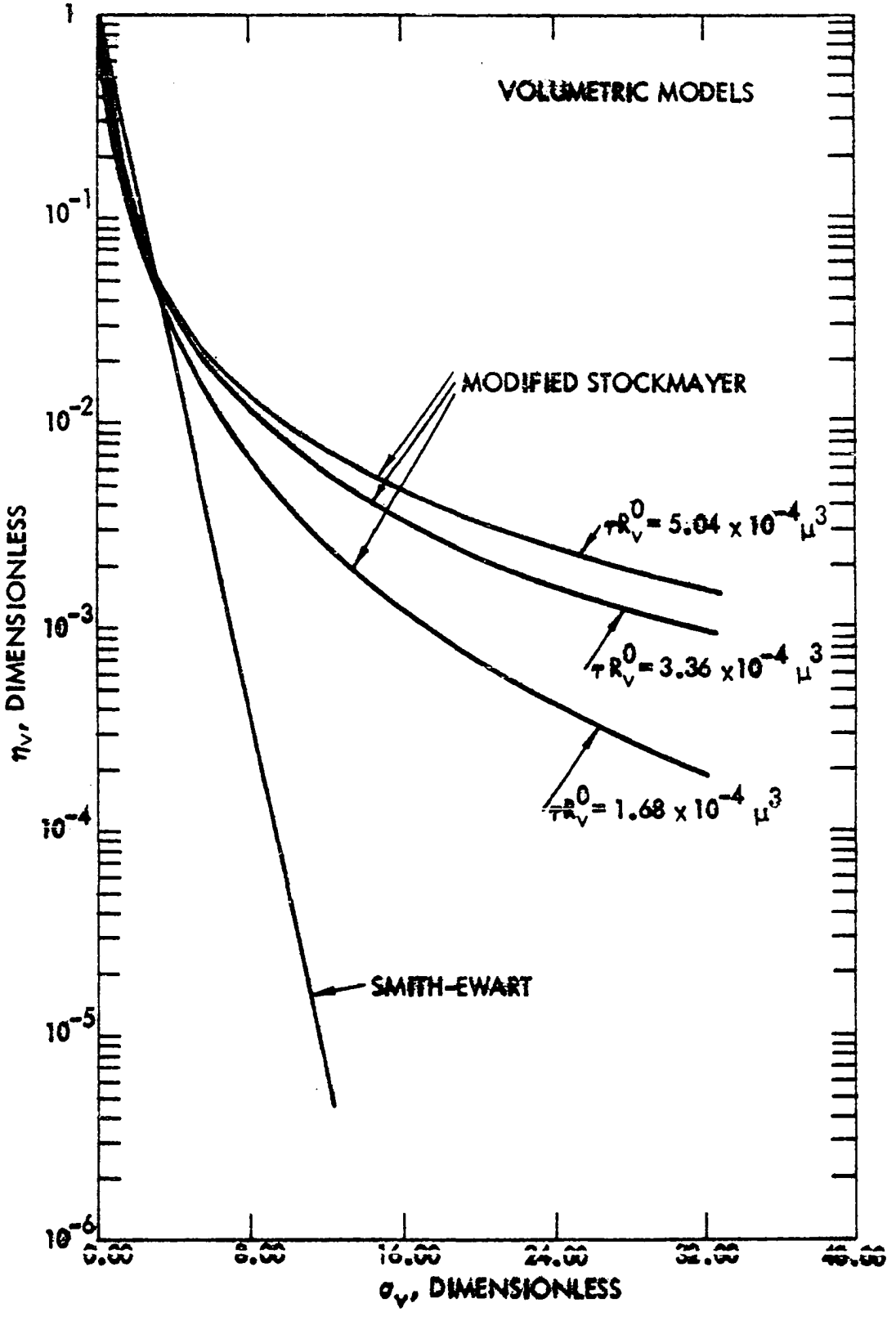
VOLUMETRIC MODELS
MODIFIED STOCKMAYER
$\tau R_v^0 = 5.04 \times 10^{-4}\ \mu^3$
$\tau R_v^0 = 3.36 \times 10^{-4}\ \mu^3$
$\tau R_v^0 = 1.68 \times 10^{-4}\ \mu^3$
SMITH-EWART
η_v, DIMENSIONLESS
σ_v, DIMENSIONLESS
1
10^{-1}
10^{-2}
10^{-3}
10^{-4}
10^{-5}
10^{-6}
0.00
8.00
16.00
24.00
32.00
40.00

Figure 11. Change in dimensionless volumetric Medvedev model due to τR_V^o

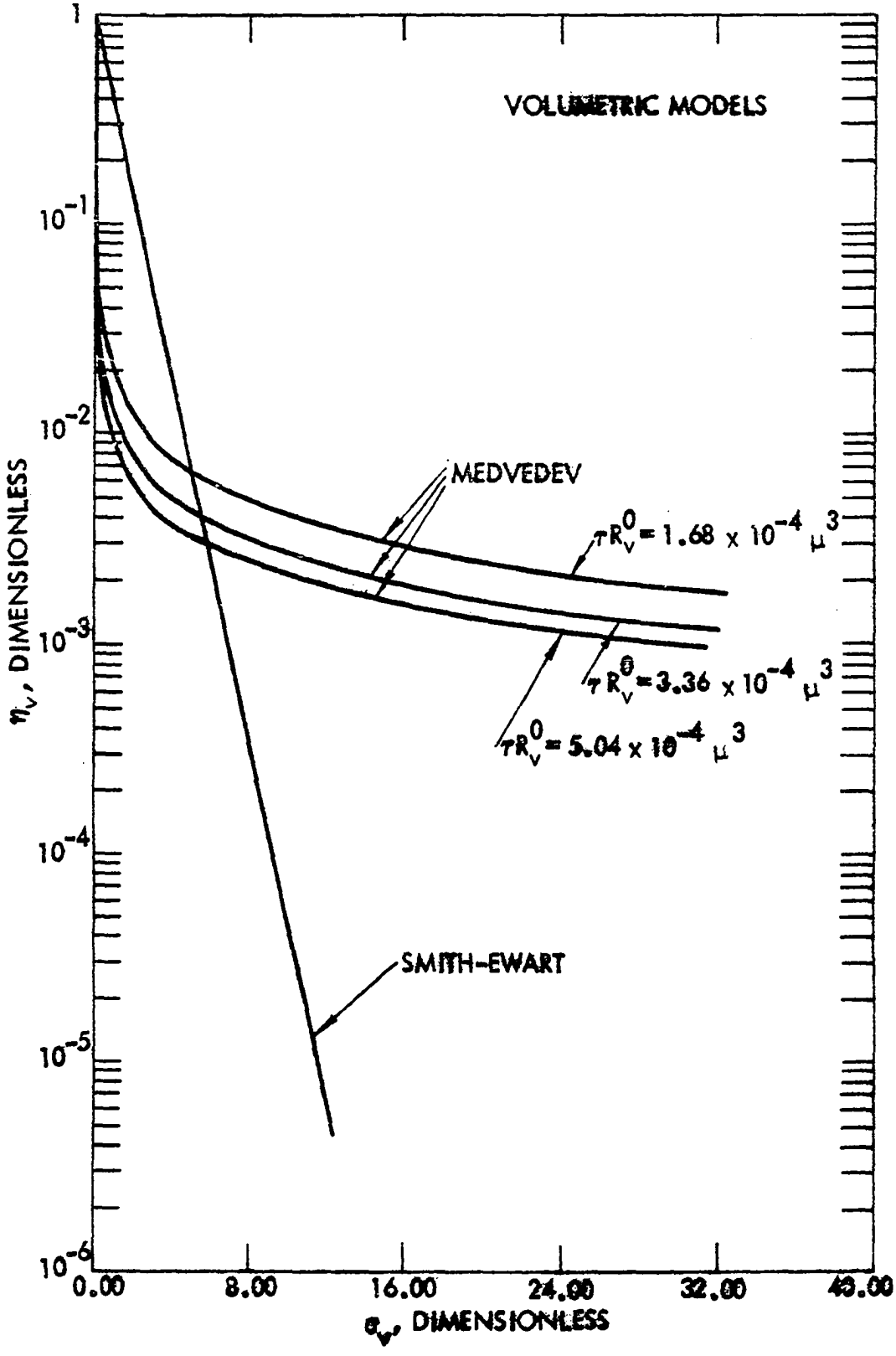
VOLUMETRIC MODELS
MEDVEDEV
$\tau R_v^0 = 1.68 \times 10^{-4}\ \mu^3$
$\tau R_v^0 = 3.36 \times 10^{-4}\ \mu^3$
$\tau R_v^0 = 5.04 \times 10^{-4}\ \mu^3$
SMITH-EWART
η_v, DIMENSIONLESS
e_v, DIMENSIONLESS
1
10^{-1}
10^{-2}
10^{-3}
10^{-4}
10^{-5}
10^{-6}
0.00
8.00
16.00
24.00
32.00
40.00

EXPERIMENTAL INVESTIGATION

The population balance has been used to develop a general representation of the population density function for the particle size distribution leaving a continuous, backmix, emulsion polymerizer. With the application of a particle growth rate model, a density function can be developed to predict the particle size distribution produced under a given set of conditions. The objective of the experimental investigation of this work was to show that the particle size distribution in the latex leaving a single, continuous, backmix polymerizer could be predicted by the representation of the distribution developed from the population balance.

Experimental Procedure

Reactants

The polymerization reaction which was chosen for the experimental study of the models was the production of polystyrene. This reaction was chosen because there is extensive published information available on styrene and the necessary parameters were available in the literature for the application to a styrene system of the Smith-Ewart and Stockmayer solution growth rate models. Gardon (9-14) has published the data in Table 5 for styrene. The following polymerization recipe has been suggested by Bovey et al. (4):

Table 5. Data for styrene at 60° C required for growth rate models

k_t/k_p	141
k_p	0.176×10^6 (cc/mole sec)
N_A	0.6023×10^{24} (#/mole)
R/(conc. of initiator in %) for potassium persulfate	0.245×10^{15} (#/cc H_2O)
S/(conc. of soap in %) for sodium lauryl sulfate	0.125×10^6 (cm^2/cc)
ρ_m	0.9050 (gm/cc)
ρ_p	1.06 (gm/cc)
ϕ_m	0.60

	Parts by weight
Styrene	100
Water	180
Sodium lauryl sulfate	5
Potassium persulfate	0.15

The styrene used was obtained from McKesson Chemical Company and contained tert-butyl catechol in a concentration of 10-15 parts per million. The catechol acts both as an inhibitor and retarding agent when present in styrene (3). In a batch system, Bovey et al. (4) reports that an inhibitor affects an emulsion polymerization by delaying the initiation of polymerization. This delay is called the induction period. The induction period is the time required for the initiator of the polymerization to react completely with the inhibitor. A retarding agent slows the polymerization rate. Bovey suggests that the length of the induction period and the magnitude the polymerization rate is a function of the initial concentration of the inhibitor.

The inhibitor was not removed from the styrene monomer because its effect can be measured by the population density analysis applied to particle size distribution data. The viscosity of the monomer was monitored to warn of any significant increase in polymer concentration in the stored monomer. Any such increase would indicate that the inhibitor level was zero.

Equipment

The polymerization system, illustrated by Figure 12, was basically simple. As shown in the schematic diagram, Figure 13, the feed streams were introduced at the latex surface through positive displacement metering pumps. The output stream used the constant head of the latex and the system pressure for its driving force. Therefore, it was possible to maintain the latex volume at a constant value.

The continuous tank polymerizer, shown in Figure 14, consisted of a section of pyrex pipe, with removable metal flanges, and stainless steel end plates. The interior of the polymerizer was equipped with a heating coil which acted as a draft tube and three baffles which prevented the formation of a vortex. The total volume of the polymerizer with the coil and baffles in place was 2.8 liters.

The flow pattern within the polymerizer was established by circulating the latex down and through the draft tube by a two inch diameter three-blade propeller located at the center of the coil. Due to the stability of the latex and the high residence times studied, the mixing was than sufficient to approach ideal mixing. The latex stability was due to the small sizes of the particles and monomer droplets.

The space between the latex surface and the fixed top of the polymerizer was filled with nitrogen gas and regulated

Figure 12. Continuous polymerization system

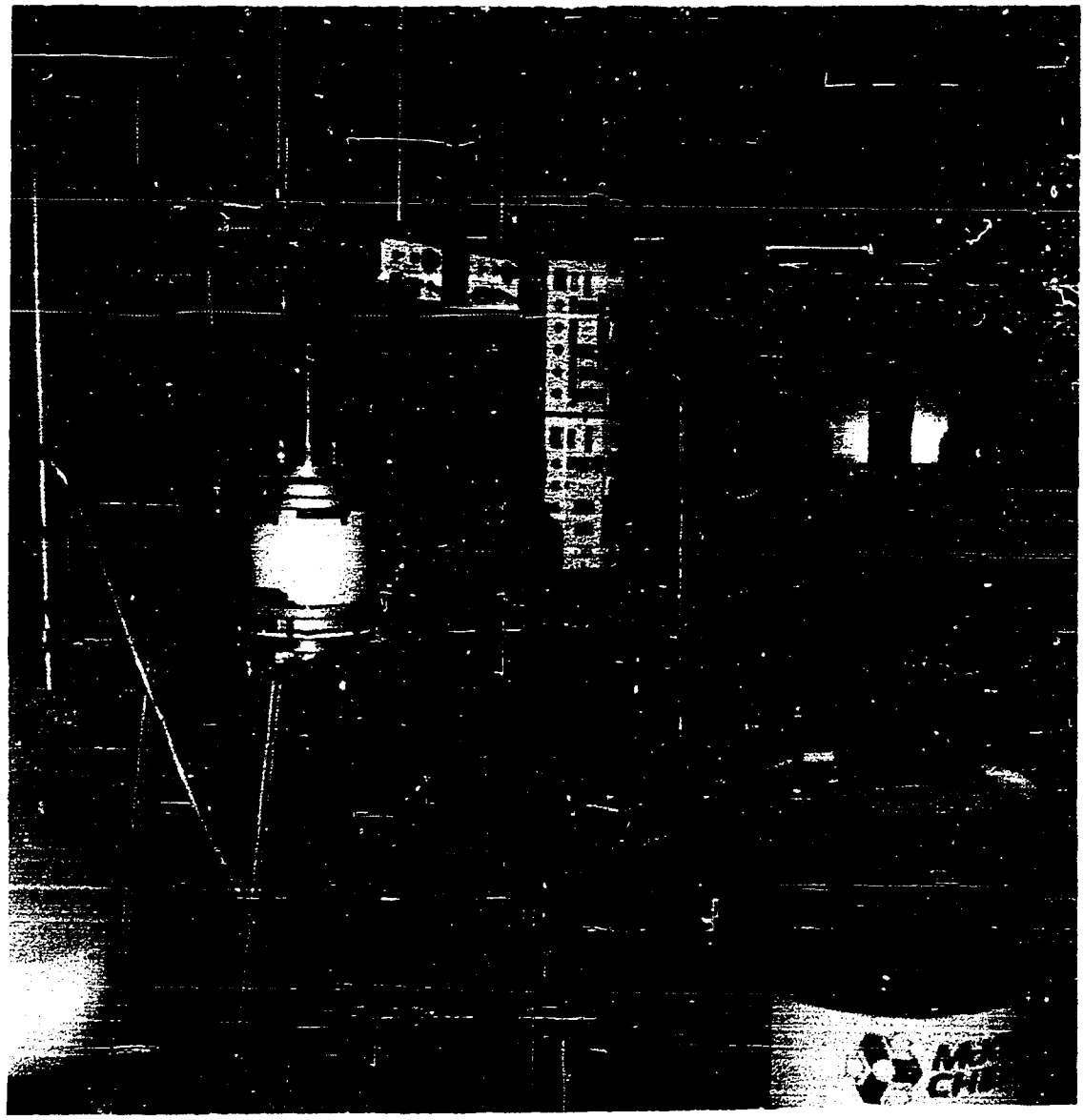

Figure 13. Schematic representation of the continuous polymerization system

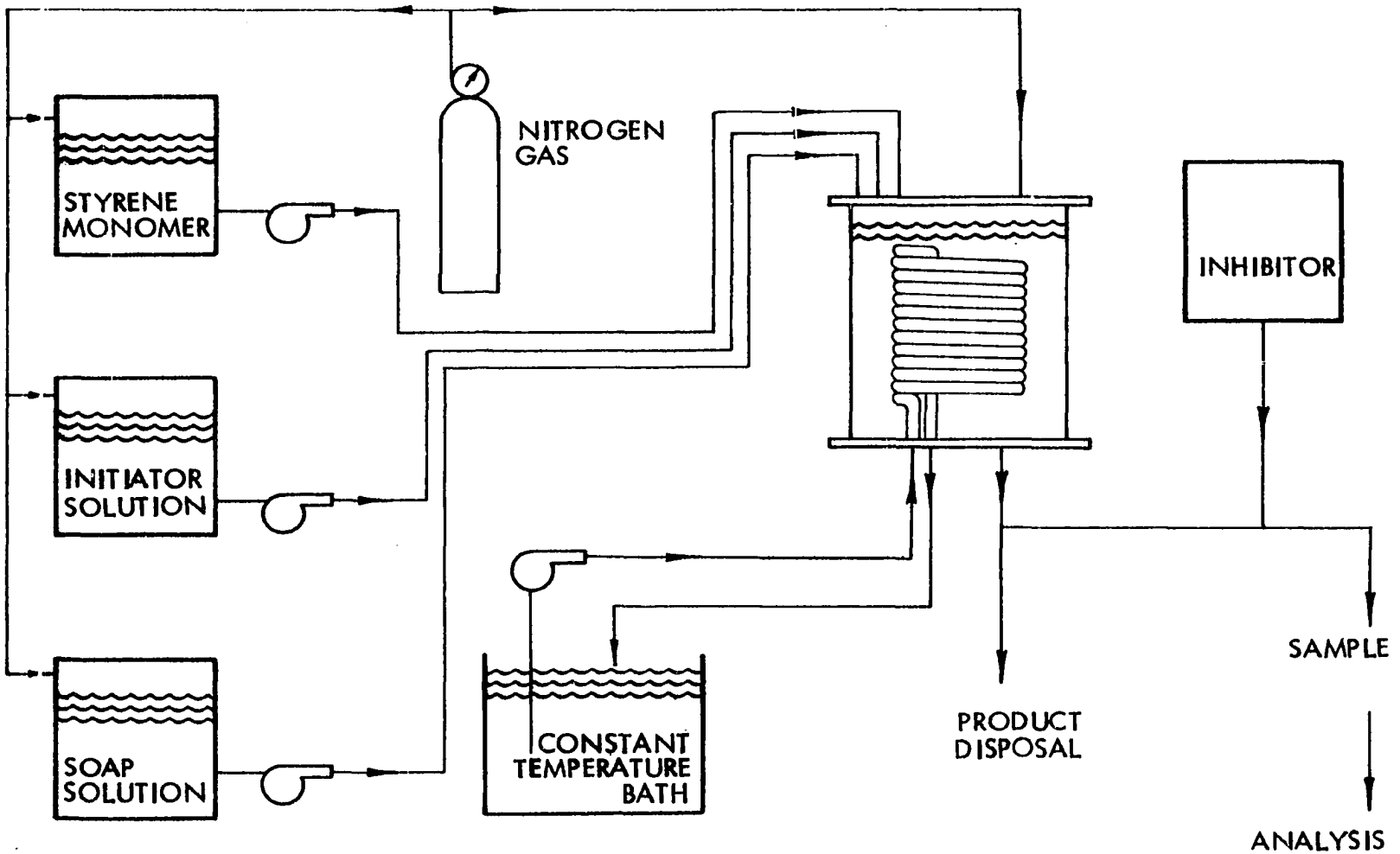
NITROGEN GAS
STYRENE MONOMER
INITIATOR SOLUTION
SOAP SOLUTION
INHIBITOR
CONSTANT TEMPERATURE BATH
PRODUCT DISPOSAL
SAMPLE
ANALYSIS

Figure 14. Top and side views of the polymerizer. Baffles are omitted in the side view. Only the outer diameter of the heat transfer coil is indicated in the top view

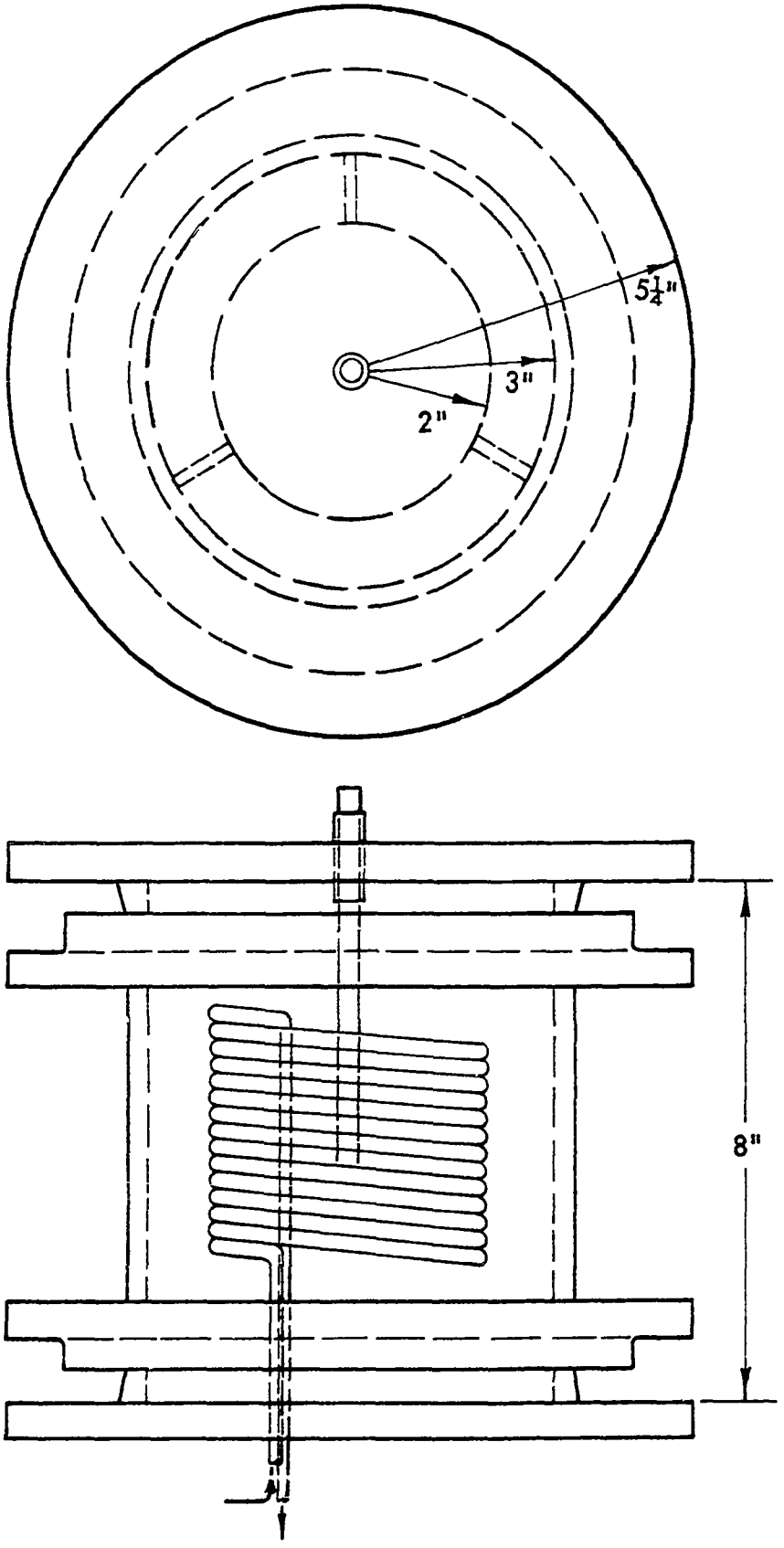
5¼"
3"
2"
8"

at approximately 8 mm Hg gauge pressure. Nitrogen was used to decrease the concentration of oxygen, a retarding agent, in the latex. The elevated pressure was maintained to insure that any gas leaks were outward.

The styrene monomer was fed into the polymerizer directly from its 55 gallon shipping drum through "viton" and stainless steel tubing. As the styrene was removed from the shipping drum, its volume was replaced by nitrogen at the polymerizer pressure. The soap and persulfate solutions were fed from separate "pyrex" jugs through "tygon" and stainless steel tubing. The volumes above these solutions were also filled with nitrogen.

Water from a constant temperature bath was circulated through the heating coils to maintain the temperature in the polymerizer at 60°C. The polymerizer temperature was monitored by a stainless steel covered thermocouple.

Analysis

The latex was sampled at steady state. The determination of steady state conditions is discussed in Appendix B. The particle size distribution of the latex was measured from photographs obtained through electron microscopy. Figure 15 is an example of the photographs used in the distribution determination. The total magnification is 175,000. One should note that Figure 15 is slightly out of focus. This increases the contrast to aid in particle measurement.

Figure 15. Polymer particles. One centimeter equals 0.057 microns

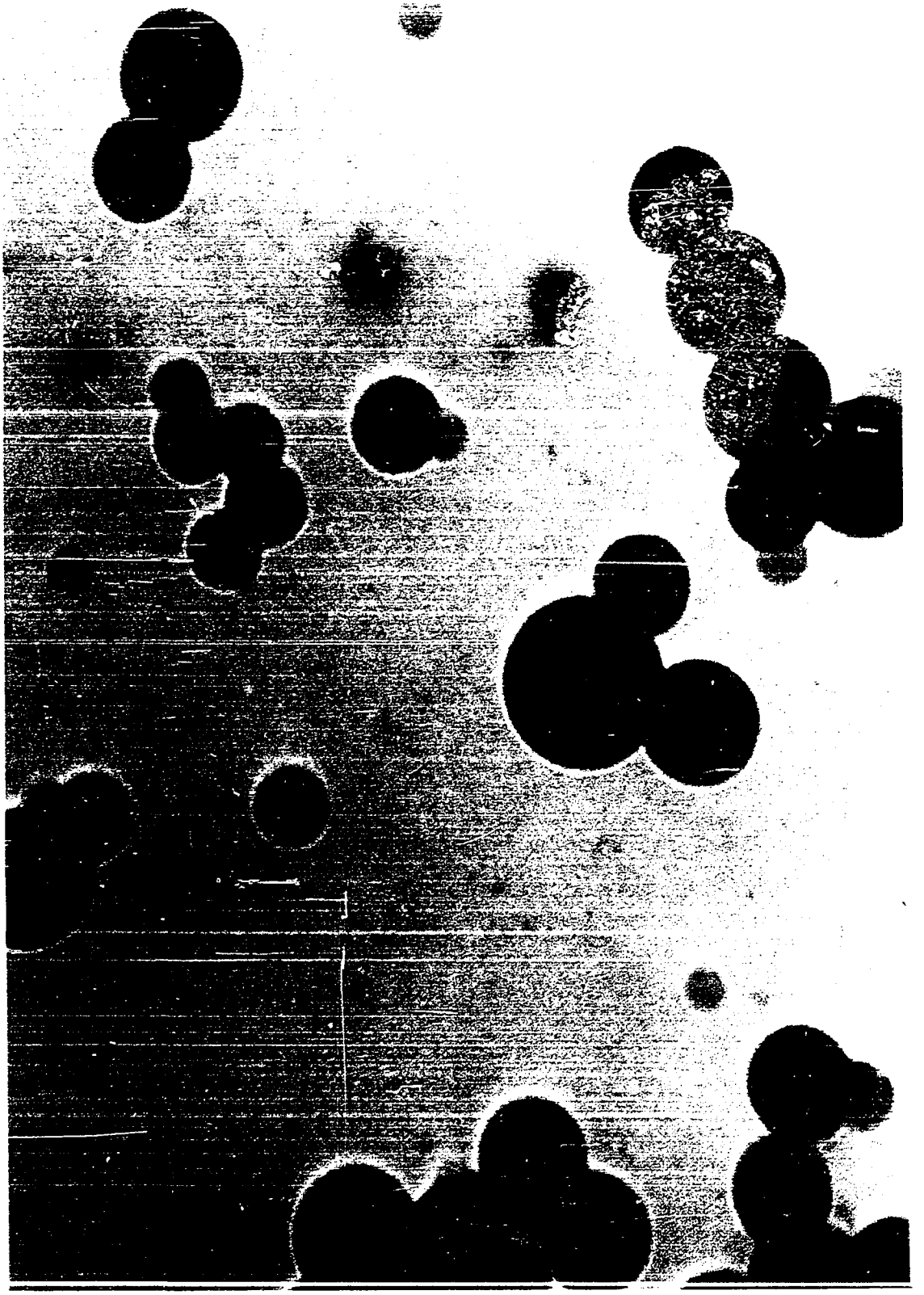

The extremely regular spherical shape of the particles present should be noted. This spherical shape is maintained even though a particle may be part of a conglomeration. The presence of ellipsoid particles would have indicated that two particles had joined together and continued to grow as one particle. Since there are no ellipsoid particles present, the particles are assumed to have grown independently and the conglomeration was formed during sampling.

When a sample was removed from the polymerizer, it was quenched by addition of hydroquinone and a 30°C decrease in temperature. The sample was prepared for the microscope by a 10:1 dilution with distilled water. The diluted latex was then deposited on a carbon grid by nebulization. That is, a drop of the diluted latex was formed into a small cloud which was allowed to settle on the grid.

Since the population density is a decreasing exponential function, the data were plotted using a graded scale which increased each successive size interval. This procedure has been suggested by the American Society for Testing Materials (2) to help equalize the number of particles in the size ranges.

Experimental Results and Discussion

The parameters which are needed to predict the polymer particle size distribution in the latex leaving a continuous polymerizer are the mean residence time for particle growth

and the radial or volumetric nuclei growth rate. If there is no inhibitor in the monomer fed to the polymerizer, the mean residence time which applies to the size distribution prediction is the ratio of the polymerizer volume to the volumetric flow rate of the latex leaving the polymerizer, i.e., there is no induction time. Also if there is no inhibitor present, the theoretical volumetric nuclei growth rate can be calculated from the data given in Table 5. Since the inhibitor, tert-butyl catechol, was left in the styrene monomer and the dissolved oxygen was not removed from the other feed streams, the theoretical values of these parameters could not be used. However, these parameters were estimated from the particle size distribution data by means of a least squares fit of the distribution data to the Smith-Ewart and modified Stockmayer models, as explained in Appendix A.

The mean residence time which is required for particle size distribution prediction is the mean residence time for growing particles. As Bovey et al. (4) states, when the inhibitor and dissolved oxygen are not removed, the mean residence time of the latex includes an induction period. Therefore, the mean residence time for growing particles has been expressed as

$$\tau = \tau_m - T \qquad (45)$$

where T is the length of the induction period and τ_m is the mean residence time of the latex.

From the least squares fit of the data to the volumetric Smith-Ewart or modified Stockmayer models, the volumetric nuclei growth rate can be related to the mean residence time of growing particles by

$$\tau R_v^o = \text{constant.} \tag{46}$$

Therefore, from a given set of data, Equations 45 and 46 represent two equations relating three unknowns; R_v^o, T, and τ. By applying the least squares fit to another set of data obtained at a different latex mean residence time, τ_m, to Equations 45 and 46, two new equations relating the unknowns are obtained while adding only one additional unknown. The additional unknown is the mean residence time of particle growth for this second set of data. These four equations are now used to calculate the induction period, T, and the volumetric nuclei growth rate, R_v^o, which can be used to predict the size distribution of polymer particles at a third latex residence time.

The sets of data used to estimate T and R_r^o were obtained for latex residence times of 2260 and 2540 seconds. Table 6 lists these values obtained using the least squares fit for both the Smith-Ewart and modified Stockmayer models.

The theoretical volumetric nuclei growth rate is 1.9 x

Table 6. Measured volumetric nuclei growth rate

	Smith-Ewart	Modified Stockmayer
R_v^o	2.6×10^{-7} μ^3/sec	2.4×10^{-7} μ^3/sec
T	1380 sec	1730 sec

10^{-7} μ^3/sec. The approximations obtained from the distribution data for both the Smith-Ewart and modified Stockmayer models are larger than the theoretical growth rate. This indicates that the retarding effect on the nuclei growth rate is very slight if it exists at all.

For the Smith-Ewart model the fit of experimental data for τ_m equal to 2260 seconds and 2540 seconds to the theoretical dimensionless predictions using the parameters from Table 6 are shown in Figures 16 and 17, respectively. Figures 18 and 19 compare the same experimental data with the modified Stockmayer model using the parameters from Table 6. These figures show that the modified Stockmayer model predicts the change in slope of the size distribution data. Although it is possible to fit these data with the straight line prediction from the Smith-Ewart growth rate model, the curved nature of the modified Stockmayer model

Figure 16. Comparison of experimental size distribution data to dimensionless volumetric Smith-Ewart model

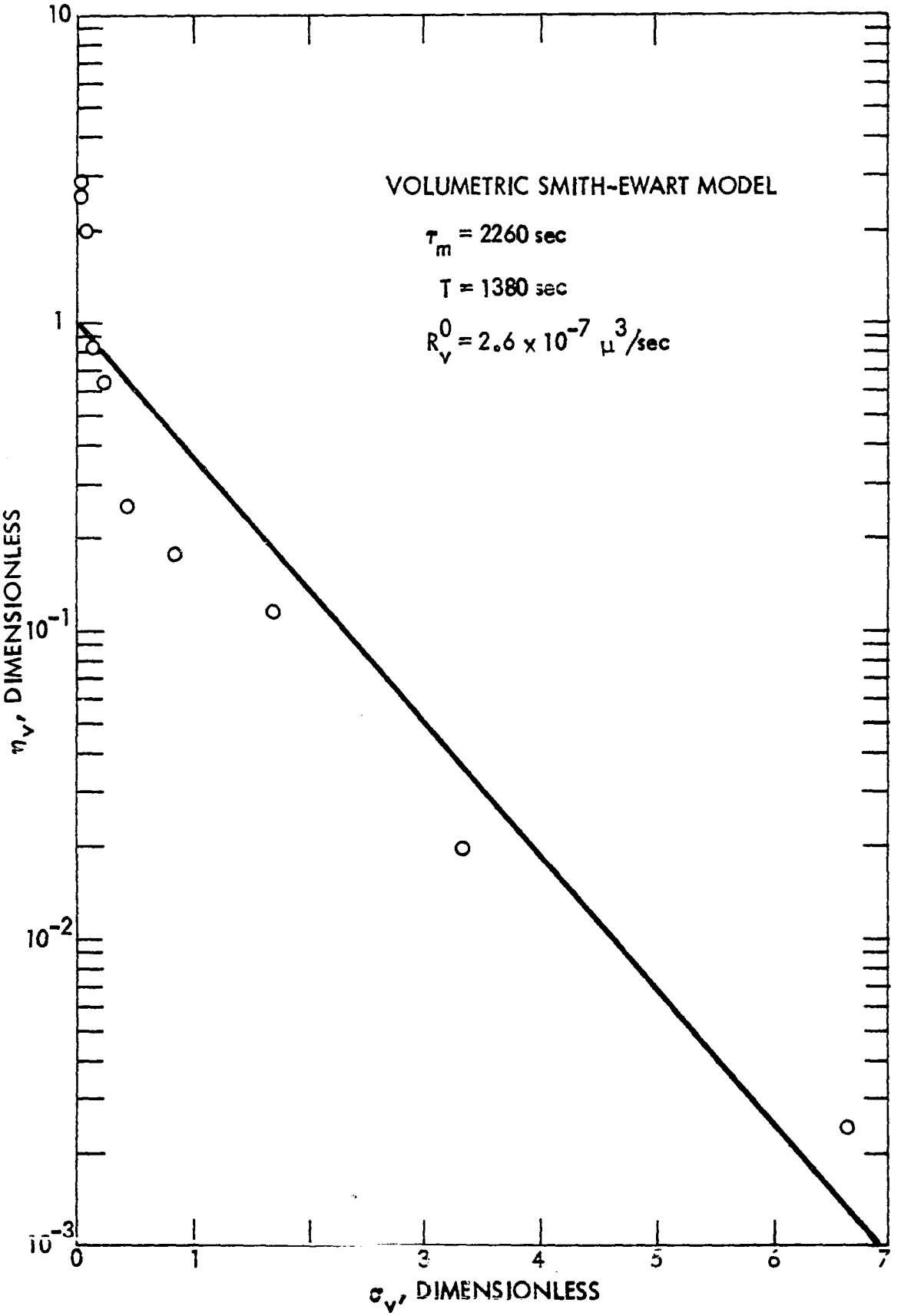
VOLUMETRIC SMITH-EWART MODEL
τ_m = 2260 sec
T = 1380 sec
$R_v^0 = 2.6 \times 10^{-7}$ μ^3/sec
η_v, DIMENSIONLESS
σ_v, DIMENSIONLESS
10
1
10^{-1}
10^{-2}
10^{-3}
0
1
3
4
5
6
7

Figure 17. Comparison of experimental size distribution data to dimensionless volumetric Smith-Ewart model

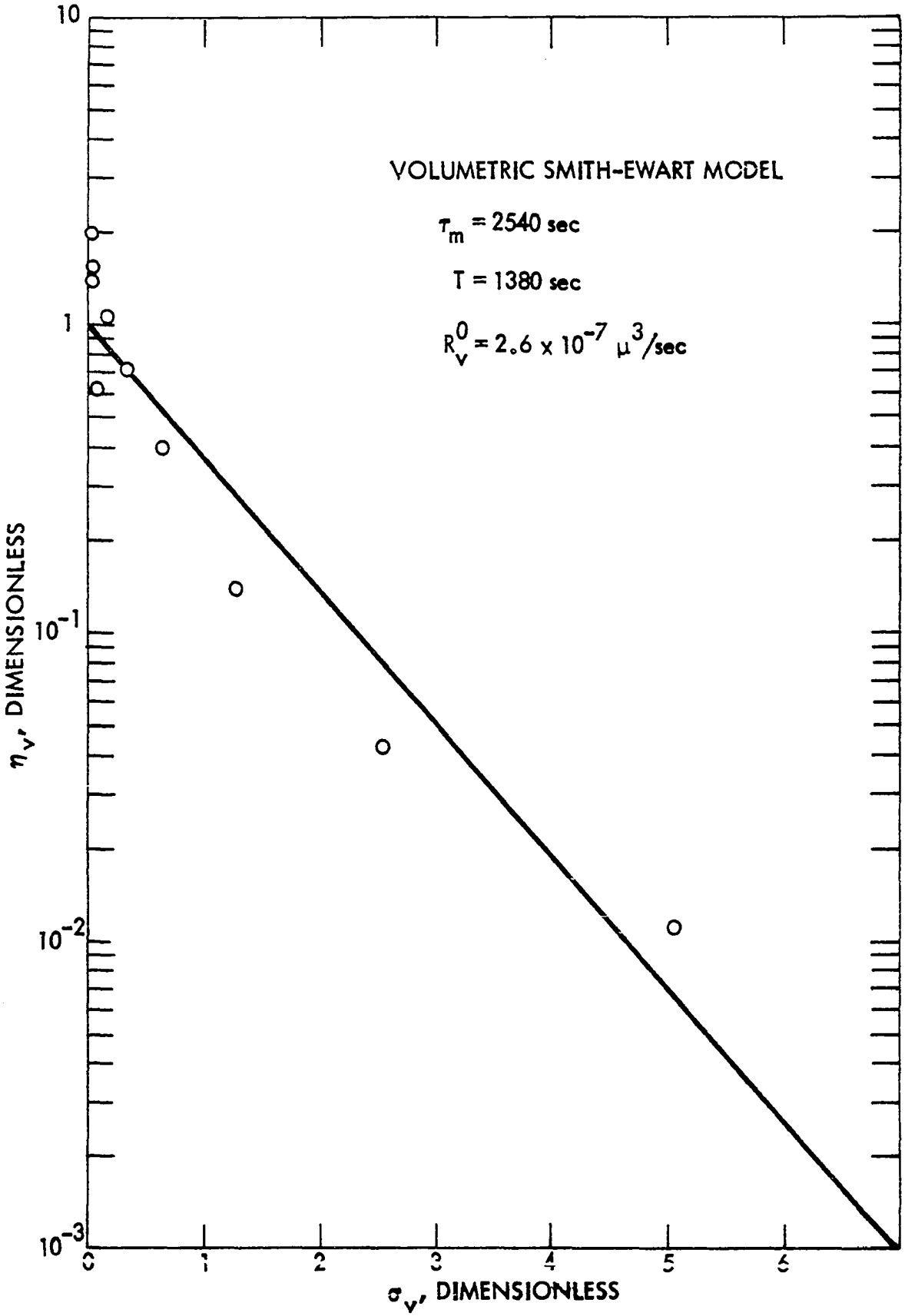
VOLUMETRIC SMITH-EWART MODEL
τ_m = 2540 sec
T = 1380 sec
$R_v^0 = 2.6 \times 10^{-7}\ \mu^3/sec$
η_v, DIMENSIONLESS
σ_v, DIMENSIONLESS
10
1
10^{-1}
10^{-2}
10^{-3}
0
1
2
3
4
5
6

Figure 18. Comparison of experimental size distribution data to dimensionless volumetric modified Stockmayer model

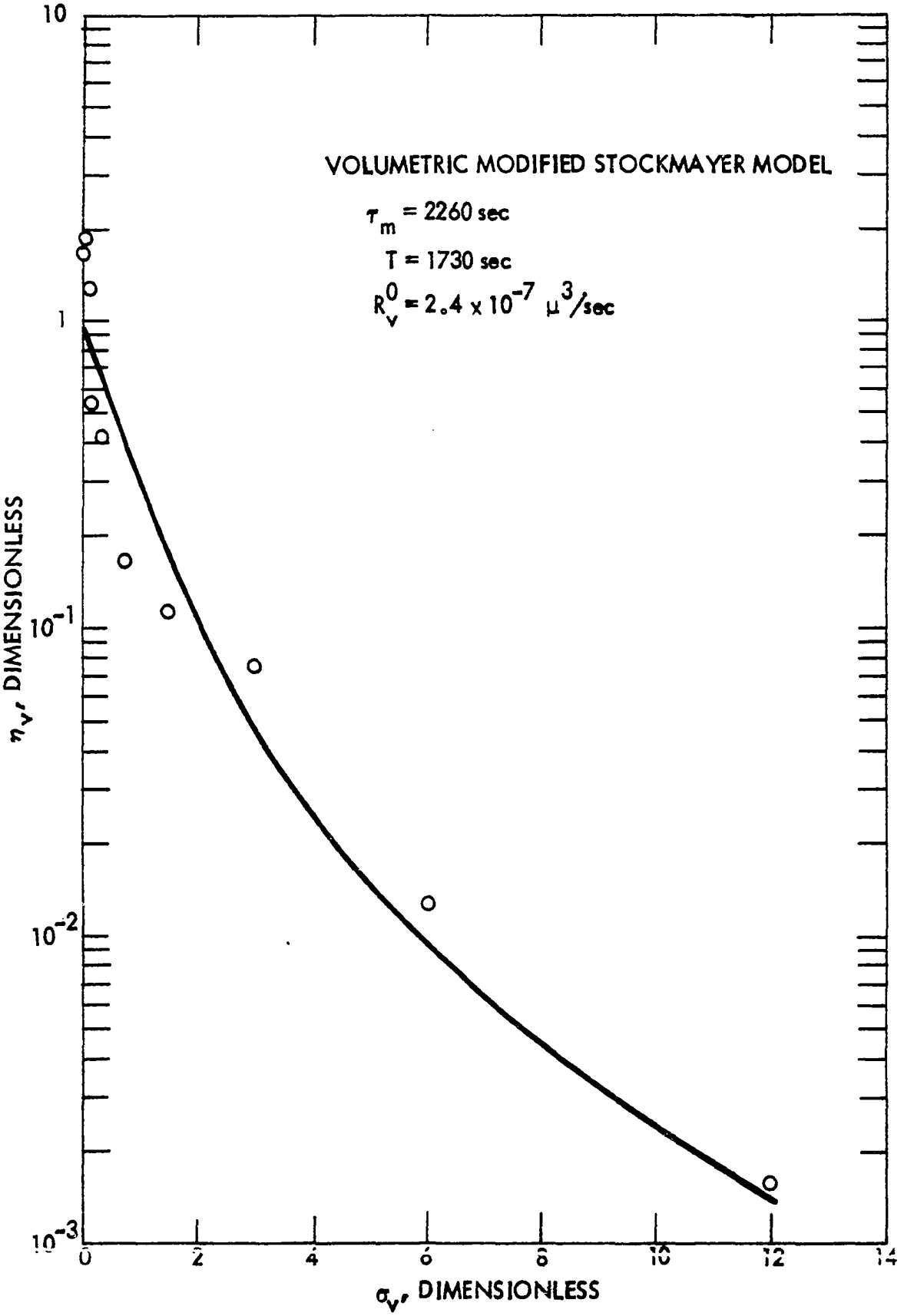
VOLUMETRIC MODIFIED STOCKMAYER MODEL
τ_m = 2260 sec
T = 1730 sec
$R_v^0 = 2.4 \times 10^{-7}$ μ^3/sec
η_v, DIMENSIONLESS
σ_v, DIMENSIONLESS
10
1
10^{-1}
10^{-2}
10^{-3}
0
2
4
6
8
10
12
14

Figure 19. Comparison of experimental size distribution data to dimensionless volumetric modified Stockmayer model

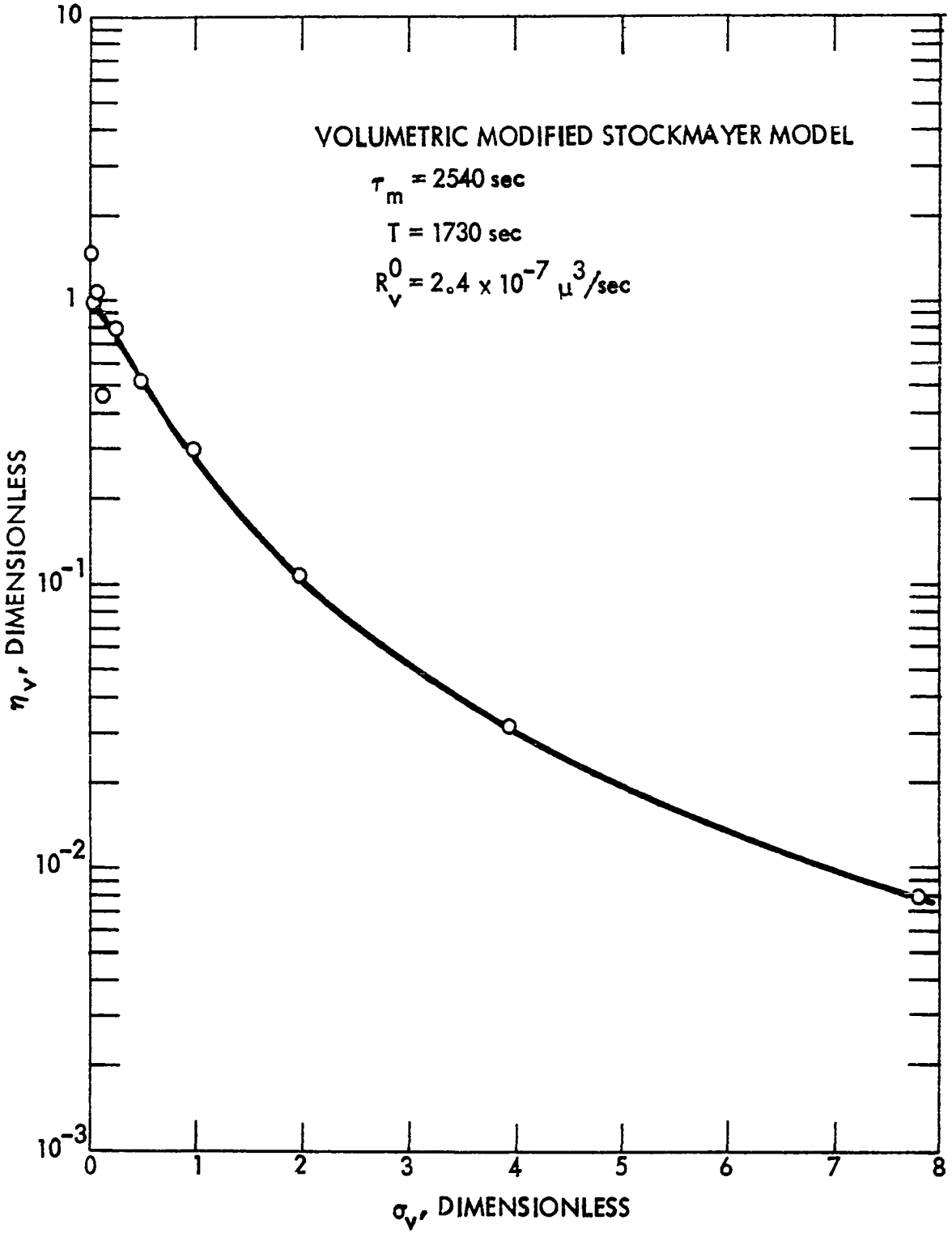
VOLUMETRIC MODIFIED STOCKMAYER MODEL
τ_m = 2540 sec
T = 1730 sec
$R_v^0 = 2.4 \times 10^{-7}$ μ^3/sec
η_v, DIMENSIONLESS
σ_v, DIMENSIONLESS
10
1
10^{-1}
10^{-2}
10^{-3}
0
1
2
3
4
5
6
7
8

exhibits a better fit.

One reason there is a greater amount of deviation from the predicted distribution at small particle sizes is the classification of particles into size intervals is the least accurate at small sizes. This occurs since the intervals at small particle sizes are smaller than at larger particle sizes, and those small intervals are the same order of magnitude as the errors involved in particle measurement.

To investigate the size distribution predictions on a radial basis, the radial nuclei growth rate must be estimated. It was not possible to obtain this from the measured volumetric nuclei growth rate since such a calculation requires accurate knowledge of the nuclei size. The size of a nucleus is not accurately known. Therefore the radial nuclei growth rate was estimated by fitting the peak of the experimental data to the peak of the dimensionless theoretical prediction for a latex residence time of 2540 seconds. These estimates are listed in Table 7 for both a fit to the Smith-Ewart and modified Stockmayer model peaks.

Table 7. Measured radial nuclei growth rate

	Smith-Ewart	Modified Stockmayer
R_r^o	0.5×10^{-3} μ/sec	0.7×10^{-3} μ/sec
T	1380 sec	1730 sec

For the Smith-Ewart model the fit of the experimental data for τ_m equal to 2260 and 2540 seconds to the dimensionless theoretical prediction using the parameters from Table 7 are illustrated in Figures 20 and 21, respectively. The modified Stockmayer model, as illustrated in Figures 22 and 23, also gives an excellent fit of these data. The modified Stockmayer model exhibits a slightly better fit of the data at the larger sizes.

When considering Figures 20, 21, 22, and 23, one must recall that the modified Stockmayer model is an extension of the Smith-Ewart model. The significant difference being that the assumption of instantaneous termination is dropped in the modified Stockmayer model. Therefore, the models should be expected to behave similarly. The fit of both the models is good because the radial nuclei growth rate used to convert the data to dimensionless quantities for each model was determined by assuming each model fit. As illustrated in Figure 3, when the same mean residence time of growth and radial nuclei growth rate are applied to the Smith-Ewart and modified Stockmayer models, the modified Stockmayer model peaks earlier. Therefore, if T and R_r^o could be estimated accurately from an independent source, the difference in the two radial models would be more pronounced.

The fit of the data to the curve of the volumetric

Figure 20. Comparison of experimental size distribution data to dimensionless radial Smith-Ewart model

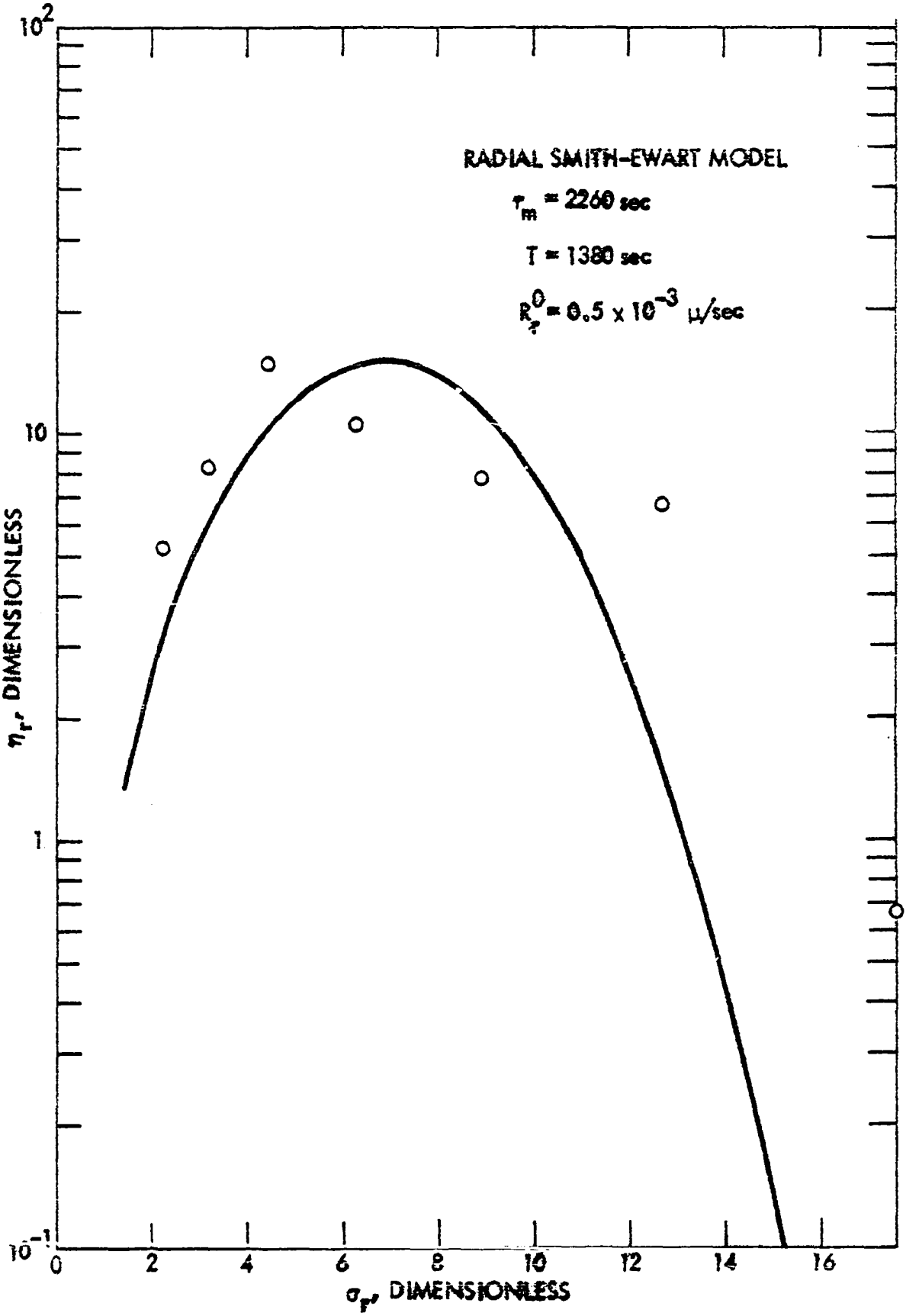
RADIAL SMITH-EWART MODEL
τ_m = 2260 sec
T = 1380 sec
R_τ^0 = 0.5 x 10^{-3} μ/sec
10^2
10
1
10^{-1}
$\eta_{r'}$ DIMENSIONLESS
0
2
4
6
8
10
12
14
16
$\sigma_{r'}$ DIMENSIONLESS

Figure 21. Comparison of experimental size distribution data to dimensionless radial Smith-Ewart model

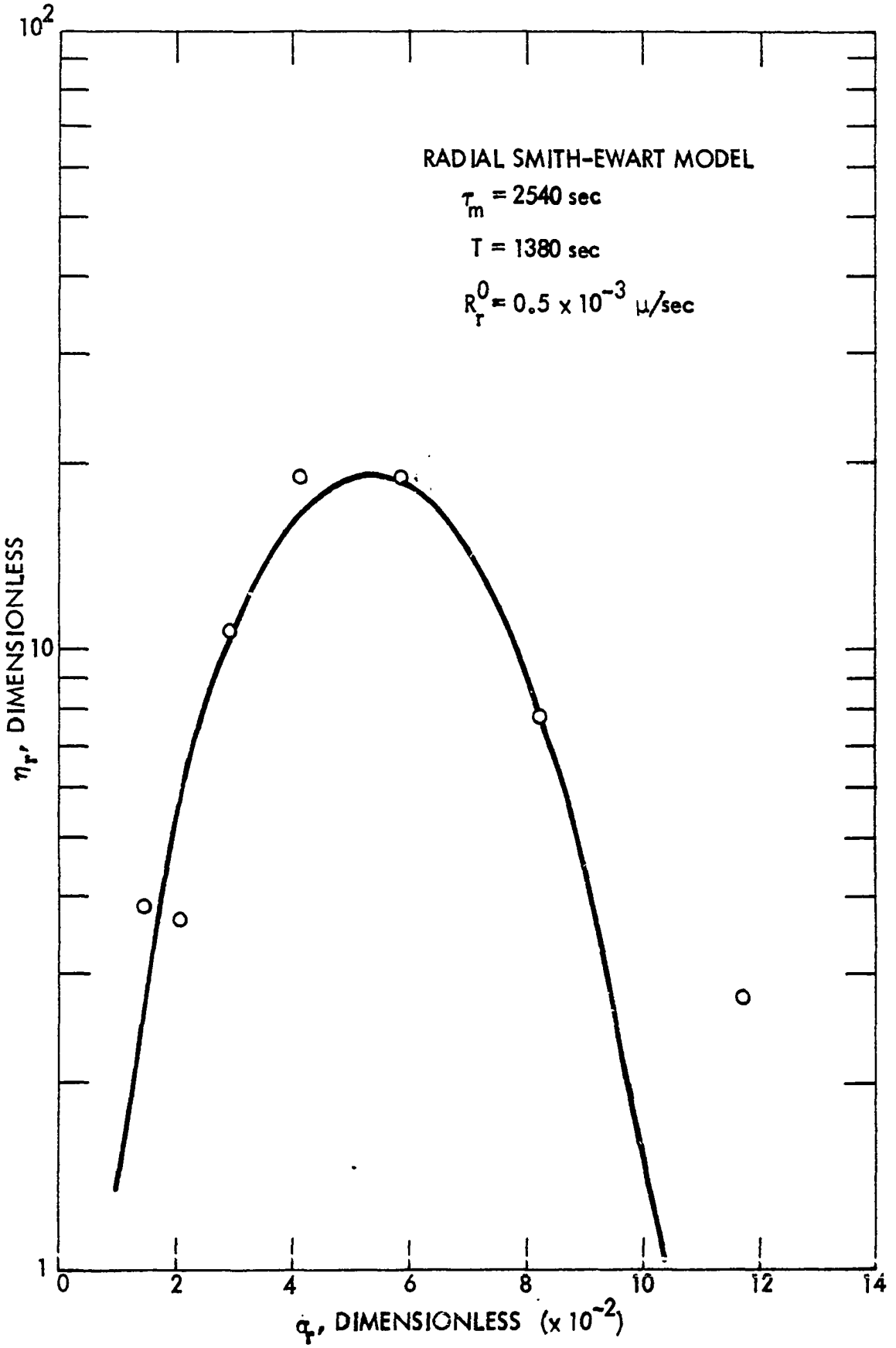
RADIAL SMITH-EWART MODEL
τ_m = 2540 sec
T = 1380 sec
R_r^0 = 0.5 x 10^{-3} μ/sec
10^2
10
1
η_r, DIMENSIONLESS
0
2
4
6
8
10
12
14
q_r, DIMENSIONLESS (x 10^{-2})

Figure 22. Comparison of experimental size distribution data to dimensionless radial modified Stockmayer model

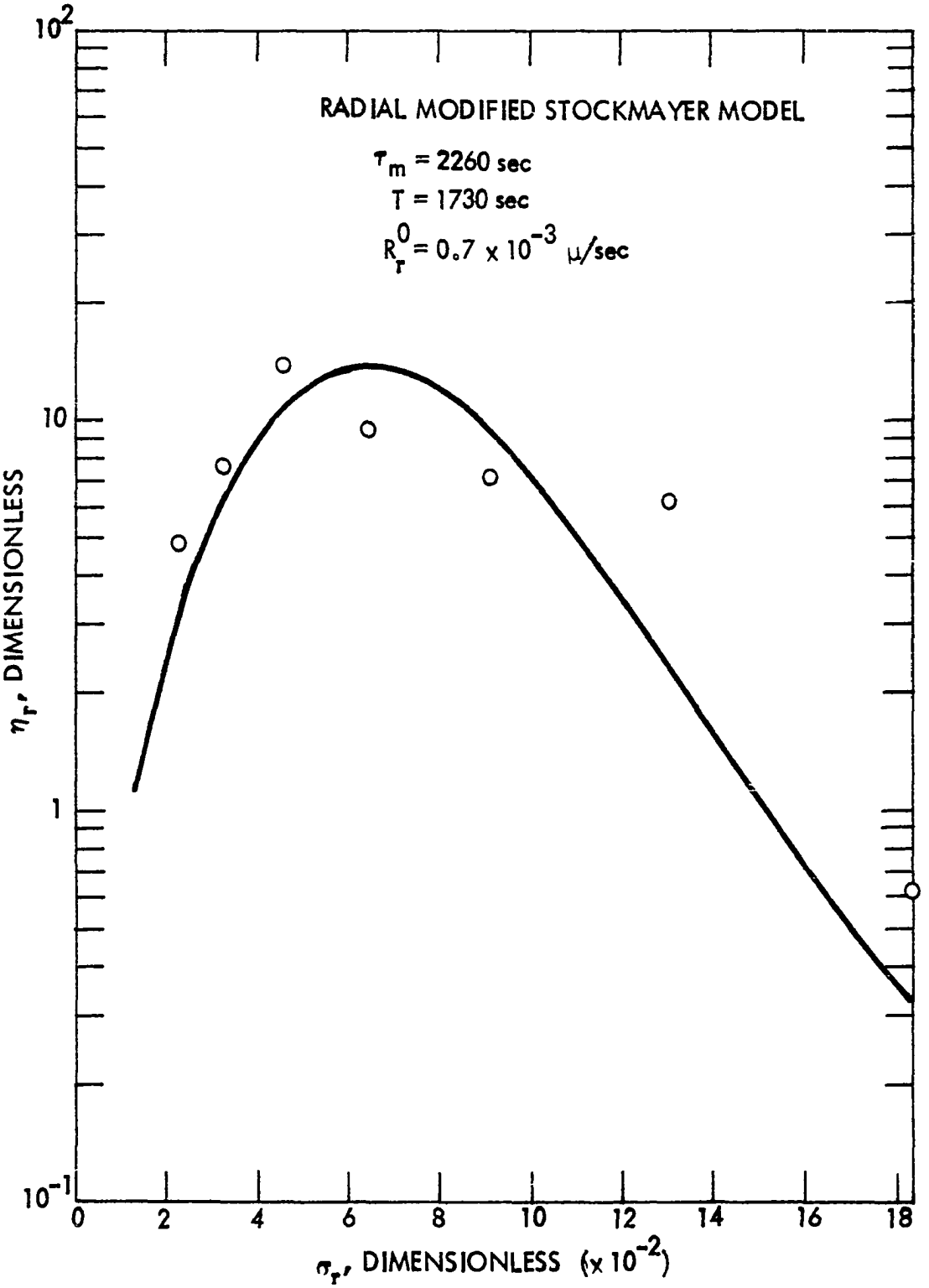
RADIAL MODIFIED STOCKMAYER MODEL
τ_m = 2260 sec
T = 1730 sec
R_r^0 = 0.7 x 10^{-3} μ/sec
10^2
10
1
10^{-1}
η_r', DIMENSIONLESS
0
2
4
6
8
10
12
14
16
18
σ_r', DIMENSIONLESS (x 10^{-2})

Figure 23. Comparison of experimental size distribution data to dimensionless radial modified Stockmayer model

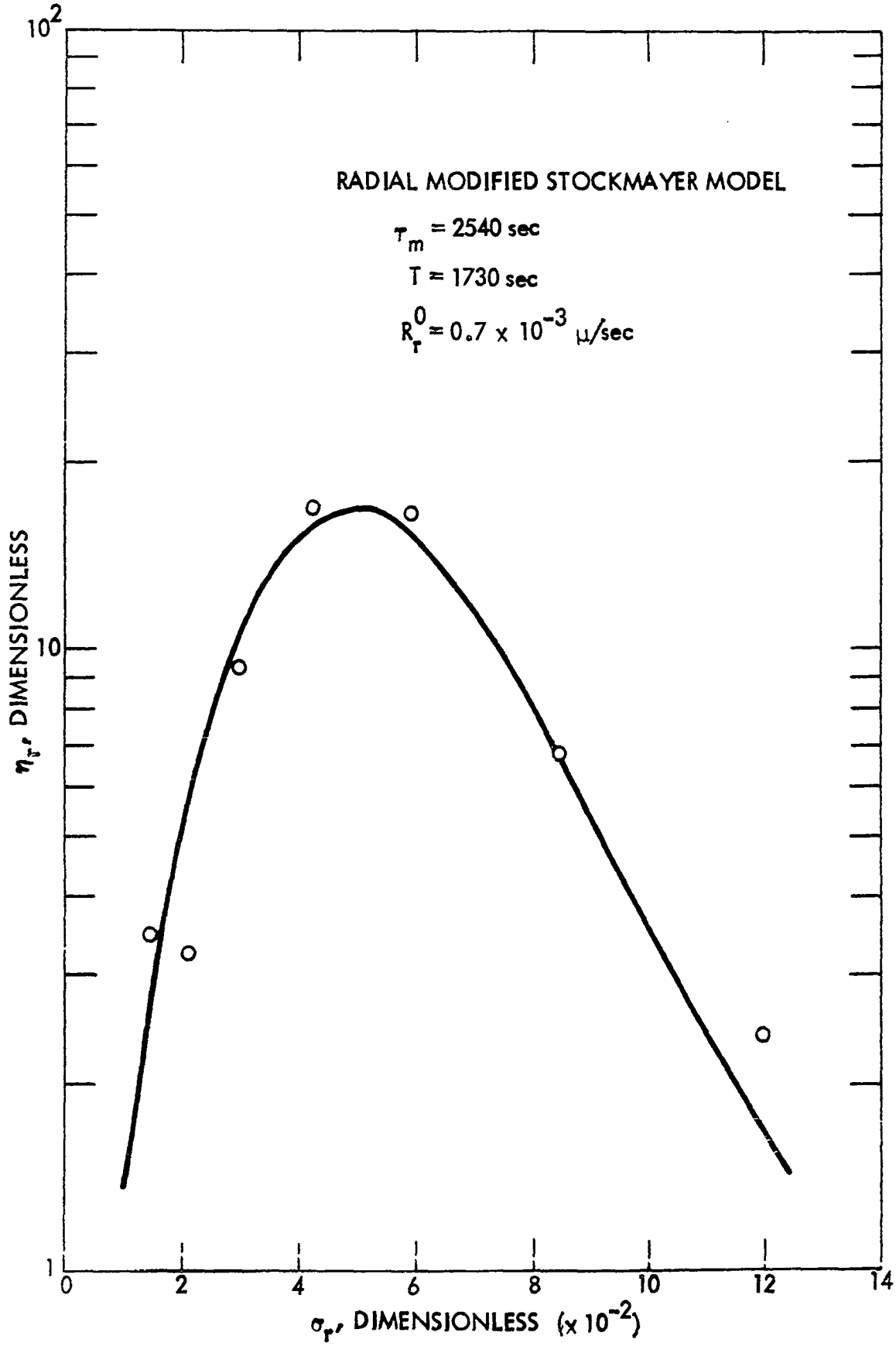
RADIAL MODIFIED STOCKMAYER MODEL
τ_m = 2540 sec
T = 1730 sec
$R_r^0 = 0.7 \times 10^{-3}$ μ/sec
10^2
10
1
η_r, DIMENSIONLESS
0
2
4
6
8
10
12
14
σ_r, DIMENSIONLESS ($\times 10^{-2}$)

prediction made by the modified Stockmayer model indicated that the modified Stockmayer represents the data with more reliability. However, when the nuclei growth rate and the induction period are estimated from utilizing the assumption of the Smith-Ewart model, the data fit the Smith-Ewart model very well.

The estimates of the induction period and the volumetric and radial nuclei growth rates listed in Tables 6 and 7 were used to predict the particle size distribution of a latex produced with a latex mean residence time of 2820 seconds. A prediction was made assuming both the Smith-Ewart and modified Stockmayer models. The comparisons of the experimental data with the Smith-Ewart model radial and volumetric predictions are illustrated by Figures 24 and 25, respectively. The same comparisons are illustrated for the modified Stockmayer radial and volumetric predictions by Figures 26 and 27, respectively. These figures illustrate the fact that when the induction period and the nuclei growth rates are determined by assumption of either the Smith-Ewart or modified Stockmayer model, those parameters may be used to predict other particle size distributions along with the model used in the parameter determination.

The three sets of data that have been mentioned were obtained over a period of eight days. This fact is important since the level of the inhibitor in the stored styrene was

Figure 24. Comparison of experimental size distribution data to dimensionless radial Smith-Ewart model

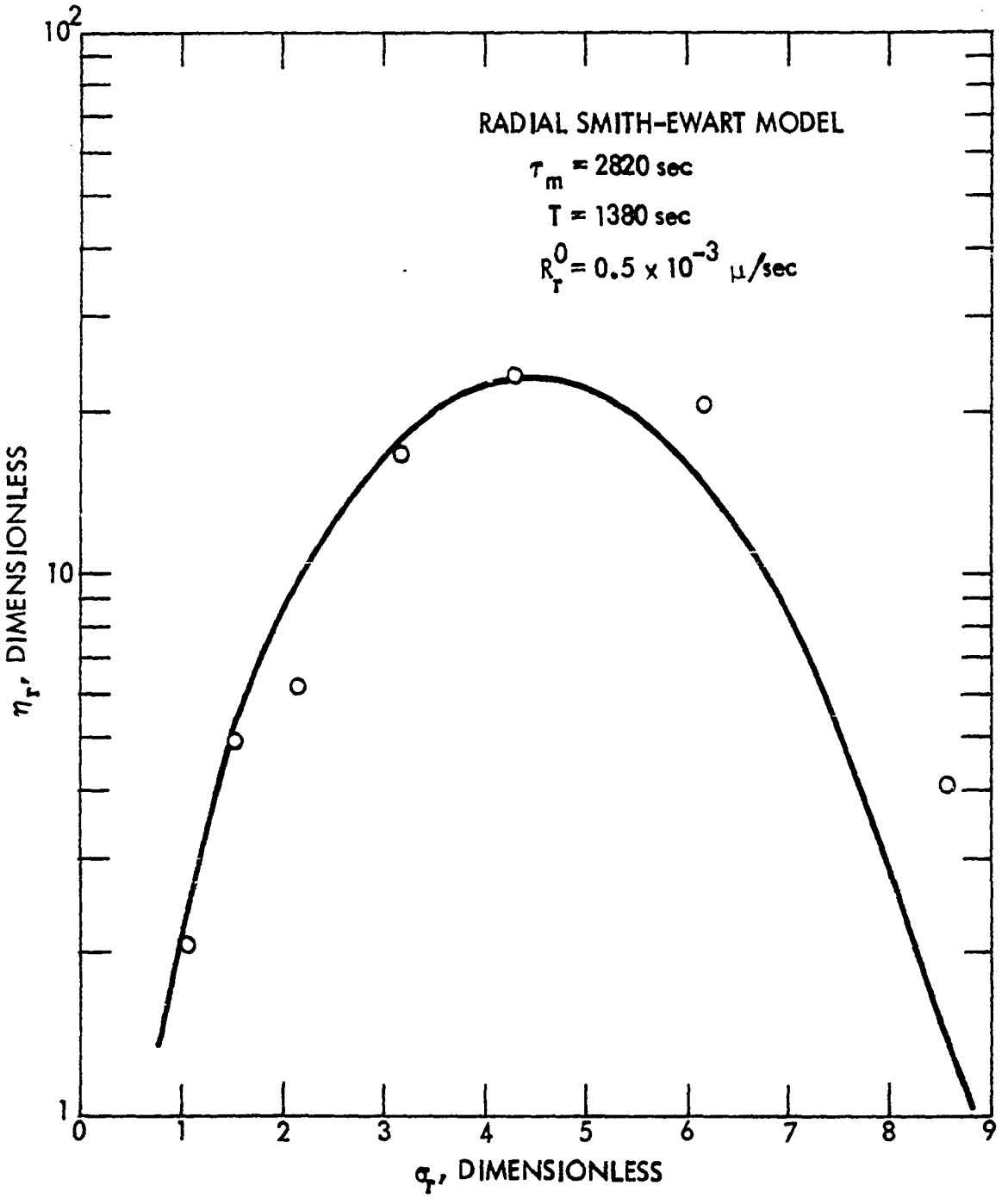
RADIAL SMITH-EWART MODEL
τ_m = 2820 sec
T = 1380 sec
R_r^0 = 0.5 x 10^{-3} μ/sec
10^2
10
1
0
1
2
3
4
5
6
7
8
9
η_r, DIMENSIONLESS
σ_r, DIMENSIONLESS

Figure 25. Comparison of experimental size distribution data to dimensionless volumetric Smith-Ewart model

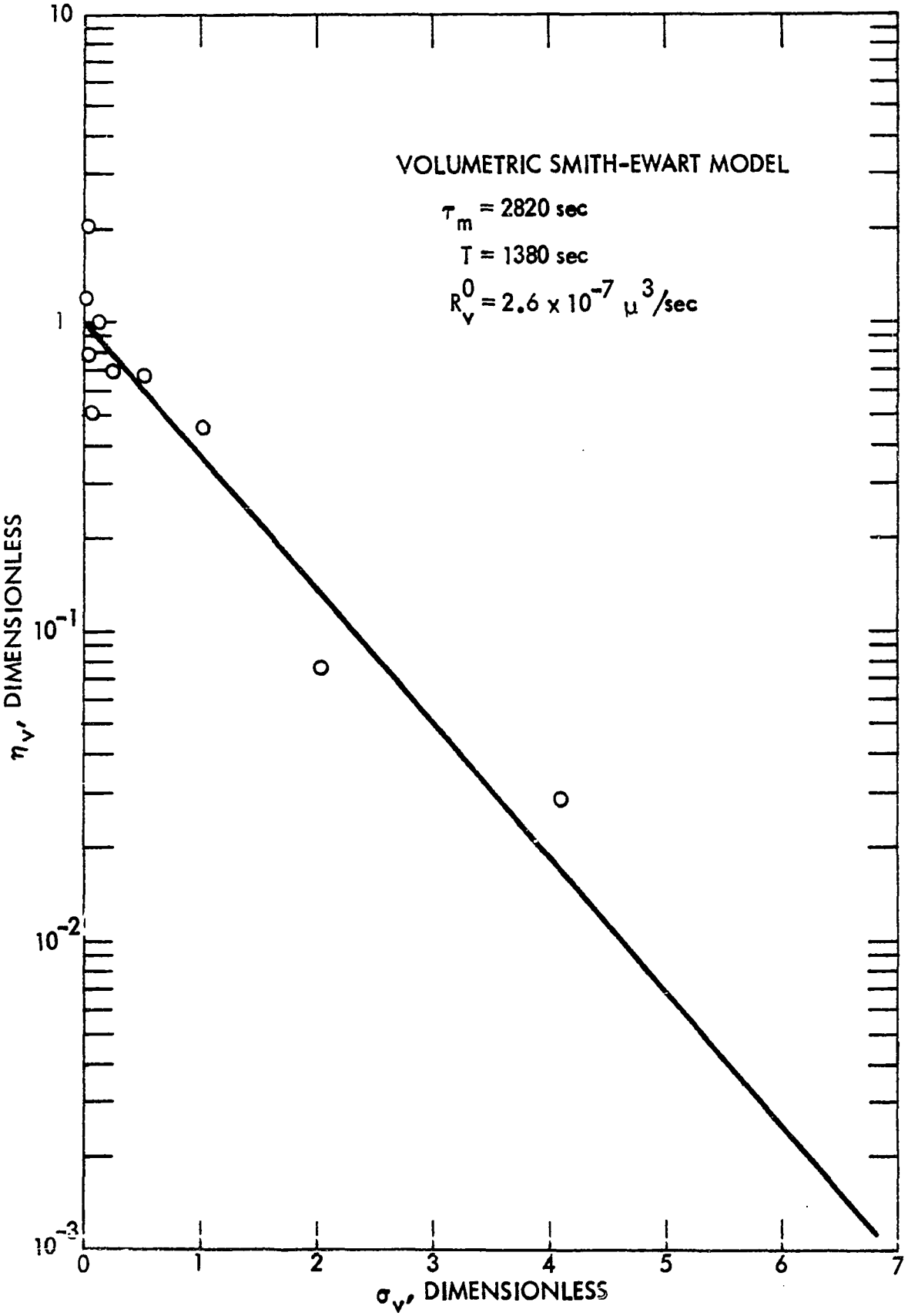
VOLUMETRIC SMITH-EWART MODEL
τ_m = 2820 sec
T = 1380 sec
$R_v^0 = 2.6 \times 10^{-7}$ μ^3/sec
η_v, DIMENSIONLESS
σ_v, DIMENSIONLESS
10
1
10^{-1}
10^{-2}
10^{-3}
0
1
2
3
4
5
6
7

Figure 26. Comparison of experimental size distribution data to dimensionless radial modified Stockmayer model

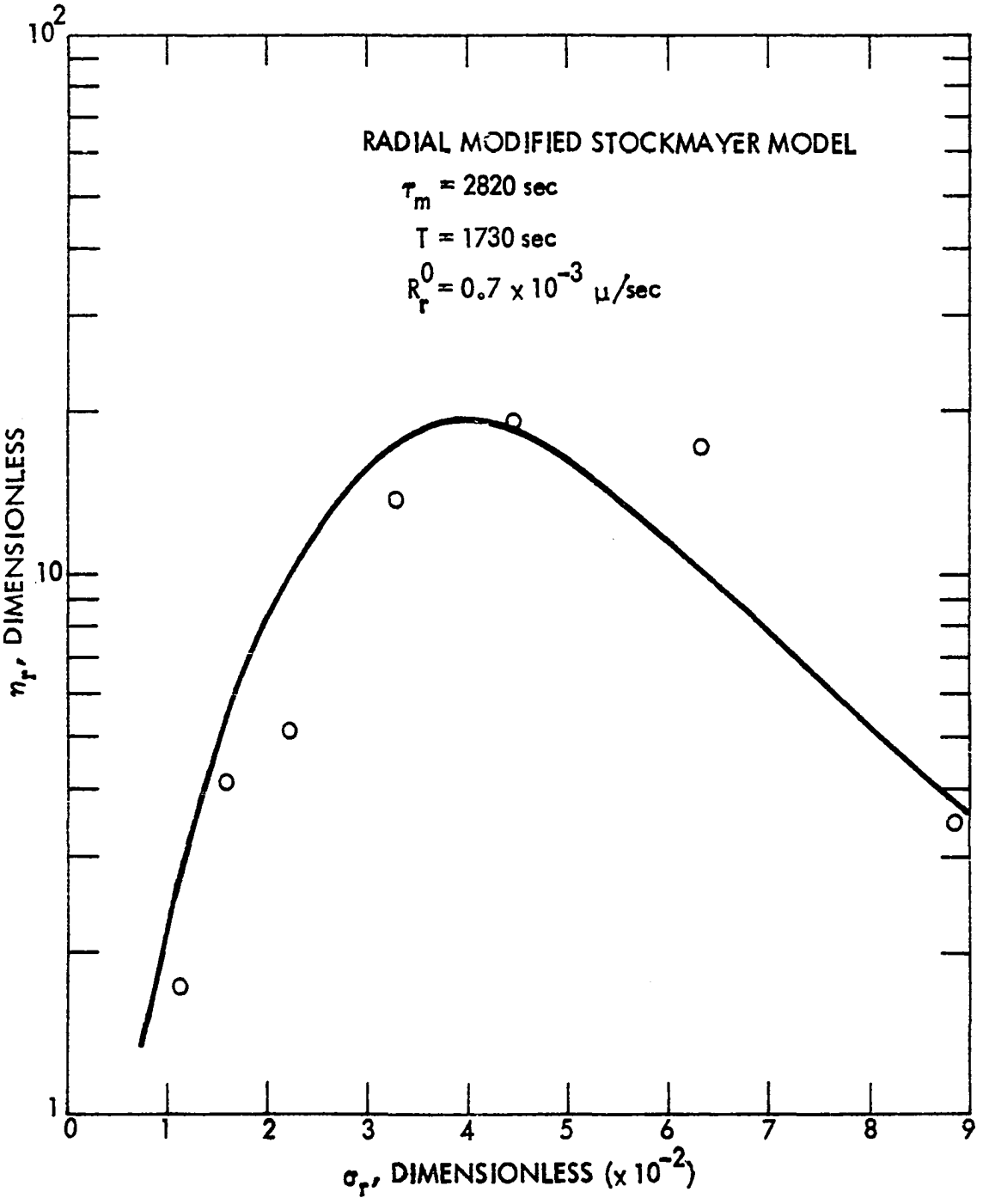
RADIAL MODIFIED STOCKMAYER MODEL
τ_m = 2820 sec
T = 1730 sec
$R_r^0 = 0.7 \times 10^{-3}$ μ/sec
10^2
10
1
η_r, DIMENSIONLESS
0
1
2
3
4
5
6
7
8
9
σ_r, DIMENSIONLESS (x 10^{-2})

Figure 27. Comparison of experimental size distribution data to dimensionless volumetric modified Stockmayer model

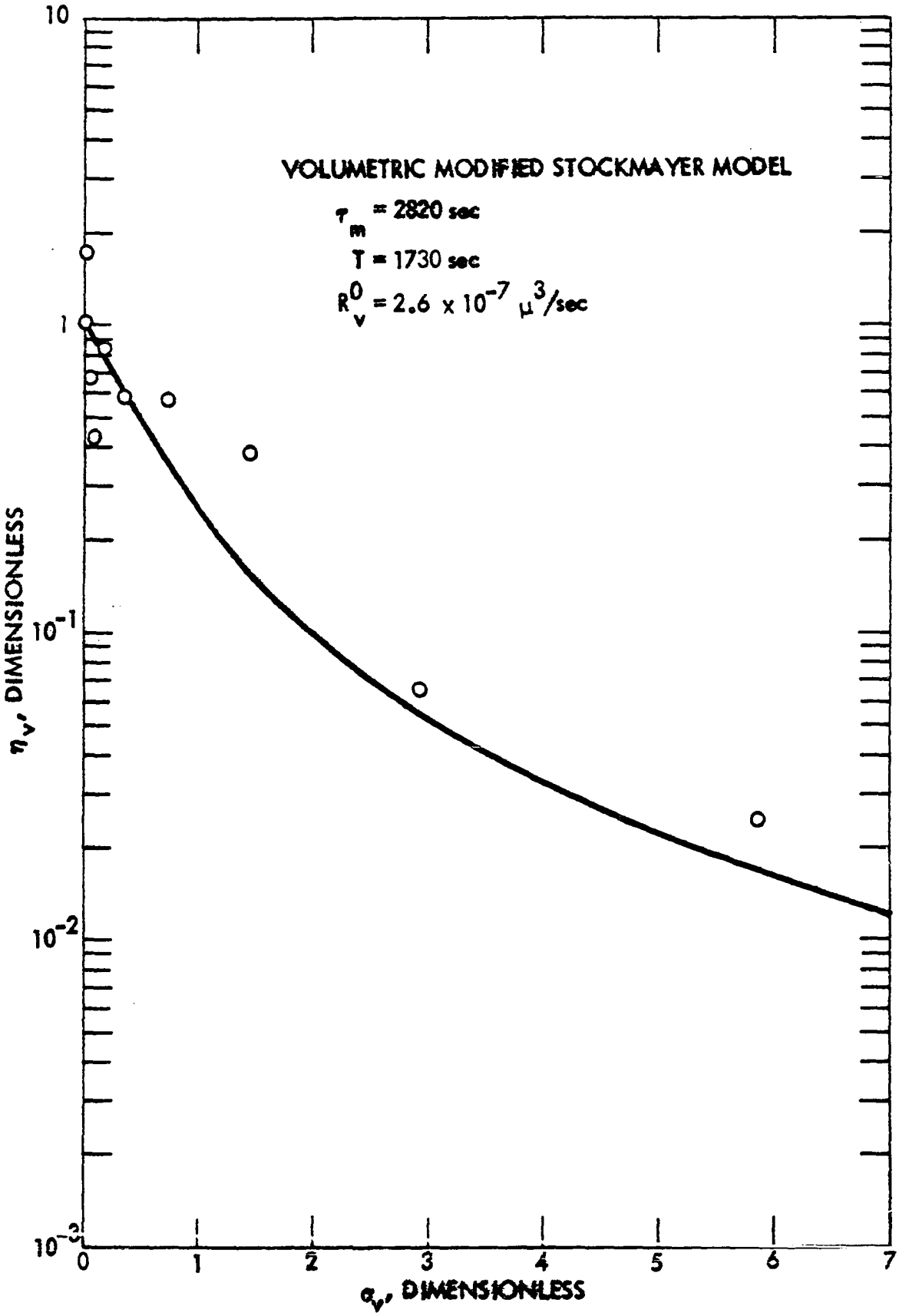
VOLUMETRIC MODIFIED STOCKMAYER MODEL
τ_m = 2820 sec
T = 1730 sec
$R_v^0 = 2.6 \times 10^{-7}\ \mu^3/sec$
10
1
10^{-1}
10^{-2}
10^{-3}
η_v, DIMENSIONLESS
0
1
2
3
4
5
6
7
α_v, DIMENSIONLESS

decreasing. As stated by Boundy (3), the inhibitor is believed to react with oxygen and oxygen-containing compounds to prevent them from initiating polymerization of the monomer. These reactions will decrease the level of the inhibitor. The inhibitor level has a direct relationship to the length of the induction period and the particle growth rate. Therefore, the estimated values for the induction period and the nuclei growth rate was affected by the inhibitor level at the time the data were obtained. No attempt was made to keep the level of the inhibitor constant since the purpose of this experimental work was to verify that the solution to the population balance for a continuous emulsion polymerizer could be used to predict the polymer particle size distribution in latex. This could be done without a constant inhibitor level since the effect of the inhibitor was minimized by making the above mentioned experiments over a short time period. However, if the level of the inhibitor is allowed to vary, the value of the induction period and nuclei growth rate must be redetermined to make an accurate prediction.

For the radial and volumetric Smith-Ewart and radial and volumetric modified Stockmayer models respectively, Figures 28, 29, 30, and 31 illustrate the effect of an inhibitor level higher than existed when the estimates for the induction period and nuclei growth rate were determined. The theoretical predictions illustrated in these figures

Figure 28. Comparison of dimensionless radial Smith-Ewart model to experimental size distribution data obtained at a high inhibitor level

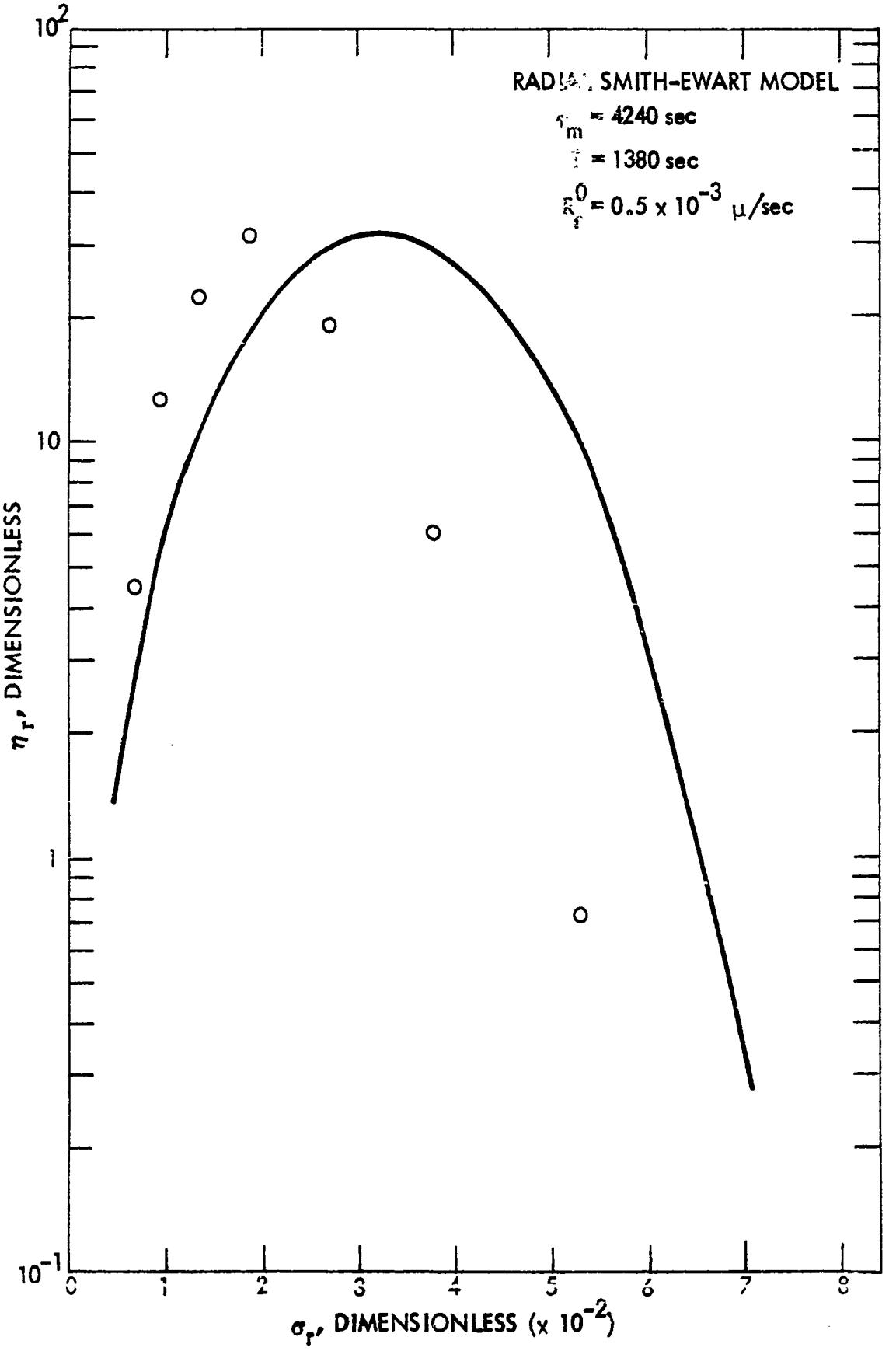
RADIAL SMITH-EWART MODEL
τ_m = 4240 sec
$\bar{\tau}$ = 1380 sec
R_f^0 = 0.5 x 10^{-3} μ/sec
10^2
10
1
10^{-1}
η_r, DIMENSIONLESS
0
1
2
3
4
5
6
7
8
σ_r, DIMENSIONLESS (x 10^{-2})

Figure 29. Comparison of dimensionless volumetric Smith-Ewart model to experimental size distribution data obtained at a high inhibitor level

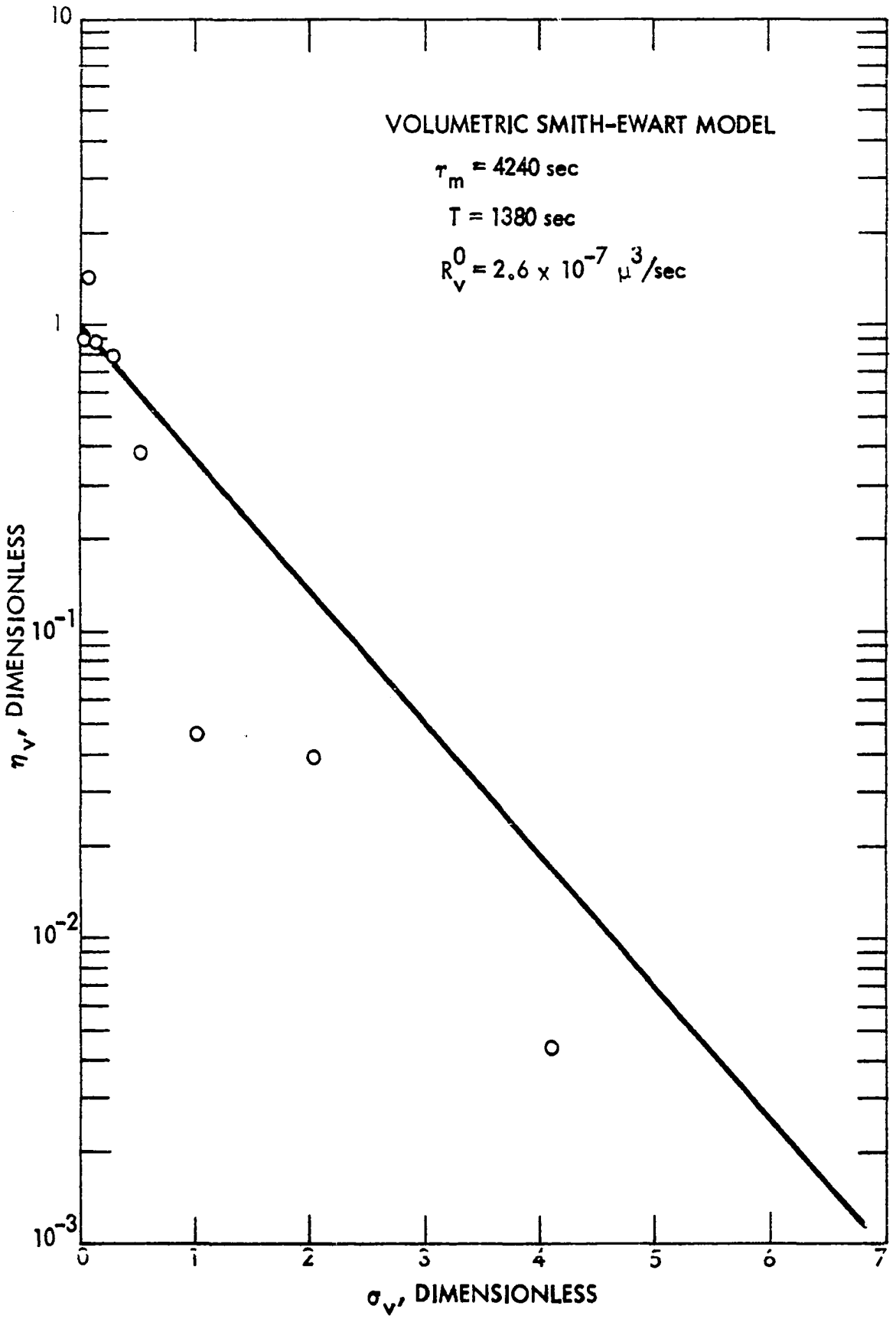
VOLUMETRIC SMITH-EWART MODEL
τ_m = 4240 sec
T = 1380 sec
$R_v^0 = 2.6 \times 10^{-7}\ \mu^3/sec$
10
1
10^{-1}
10^{-2}
10^{-3}
η_v, DIMENSIONLESS
0
1
2
3
4
5
6
7
σ_v, DIMENSIONLESS

Figure 30. Comparison of dimensionless radial modified Stockmayer model to experimental size distribution data obtained at a high inhibitor level

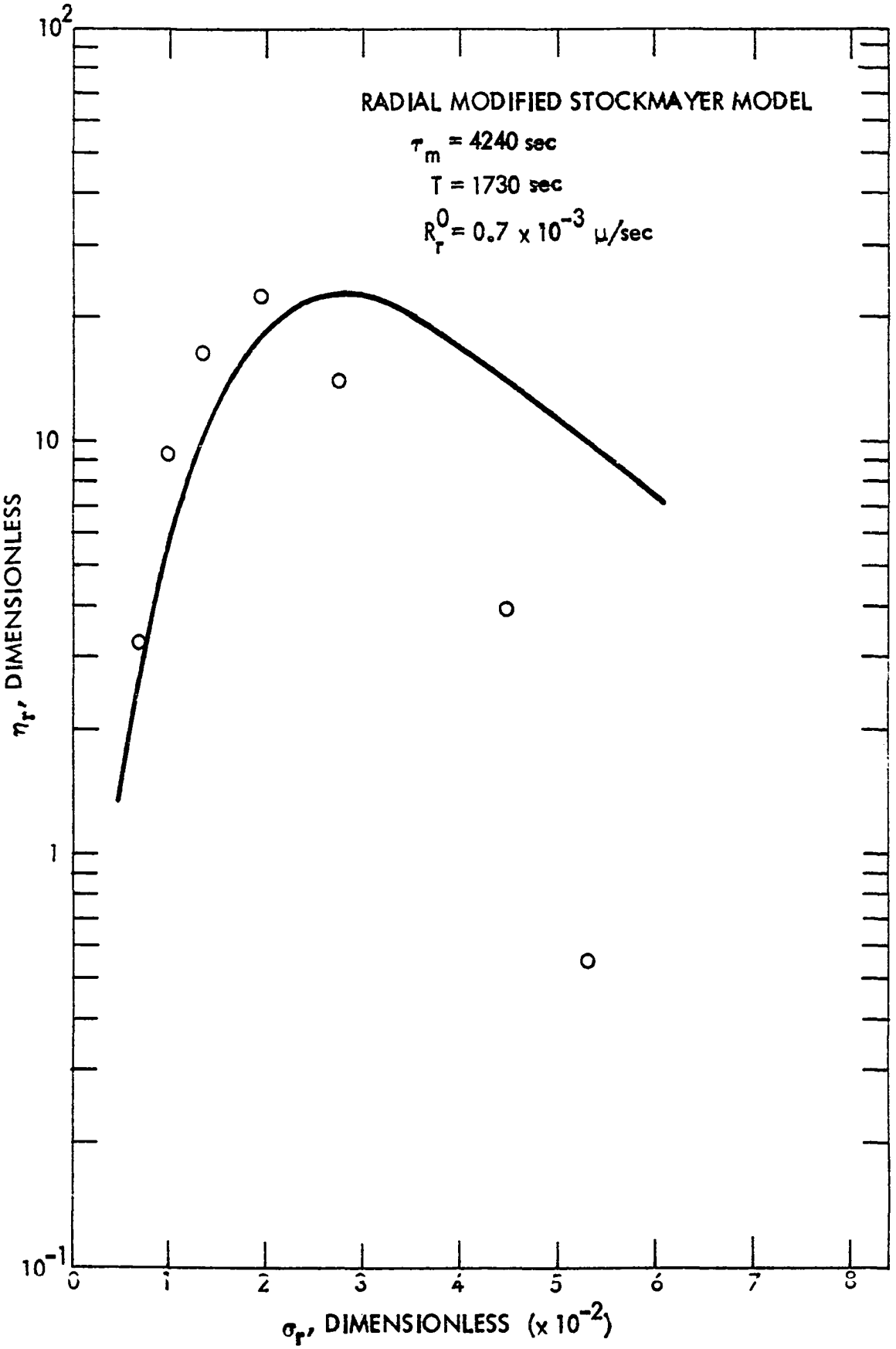
RADIAL MODIFIED STOCKMAYER MODEL
τ_m = 4240 sec
T = 1730 sec
R_r^0 = 0.7 x 10^{-3} μ/sec
10^2
10
1
10^{-1}
η_r', DIMENSIONLESS
0
1
2
3
4
5
6
7
8
σ_r', DIMENSIONLESS (x 10^{-2})

Figure 31. Comparison of dimensionless volumetric modified Stockmayer model to experimental size distribution data obtained at a higher inhibitor level

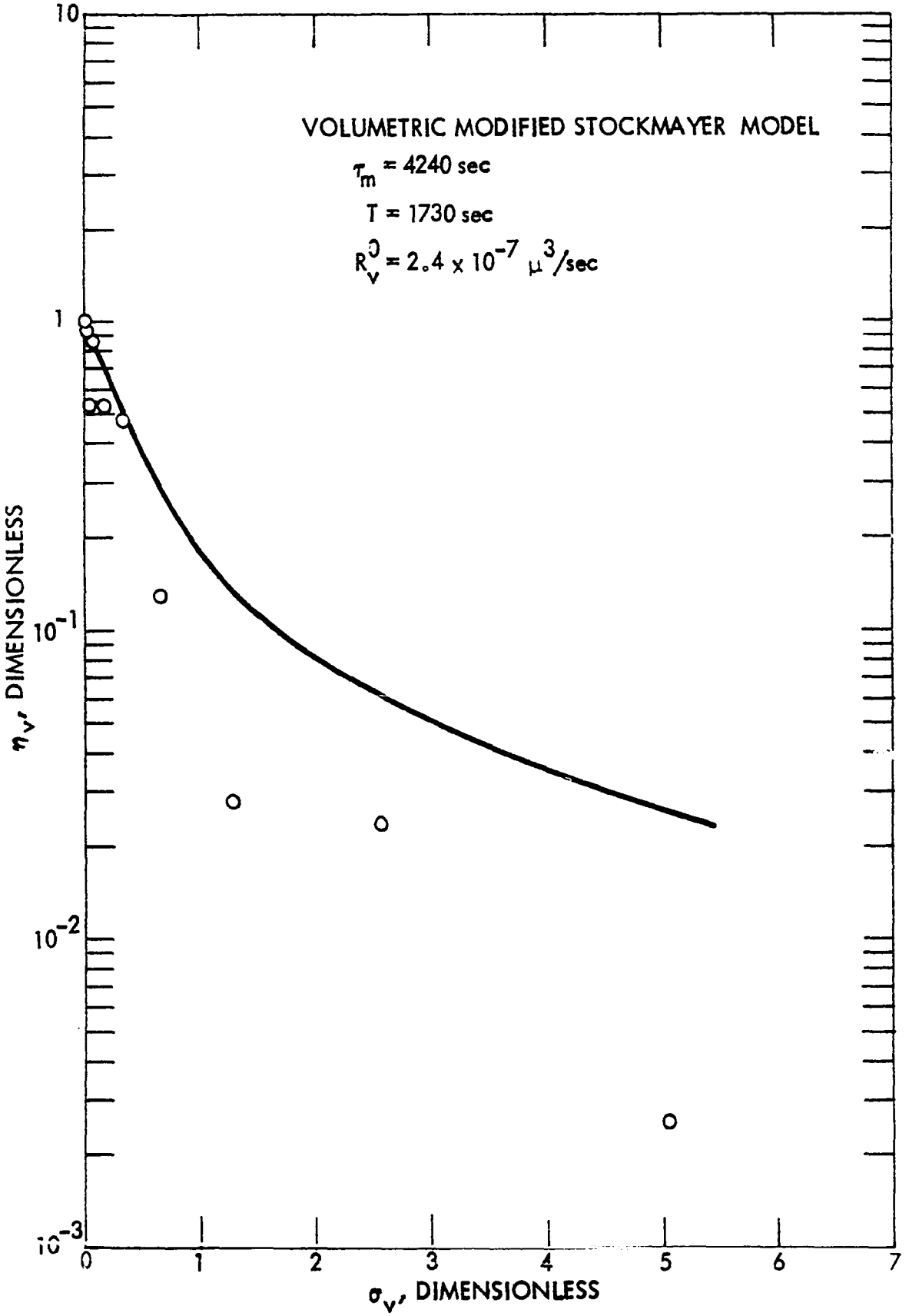
VOLUMETRIC MODIFIED STOCKMAYER MODEL
τ_m = 4240 sec
T = 1730 sec
$R_v^0 = 2.4 \times 10^{-7}$ μ^3/sec
10
1
10^{-1}
10^{-2}
10^{-3}
η_v, DIMENSIONLESS
0
1
2
3
4
5
6
7
σ_v, DIMENSIONLESS

were obtained using the parameters listed in Tables 4 and 5. However, the data show that particles smaller than predicted were produced. This indicated that the growth rate was lower and the induction period was longer than the estimates used in the prediction.

For the radial and volumetric Smith-Ewart and radial and volumetric Stockmayer models respectively, Figures 32, 33, 34, and 35 illustrate the effect of an inhibitor level lower than existed when the estimates for the induction period and nuclei growth rate were determined. The theoretical predictions indicate much smaller particles than were actually produced. This lack of fit was due to an induction period which was shorter and a particle growth rate which was greater than when the estimates used in the size distribution prediction were obtained.

To observe the effect of the decreasing inhibitor level, the measured volumetric nuclei growth rates from each experiment discussed for the modified Stockmayer model are listed in Table 8. Since both the induction period and nuclei growth rate cannot be calculated for a single set of data, the induction period was set at a value of 1730 seconds to calculate the nuclei growth rate.

The second, third, and fourth experiments were made over an eight day period and the growth rates measured are approximately equal. However, there was an 11 day span between the

Figure 32. Comparison of dimensionless radial Smith-Ewart model to experimental size distribution data obtained at a low inhibitor level

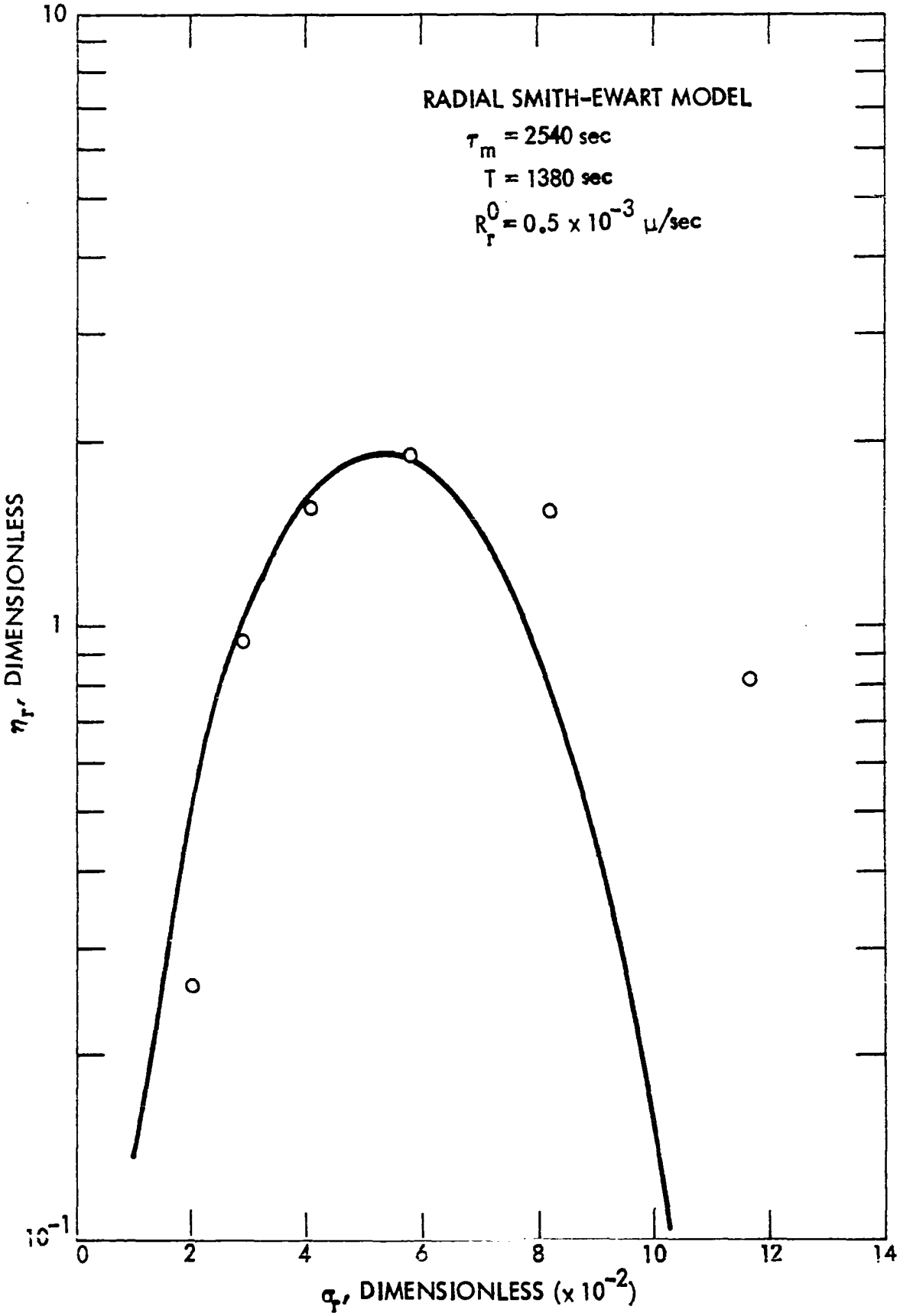
RADIAL SMITH-EWART MODEL
τ_m = 2540 sec
T = 1380 sec
R_r^0 = 0.5 x 10^{-3} μ/sec
η_r, DIMENSIONLESS
σ_r, DIMENSIONLESS (x 10^{-2})
10
1
10^{-1}
0
2
4
6
8
10
12
14

Figure 33. Comparison of dimensionless volumetric Smith-Ewart model to experimental size distribution data obtained at a low inhibitor level

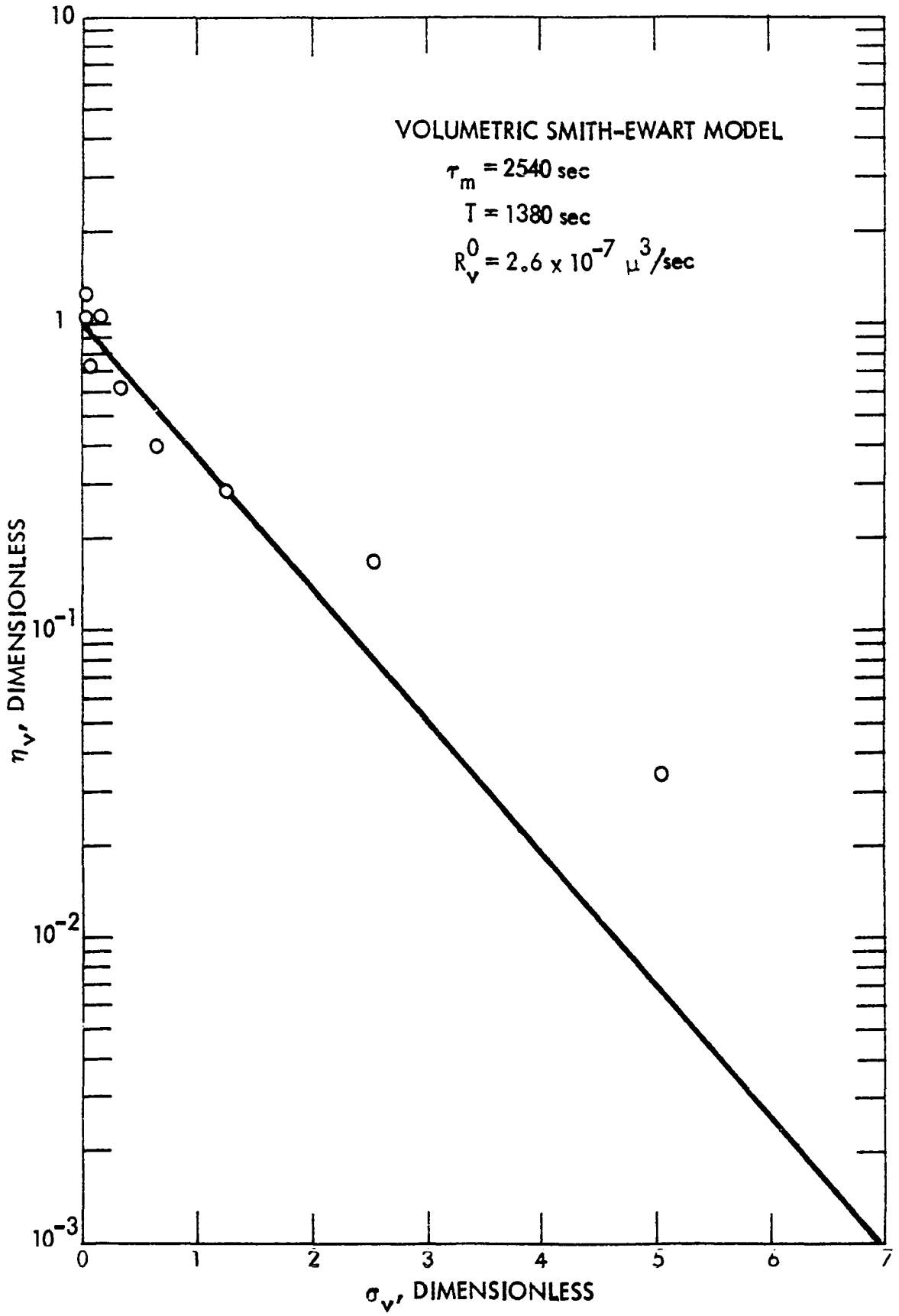
VOLUMETRIC SMITH-EWART MODEL
τ_m = 2540 sec
T = 1380 sec
$R_v^0 = 2.6 \times 10^{-7}$ μ^3/sec
η_v, DIMENSIONLESS
σ_v, DIMENSIONLESS
10
1
10^{-1}
10^{-2}
10^{-3}
0
1
2
3
4
5
6
7

Figure 34. Comparison of dimensionless radial modified Stockmayer model to experimental size distribution data obtained at a low inhibitor level

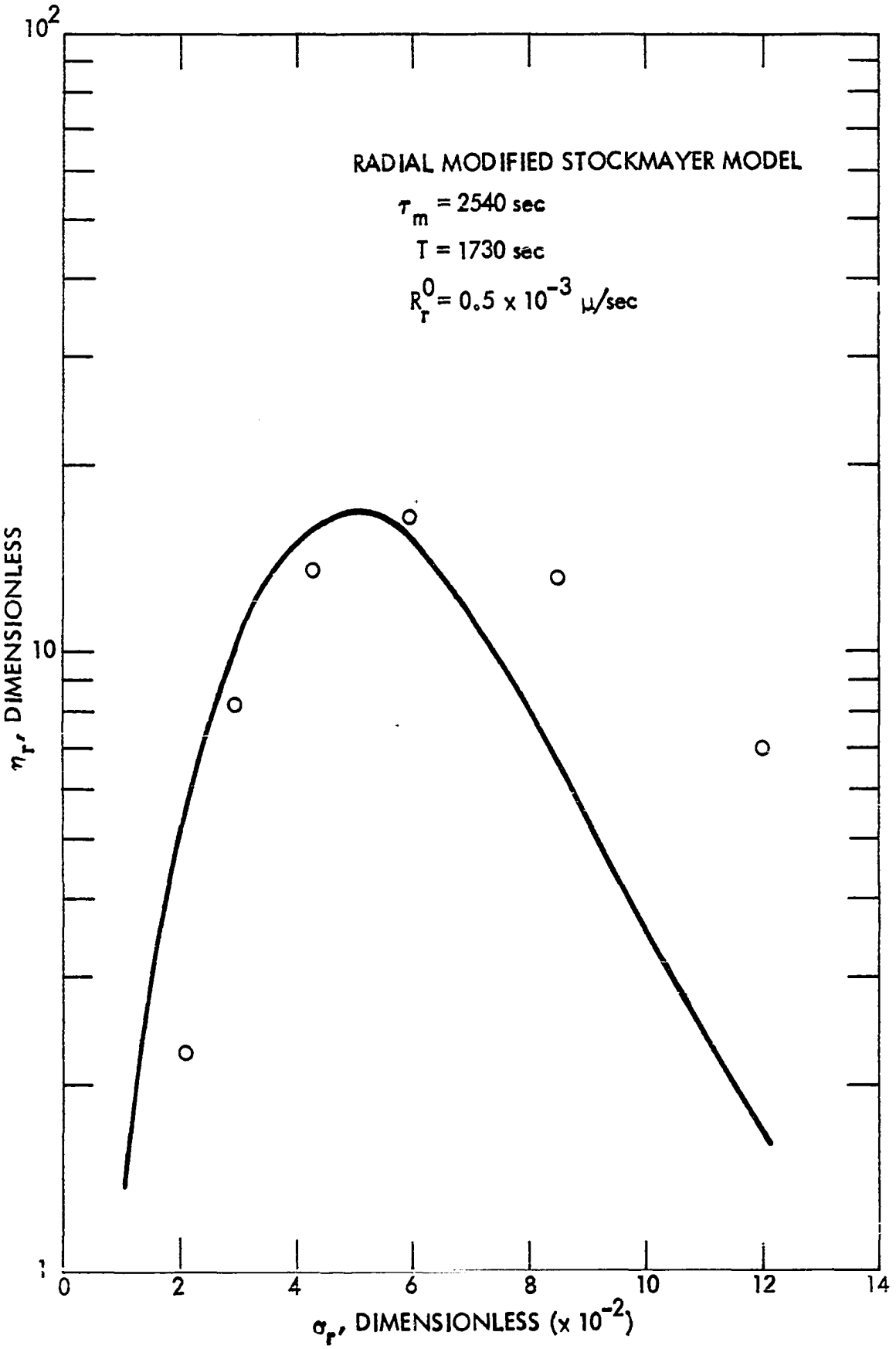
RADIAL MODIFIED STOCKMAYER MODEL
τ_m = 2540 sec
T = 1730 sec
R_r^0 = 0.5 x 10^{-3} μ/sec
10^2
10
1
η_r, DIMENSIONLESS
0
2
4
6
8
10
12
14
σ_r, DIMENSIONLESS (x 10^{-2})

Figure 35. Comparison of dimensionless volumetric modified Stockmayer model to experimental size distribution data obtained at a low inhibitor level

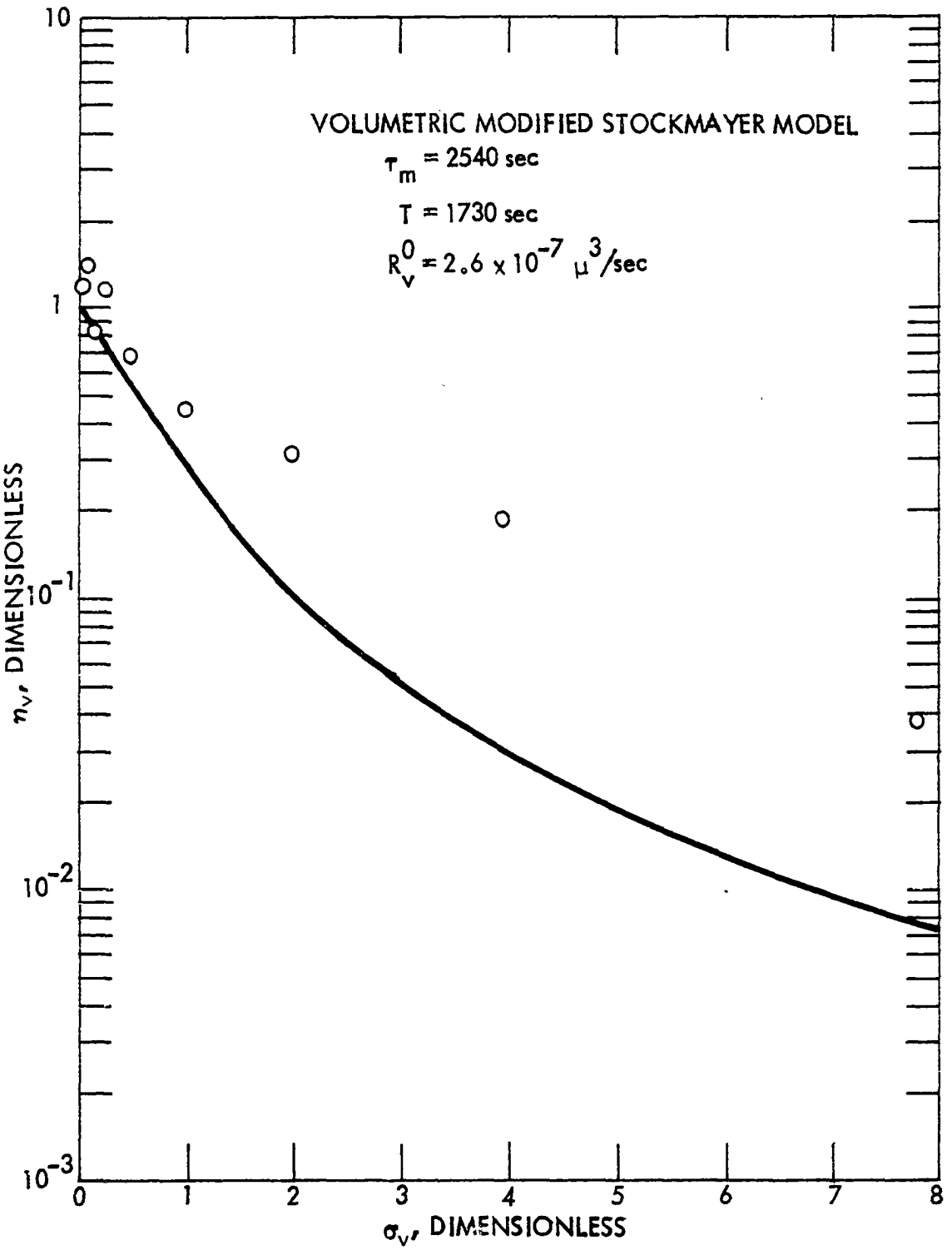
VOLUMETRIC MODIFIED STOCKMAYER MODEL
τ_m = 2540 sec
T = 1730 sec
$R_v^0 = 2.6 \times 10^{-7}$ μ^3/sec
η_v, DIMENSIONLESS
σ_v, DIMENSIONLESS
10
1
10^{-1}
10^{-2}
10^{-3}
0
1
2
3
4
5
6
7
8

Table 8. Change due to decreasing inhibitor level

Date of measurement	τ_m (sec)	$R_v^o \times 10^7$ (μ^3/sec)	T (sec)
July 31	4240	0.98	3200
August 11	2820	3.2	1400
August 13	2260	2.4	1700
August 19	2540	2.4	1700
August 28	2540	7.5	40

first and second experiment, and the growth rate increased by a factor of approximately 2.9. There was a nine day span between the fourth and fifth experiment and a 2.8 factor increase in the nuclei growth rate. A similar effect is shown by the change in the induction period calculated for each experiment assuming a growth rate of 2.4×10^{-7} μ^3/sec. That is, Table 8 shows that the induction period is approximately constant for the second, third, and fourth experiment, and a higher or lower inhibitor level exhibits a longer or shorter induction period respectively.

This indicates that estimates of the induction period and nuclei growth rate cannot be used in further predictions unless the inhibitor level is approximately the same as when the estimates were made. For the three sets of data over a

limited time period, the estimates of the induction period and nuclei growth rate were accurate enough to demonstrate that the modified Stockmayer model can be used to predict the particle size distribution when the needed parameters are known. Also when these parameters are determined through the assumption of the Smith-Ewart model as done with the data presented, the Smith-Ewart model can be used to predict the particle size distribution as a simplification of the modified Stockmayer model over the particle size range produced in this work. The particle diameters ranged up to 0.2 microns.

CONCLUSIONS

1. The solution of the equation resulting from the population balance can be used to represent the polymer particle size distribution of the latex leaving a continuous emulsion polymerizer. This representation will be in the form of a population density function. To apply this representation, a model describing the particle growth rate as a function of particle size must be known. In dimensionless form, this representation can be used in either of the forms

$$\eta_v = \exp\left[- \int_{\sigma_v^o}^{\sigma_v} \frac{1}{\rho_v} \frac{d\rho_v}{d\sigma_v} + \frac{1}{\rho_v} \right] d\sigma_v \qquad (47)$$

$$\eta_r = \exp\left[- \int_{\sigma_r^o}^{\sigma_r} \frac{1}{\rho_r} \frac{d\rho_r}{d\sigma_r} + \frac{1}{\rho_r} \right] d\sigma_r \qquad (48)$$

when dealing in terms of volumetric or radial model respectively. In order to be able to use the dimensionless size distribution prediction, the nuclei growth rate and the mean residence time of particle growth must be known.

2. There are three particle growth rate models which have been discussed. The Smith-Ewart and Medvedev models can be applied directly to the representations of particle size distribution given in Equations 47 and 48. When this is done the volumetric and radial Smith-Ewart and

volumetric and radial Medvedev representations of the size distribution become respectively

$$n = n^{o} \exp [-(V - V^{o})/\tau R_{V}] \tag{49}$$

$$m = m^{o} \exp [\ln(r^{o}/r)^{2} - \frac{8\pi}{3K\tau} (r^{3} - r^{o3})] \tag{50}$$

$$n = n^{o} \exp [\ln(V^{o}/V)^{2/3} - 3(V^{1/3} - V^{o1/3})/\tau k_{M}] \tag{51}$$

$$m = m^{o} \exp [-(r - r^{o})/R_{r}\tau]. \tag{52}$$

The Stockmayer model must be modified to be applied to a continuous, backmix polymerizer. When this modification is made the dimensionless volumetric and radial modified Stockmayer representations of the size distribution become respectively

$$n = n^{o} \exp [\ln(R_{V}^{o}/R_{V}) - \int_{V^{o}}^{V} dV/R_{V}\tau] \tag{53}$$

$$m = m^{o} \exp [\ln(R_{r}^{o}/R_{r}) - \int_{r^{o}}^{r} dr/R_{r}\tau]. \tag{54}$$

3. The Medvedev model, when applied to the population balance, predicted particles that were much larger than the particles that were experimentally produced. The Medvedev model also predicted a particle size distribution which would be a straight line on a semi-log scale as a function of particle radius. Since this relation did not agree with experimental results, the Medvedev model should not

be applied to the emulsion polymerization of styrene.

If the induction period and nuclei growth rate are determined by a least squares fit of particle size data as in this work, either the modified Stockmayer or the Smith-Ewart model, when applied to the population balance solution, may be used to predict the particle size distribution for a latex produced in a continuous emulsion polymerizer from styrene monomer. Since the modified Stockmayer model gives a more accurate prediction at the larger particle sizes, it should be used to describe the particle size distribution produced at longer residence times since longer residence times would produce larger particles. The Smith-Ewart model is only recommended for use as a simplification of the modified Stockmayer to predict the particle size distribution when approximately 90 percent of the particles are below a diameter of 0.2 microns, which is the approximate size range of this work.

4. In a continuous emulsion polymerization system, the mean residence time of particle growth can be described as the latex residence time minus the induction period produced by an inhibitor present. The residence time for particle growth is of interest since it is the fundamental parameter which determines the final size a particle will attain. The residence time for particle

growth along with the nuclei growth rate can be measured from the particle size data from two experiments made at different latex residence times and at the same inhibitor level by means of a least squares fit of a linear regression to the particle size data.

5. The application of measured induction periods and nuclei growth rates to particle size distribution predictions will not be accurate if the inhibitor level is not maintained at a constant value. However, if the inhibitor level changes only slightly, the measured parameters may be used as an approximation to the induction period and nuclei growth rate at the new inhibitor level.

SUGGESTED FURTHER WORK

1. In many uses for a polymer product of emulsion polymerization, the molecular weight distribution is of more interest than the particle size distribution. Due to the effect of the particle size on the termination rate within a particle described by the Stockmayer theory, the molecular weight distribution within a particle is expected to be a function of the size of that particle. Therefore the development of a model which could describe the molecular weight distribution within a particle and could be superimposed on the representation of the particle size distribution would be very useful.
2. Much of the industrial application of backmix polymerizers to emulsion polymerization is in the form of a cascade or series of polymerizers. In such a system the number of parameters which may be varied is very large. The population balance can be used to produce a useful description of the particle size distribution in each polymerizer of such a cascade as well as the final product.
3. The non-steady state equation resulting from the population balance has been presented in this work. Its solution should provide additional insight which would aid in the process design of continuous emulsion polymerization systems.

4. The steady state representation of the particle size distribution presented in this work describes the effect of all system parameters on the particle size distribution. Since only experimental verification with the latex residence time as a variable has been presented, an experimental study of all possible parameters of the system would be a significant addition to emulsion polymerization process design capability.

LITERATURE CITED

1. Allen, R. B., Yates, L. D. and Alfrey, T., Jr. Emulsion polymerization in continuous reactor systems: Particle size distribution calculation. American Chemical Society, Division of Organic Coatings and Plastics Chemistry Preprints No. 1, 23: 186-196. 1963. Abstracted in Chemical Abstracts 62: 641d. 1965.

2. American Society for Testing Materials. Recommended practice for analysis by microscopical methods for particle size distribution of particulate substances of subsievesizes. A.S.T.M. Designation E20-68. A.S.T.M. Standards, Part 30. 1968.

3. Boundy, R. H. Styrene. New York, N.Y., Reinhold Publishing Corporation. 1952.

4. Bovey, F. A., Kolthoff, I. M., Medalia, A. I. and Mechan, E. J. Emulsion polymerization. New York, N.Y., Interscience Publishers. 1955.

5. Brodnyan, J. G. Emulsion particle size. III. Particle size distributions determined by various growth mechanisms. Journal of Colloid Science 15: 573-577. 1960.

6. Brodnyan, J. G., Cala, J. A., Konen, T. and Kelley, E. L. The mechanism of emulsion polymerization. I. Studies of the polymerization of methyl methacrylate and N-butyl methacrylate. Journal of Colliod Science 18: 73-90. 1963.

7. DeGraff, A. W. and Poehlin, G. W. Continuous emulsion polymerization paper presented at the 65th national meeting of American Institute of Chemical Engineering, Cleveland, Ohio, May 4-7, 1969. Bethlehem, Pennsylvania, Department of Chemical Engineering, Lehigh University. 1964.

8. Ewart, R. H. and Carr, C. I. The distribution of particle sizes in polystyrene latex. Journal of Physical Chemistry 58: 640-644. 1954.

9. Gardon, J. L. Emulsion polymerization. I. Recalculation and extension of the Smith-Ewart theory. Journal of Polymer Science, Part A-1, 6: 623-641. 1968.

10. Gardon, J. L. Emulsion polymerization. II. Review of experimental data in the context of the revised Smith-Ewart theory. Journal of Polymer Science, Part A-1, 6: 643-644. 1968.

11. Gardon, J. L. Emulsion polymerization. III. Theoretical prediction of the effects of slow termination rate within latex particles. Journal of Polymer Science, Part A-1, 6: 665-685. 1968.

12. Gardon, J. L. Emulsion polymerization. IV. Experimental verification of theory based on slow termination rate within latex particles. Journal of Polymer Science, Part A-1, 6: 687-710. 1968.

13. Gardon, J. L. Emulsion polymerization. V. Lowest theoretical limit of the ratio k_t/k_p. Journal of Polymer Science, Part A-1, 6: 2853-2857. 1968.

14. Gardon, J. L. Emulsion polymerization. VI. Concentration of monomers in latex particles. Journal of Polymer Science, Part A-1, 6: 2859-2879. 1968.

15. Gershberg, D. B. and Longfield, J. E. Unpublished paper presented at Symposium on Polymerization Kinetics and Catalyst Systems: Part I. 54th meeting, American Institute of Chemical Engineering, December 2-7, 1961. Original not available; cited in DeGraff, A. W. and Poehlin, G. W. Continuous emulsion polymerization. Paper presented at 65th national meeting of American Institute of Chemical Engineering, Cleveland, Ohio, May 4-7, 1969.

16. Harkins, W. D. A general theory of the mechanism of emulsion polymerization. Journal of the American Chemical Society 69: 1428-1444. 1947.

17. Harkins, W. D. General theory of mechanism of emulsion polymerization II. Journal of Polymer Science 5: 217-251. 1950.

18. Hartley, G. S. Aqueous solution of paraffin-chain salts. Paris, Hermann et Cie. 1936.

19. Hildebrand, F. B. Introduction to numerical analysis. New York, N.Y., McGraw Hill Book Co., Inc. 1956.

20. Katz, S. and Shinnar, R. Particulate methods in probability systems. Industrial and Engineering Chemistry 61, No. 4: 60-73. 1969.

21. McBain, J. W. Colloid Science. Boston, Mass., D. C. Heath and Co. 1950.

22. Medvedev, S. S. Mechanism of emulsion polymerization (Translated title). Ricerca scientifica, Supplemento, Simposio internacional chim macromol. Milan - Turin 25: 897-908. 1954. Abstracted in Chemical Abstracts 54: 12631h. 1960.

23. Morton, M., Kaizerman, S. and Altier, M. W. Swelling of latex particles. Journal of Colloid Science 9: 300-312. 1954.

24. O'Toole, J. T. Kinetics of emulsion. Journal of Applied Polymer Science 9: 1291-1297. 1965.

25. Randolph, A. D. and Larson, M. A. Transient and steady state size distributions in continuous mixed suspension crystallizers. American Institute of Chemical Engineering Journal 8, No. 5: 639-645. 1962.

26. Roe, C. P. Surface chemistry aspects of emulsion polymerization. Industrial and Engineering Chemistry 60, No. 9: 20-33. 1968.

27. Sato, T. and Taniyama, I. Kinetics of emulsion polymerization (Translated title). Kogyo Kagaku Zasshi 68, No. 1: 67-72. 1965.

28. Sato, T. and Taniyama, I. Continuous emulsion polymerization (Translated title). Kogyo Kagaku Zasshi 68, No. 1: 106-109. 1965.

29. Smith, W. V. The kinetics of styrene emulsion polymerization. Journal of American Chemical Society 70: 3695-3702. 1948.

30. Smith, W. V. and Ewart, R. H. Kinetics of emulsion polymerization. Journal of Chemical Physics 16, No. 6: 592-599. 1948.

31. Stockmayer, W. H. Note on the kinetics of emulsion polymerization. Journal of Polymer Science 24: 314-317. 1957.

32. Ugelstad, J., Mork, P. C., and Aasen, J. O. Kinetics of emulsion polymerization. Journal of Polymer Science, Part A-1, 5: 2281-2288. 1967.

33. Vanderhoff, J. W., Vitkuske, J. F., Bradford, E. G., and Alfrey, T., Jr. Some factors involved in the preparation of uniform particle size latexes. Journal of Polymer Science 20: 225-234. 1956.

34. Wall, F. T., Delbecq, C. J., and Florin, R. E. Studies in continuous polymerization. Journal of Polymer Science 9: 177-192. 1952.

35. Wine, R. L. Statistics for scientists and engineers. Englewood Cliffs, N.J., Prentice Hall, Inc. 1964.

ACKNOWLEDGEMENTS

The author is indebted to his advisor, Dr. J. D. Stevens, whose aid and encouragement was deeply appreciated. Dr. Stevens, who doubled as a playing partner in the Chemical Engineering golf league, could only have improved his relationship with the author by improving his putting.

The author also wishes to thank Dr. M. A. Larson whose aid was invaluable in completing this work in the absence of Dr. Stevens.

The machine computation time was donated by the Iowa State University computation center. The Electron Microscope Lab of the Engineering Research Institute of Iowa State University provided the technical assistance necessary to obtain the particle size measurement.

The author wishes to acknowledge financial support during his graduate study by a National Defense Education Act, Monsanto, and American Cyanamid Fellowships.

Finally, the author wishes to thank his wife, Linda, whose contributions to this work were freely given. Her support and encouragement made the author's life more than bearable throughout the long working hours of graduate school.

NOMENCLATURE

A_T	cumulative surface area of particles, L^2/L^3
a	parameter in the Stockmayer theory
$\bar{a}$	particle average surface area, L^2
b	parameter in the modified Stockmayer theory
I_o, I_1	Bessel functions of the first kind
K	volumetric growth rate constant, L^3/t
k	specific rate constant
k_M	proportionality constant for Medvedev radial growth rate
k_p	specific rate constant of propagation, $L^3/(\text{mole } t)$
k_t	specific rate constant of termination, $L^3/(\text{mole } t)$
M	monomer concentration at polymerization loci, mole/L^3
m	particle population density as a function of radius, $\#/(L\ L^3)$
m^o	nuclei population density as a function of radius, $\#/(L\ L^3)$
N	total number of polymer particles per cc of water, $\#/L^3$
N^o	total number of nuclei per cc of water, $\#/L^3$
N_A	Avogadro's number, #/mole
N_q	total number of particles with q radicals, #
n	particle population density, $\#/L^3$
$\bar{n}$	point population density, $\#/(L^3\ L^3)$
$\bar{n}_i$	point population density in the input stream, $\#/(L^3\ L^3)$
$\bar{n}_o$	point population density in the output stream. $\#/(L^3\ L^3)$

$\bar{n}_s$	point population density at latex surface, $\#/(L^3\ L^3)$
n^o	nuclei population density, $\#/(L^3\ L^3)$
n_q	population density for particles with q radicals, $\#/(L^3\ L^3)$
Q	average number of radicals in a particle, #
Q_i	input volumetric flow rate, L^3/t
Q_o	output volumetric flow rate, L^3/t
q	number of radicals in a particle, #
R	rate of radical production per cc of water, $\#/(t\ L^3)$
R_r	radial growth rate, L/t
R_r^o	radial growth rate of nuclei, L/t
R_T	cumulative particle radius L/L^3
R_v	volumetric growth rate, L^3/t
R_v^o	volumetric growth rate of nuclei, L^3/t
r	radius of a particle, L
r^o	nuclei radius, L
r_p	rate of propagation, mole/t
$\|r\|$	estimator for correlation coefficient
S	interfacial area of the soap present in one cc of water, L^2/L^3
T	induction period, t
t	time, t
V	particle volume, L^3
V^o	nuclei volume, L^3
$\bar{V}$	average particle volume, L^3
V'	latex volume, L^3

V_T cumulative particle volume, L^3/L^3

α parameter in Stockmayer theory

β parameter in modified Stockmayer theory

γ constant

η_r dimensionless population density based on radius

η_r^o dimensionless nuclei population density based on radius

η_r^* ratio of radial population density to total numbers

η_v dimensionless population density based on volume

η_v^o dimensionless nuclei population density based on volume

θ dimensionless time

ρ_m monomer density in a particle, M/L^3

ρ_p polymer density in a particle, M/L^3

ρ_r dimensionless radial growth rate

ρ_v dimensionless volumetric growth rate

σ_r dimensionless particle radius

σ_r^o dimensionless nuclei radius

σ_v dimensionless particle volume

σ_v^o dimensionless nuclei volume

τ mean residence time for particle growth, t

τ_m mean latex residence time, t

ϕ_m monomer volume fraction in a particle, L^3/L^3

APPENDIX A. LINEAR REGRESSION ANALYSIS

Smith-Ewart Model

The volumetric Smith-Ewart model predicts a straight line for the population density function on a semi-log scale. The population density takes the form

$$\ln n = \ln n^{o} - \frac{1}{\tau R_{v}^{o}} V. \tag{55}$$

Therefore the one can perform a least squares fit of experimental data to the regression

$$y = a + bx \tag{56}$$

to obtain experimental values of n^{o} and τR^{o}. These values are presented in Table 9 for the data obtained in this work along with the correlation coefficient in each case.

Table 9. Smith-Ewart least squares fit data

τ_m (sec)	n^{o} (#/(μ^3 cc))	$R_v^{o}\ \tau \times 10^4$ (μ^3)	$\lvert r \rvert$
4240	2.09	5.11	0.950
2820	2.07	4.01	0.947
2260	6.10	2.31	0.940
2540	2.51	3.04	0.958
2540	2.72	4.55	0.974

Modified Stockmayer Model

The volumetric modified Stockmayer model can be arranged in linear form. Even though the actual nuclei growth may be unknown, the ratio of the particle growth rate to the nuclei growth rate, ρ_r, may be evaluated as

$$\rho_r = 2\,Q \tag{57}$$

Therefore the population density

$$n = n^o \exp\left[\ln 1/\rho_V - \int_{V^o}^{V} \frac{dV}{R_V \tau}\right] \tag{58}$$

which leads to

$$\ln n = \ln n^o - \ln \rho_V - \frac{1}{R_V^o \tau} \int_{V^o}^{V} \frac{dV}{\rho_V} \tag{59}$$

or

$$\ln (n\,\rho_V) = \ln n^o - \frac{1}{R_V^o \tau} \int_{V^o}^{V} \frac{dV}{\rho_V} \tag{60}$$

Since ρ_V is known and the integral can be evaluated by numerical methods, one can perform a least squares fit of experimental data to the regression

$$y = a + bx \tag{61}$$

to obtain experimental values of n^o and τR_V^o. The values are presented in Table 10 for the data obtained in this work along with the correlation coefficient in each case.

Table 10. Modified Stockmayer least squares fit data

τ_m (sec)	n^o (#/(μ^3 cc))	$R_v^o \tau \times 10^4$ (μ^3)	$\|r\|$
4240	3.46	2.46	0.951
2820	2.43	3.46	0.813
2260	9.30	1.28	0.950
2540	3.39	1.95	0.970
2540	3.08	6.05	0.823

APPENDIX B. STEADY STATE DETERMINATION

Figure 36 illustrates the relative radial population densities for samples taken after the experiment had been in progress for 12, 16, and 18 latex residence times. In this case the population density is defined as

$$n_r^* = \frac{n_r}{N} \tag{62}$$

where N is the total number of particles counted.

These data were obtained at a latex residence time of 2820 seconds. Since data were obtained before the analytical procedure was finalized it is believed that the particles grew after sampling. However each of the three samples were handled identically and the resulting population densities were assumed to be close enough to state that steady state conditions were reached after 12 residence times. The population densities are the most similar near the peaks which accounts for the majority of the particles produced.

Figure 36. Change in relative radial population densities of latex samples obtained after 12, 16, and 18 residence times

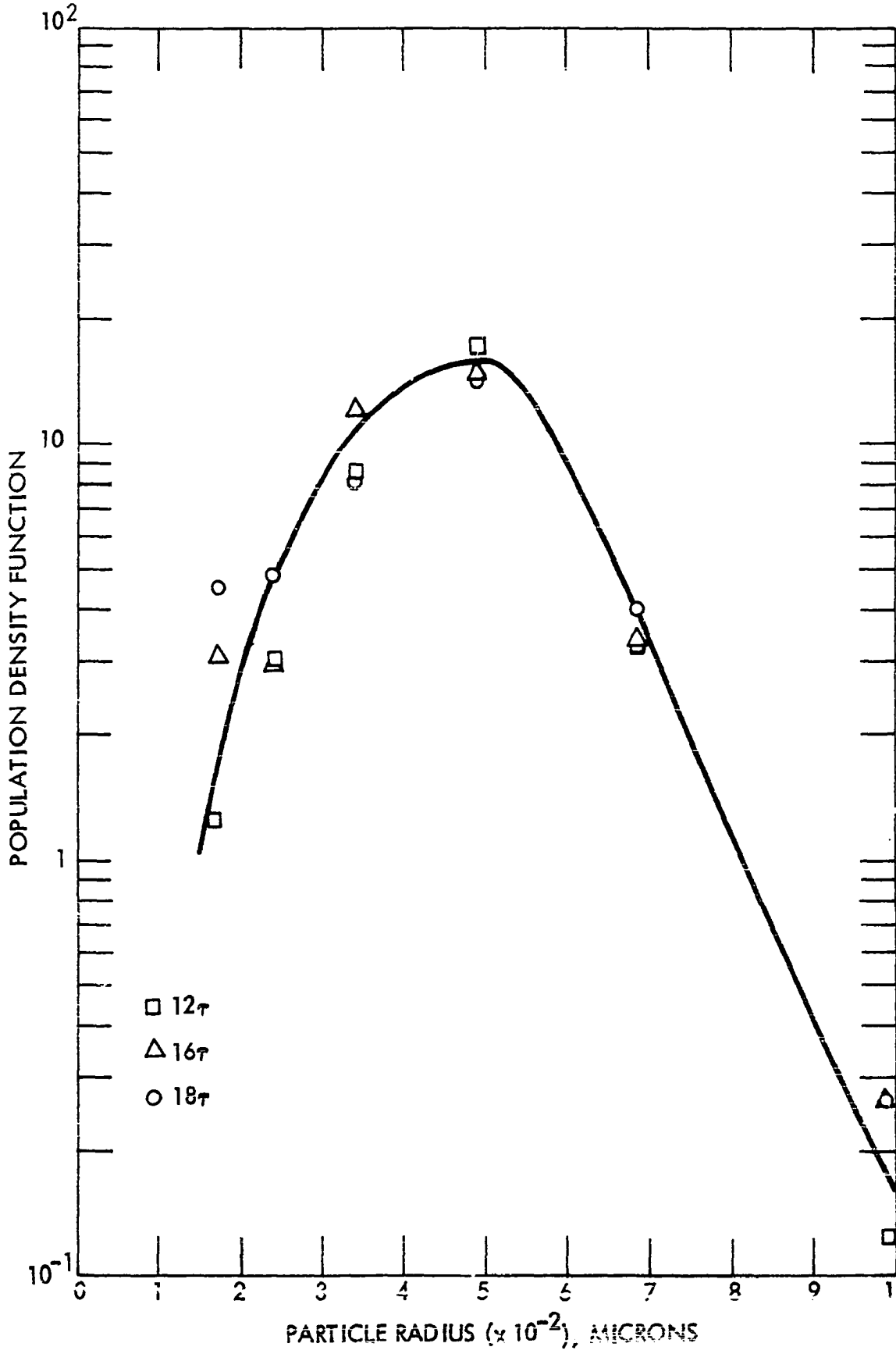
10^2
10
1
10^{-1}
POPULATION DENSITY FUNCTION
□ 12τ
△ 16τ
○ 18τ
0
1
2
3
4
5
6
7
8
9
10
PARTICLE RADIUS (x 10^{-2}), MICRONS

APPENDIX C. DERIVATION OF MODIFIED STOCKMAYER CHANGE IN Q

The derivation of volume rate of change of the average number of radicals in a particle, dQ/dV, is obtained for the modified Stockmayer solution as follows:

$$Q = (b/4)\, I_0(b)/I_1(b) \tag{63}$$

$$b^2 = 8s \tag{64}$$

$$s = \left[\frac{R}{S} (4.84) \frac{N_A}{k_t} \right] V^{5/3} \tag{65}$$

Combining Equations 64 and 65 and taking the differential, leads to

$$da^2 = 8 \left[\frac{R}{S} (4.84) \frac{N_A}{k_t} \right] dV^{5/3} \tag{66}$$

$$2ada = \frac{40}{3} \left[\frac{R}{S} (4.84) \frac{N_A}{k_t} \right] V^{2/3}\, dV \tag{67}$$

$$da = K' \frac{dV}{V^{1/6}} \tag{68}$$

where

$$K' = \frac{20}{6\sqrt{2}} \left[\frac{R}{S} (4.84) \frac{N_A}{k_t} \right]^{0.5} . \tag{69}$$

Now apply Equation 68 to the modified Stockmayer solution.

$$\frac{dQ}{dV} = \frac{d}{dV} \left[\frac{b}{4} \frac{I_0(b)}{I_1(b)} \right] = \frac{K'}{V^{1/6}} \frac{d}{db} \left[\frac{b}{4} \frac{I_0(b)}{I_1(b)} \right] . \tag{70}$$

To obtain this derivative, two Bessel function identities

are combined

$$x^{v}I_{v}'(x) + vx^{v-1}I_{v}(x) = x^{v}I_{v-1}(x) \tag{71}$$

$$x^{-v}I_{v}'(x) - vx^{-v-1}I_{v}(x) = x^{-v}I_{v+1}(x) \tag{72}$$

and the following was developed:

$$I_{v}'(x) = -vx^{-1}I_{v}(x) + I_{v-1}(x) = vx^{-1}I_{v}(x) + I_{v+1}(x) . \tag{73}$$

Equation 70 leads to

$$\frac{d}{db}\left[\frac{b}{4}\frac{I_o(b)}{I_1(b)}\right] = \frac{1}{4}\left[\frac{I_o(b)}{I_1(b)} + b\left(\frac{I_1(b)\frac{dI_o(b)}{db} - I_o\frac{dI_1(b)}{db}}{I_1^2(b)}\right)\right] \tag{74}$$

applying Equation 73

$$\frac{d}{db}\left[\frac{b}{4}\frac{I_o(b)}{I_1(b)}\right] = \frac{1}{4}\left[\frac{I_o(b)}{I_1(b)} + b\left(\frac{I_1^2(b) - I_o(b)I_o(b) - b^{-1}I_1(b)}{I_1^2(b)}\right)\right] \tag{75}$$

$$\frac{d}{db}\left[\frac{b}{4}\frac{I_o(b)}{I_1(b)}\right] = \frac{1}{4}\left[\frac{b\,I_1^2(b) + 2I_1(b)I_o(b) - b\,I_o^2(b)}{I_1^2(b)}\right]. \tag{76}$$

Therefore combining Equations 69 and 70

$$\frac{dQ}{dV} = \frac{K'}{4V^{1/6}}\left[\frac{b\,I_1^2(b) + 2I_1(b)I_o(b) - a\,I_o^2(b)}{I_1^2(b)}\right]. \tag{77}$$

This is the form which was applied to the volumetric modified Stockmayer growth rate model.